8-22-2022 4:30 PM

The Design and Evaluation of a Subacromial Implant in Restoring Normal Glenohumeral Joint Stability in the Presence of a Massive Irreparable Rotator Cuff Tear

Cole T. Fleet, *The University of Western Ontario*

Supervisor: Johnson, James A., *The University of Western Ontario*
Co-Supervisor: Athwal, George S., *The University of Western Ontario*
A thesis submitted in partial fulfillment of the requirements for the Master of Engineering Science degree in Mechanical and Materials Engineering

Abstract

Massive irreparable rotator cuff tears are a common cause of pain and disability. Several different treatment options are available for this pathology; however, these treatments have been associated with poor clinical outcomes when used to treat younger (<65 years), more active patients. The purpose of this thesis was to design and evaluate a subacromial implant in its ability to restore normal glenohumeral stability and range of motion. The implant was created as a modular device, which captured different implant thicknesses (5mm and 8mm) and constraints (high and low) within its design. In-vitro testing compared the ability of these implants to restore normal shoulder biomechanics. The results indicated the 5mm high constraint implant to be the most effective in restoring normal joint position. Furthermore, range of motion increased when the implant was paired with a tuberoplasty procedure. These results suggest this implant may be advantageous in treating younger patients.

Keywords

Subacromial implant, massive irreparable rotator cuff tear, humeral head translation, range of motion, modular, impingement

Summary for Lay Audience

One of the primary joints in the human shoulder is the glenohumeral joint, defined as the articulation between the humerus and scapula. This joint is largely supported by a group of muscles called the rotator cuff. However, when large tears occur in two or more of the units connecting these muscles to bone, patients can experience pain and loss of function. These tears can also cause unnatural translation of the humerus at the glenohumeral articulation, which can lead to further injury. Several surgical interventions are available for treating this type of injury, which have shown to have promising results when treating older (<65 years), less active patients. However, for more active patients who are younger than 65 years of age, the effectiveness of these treatments has been called into question as poor results have been shown when treating this patient group.

Recently, the concept of a subacromial implant has been proposed for this patient demographic, as it may contain several attributes that are advantageous to this specific patient population. Therefore, this thesis served to design and evaluate a subacromial implant in its ability to prevent translation of the humerus and restore normal range of motion. Four different implant models were created with varying thickness (5mm and 8mm) and constraint (high and low constraint) to determine which model was most effective at treating this injury. Testing was performed using a series of cadaver shoulders, which compared the normal, healthy shoulder to an injured shoulder state treated with the four different implant designs. Further testing was also conducted that paired the insertion of the subacromial implants with a tuberoplasty procedure which is used to improve the articulation at the glenohumeral joint.

The results indicated the 5mm high constraint implant to be most effective in restoring the normal position of the humerus within the shoulder. Furthermore, it was found that the addition of the tuberoplasty procedure increased the shoulder's allowable range of motion. These early results suggest this device may be an effective treatment options for younger, more active patients, and could improve their quality of life.

Co-Authorship Statement

Chapter 1: CT Fleet – Sole Author

Chapter 2: CT Fleet – Implant Design, implant evaluation, data collection, wrote manuscript

DS McNeil – Specimen preparation, implant evaluation

GS Athwal – Reviewed manuscript

JA Johnson – Reviewed manuscript

Chapter 3: CT Fleet – Study design, data collection, statistical analysis, wrote manuscript

DS McNeil – Study design, specimen preparation, reviewed manuscript

GS Athwal – Study design, reviewed manuscript

JA Johnson – Study design, reviewed manuscript

Chapter 4: CT Fleet – Study design, simulator design changes, data collection, statistical analysis, wrote manuscript

DP Ferguson – Study design, specimen preparation, data collection

GS Athwal – Study design

JA Johnson – Study design, reviewed manuscript

Chapter 5: CT Fleet – Sole author

Acknowledgments

I would first like to thank my primary supervisor, Dr. Johnson, for taking me on as a student and for the immense support he has provided me throughout the entirety of my Master's degree. Your work ethic both in the lab and in the classroom is truly inspirational. I will never forget you taking time out of your busy schedule to meet with me and provide support on any topic, your incredible lectures, and your chip in on the 18th.

I would additionally like to thank my co-supervisor, Dr. Athwal. From the moment I started at the hospital, you have provided me countless opportunities to partake in the most interesting and novel research studies, for which I am so grateful. Your passion and drive for research is truly remarkable and motivating.

Thank you to both Dr. McNeil and Dr. Ferguson. I cannot put into words my appreciation for all of your hard work and efforts in the lab during the long testing days. Your insight and feedback regarding the design of the subacromial implant was of immense value and will serve to drive further implant optimization. I wish you both all the best on what I am sure will be your incredible future careers as Orthopaedic surgeons.

I would also like to thank my entire family for their continuous support throughout my education. To my parents for proofreading countless documents throughout my entire education and for always being there for me; and to Neila for always supporting and believing in me. I could not have made it this far without you all.

Thank you to all my past and current fellow lab mates (both graduate and undergraduate) at the HULC research lab for providing such an incredible work environment. Nick Van Osch, the mentorship you provided me was truly invaluable. Thank you David Cunningham for continually pushing me to expand my computational knowledge and for making all TA duties so much more enjoyable.

I would also like to acknowledge NSERC as an external source of funding throughout my graduate degree.

Table of Contents

List of Figures

Chapter 1

1 Introduction

This chapter will review the fundamental anatomy of the human shoulder complex with emphasis placed on the structure and function of the osseous and soft tissue structures surrounding the glenohumeral joint. The stability of the joint will then be discussed, with specific focus on the different mechanisms that contribute to joint stability throughout full range of motion. This will be followed with a section detailing rotator cuff pathology and the effect this has on glenohumeral joint stability. Furthermore, focus will be placed on massive irreparable rotator cuff tears; a type of rotator cuff tear that can disrupt the normal stability of this joint and can be treated using numerous surgical interventions. Finally, the rationale for this thesis will be introduced which serves to propose a novel surgical treatment for massive irreparable rotator cuff tears.

1.1 The Shoulder[1]

The human shoulder complex serves to connect the upper limb to the thorax. The components of the shoulder that allow for a wide range of motion include three bones and an assortment of passive and active soft tissue structures. These structures give rise to four articulations including the glenohumeral joint, acromioclavicular joint, scapulothoracic joint, and sternoclavicular joint (Figure 1-1). While all four articulations are important for overall shoulder function and motion, this thesis will focus on the glenohumeral joint. The glenohumeral joint, a shallow ball and socket joint, is the articulation between the scapula and humerus. It is the shallow nature of this joint that makes the surrounding soft tissue vital for maintaining joint stability. The following sections will discuss the structure and functions of the osseous and soft tissue anatomy that contribute to glenohumeral joint stability.

---

[1] All anatomical terms and definitions were referenced using the same resources[68,81,206,212]

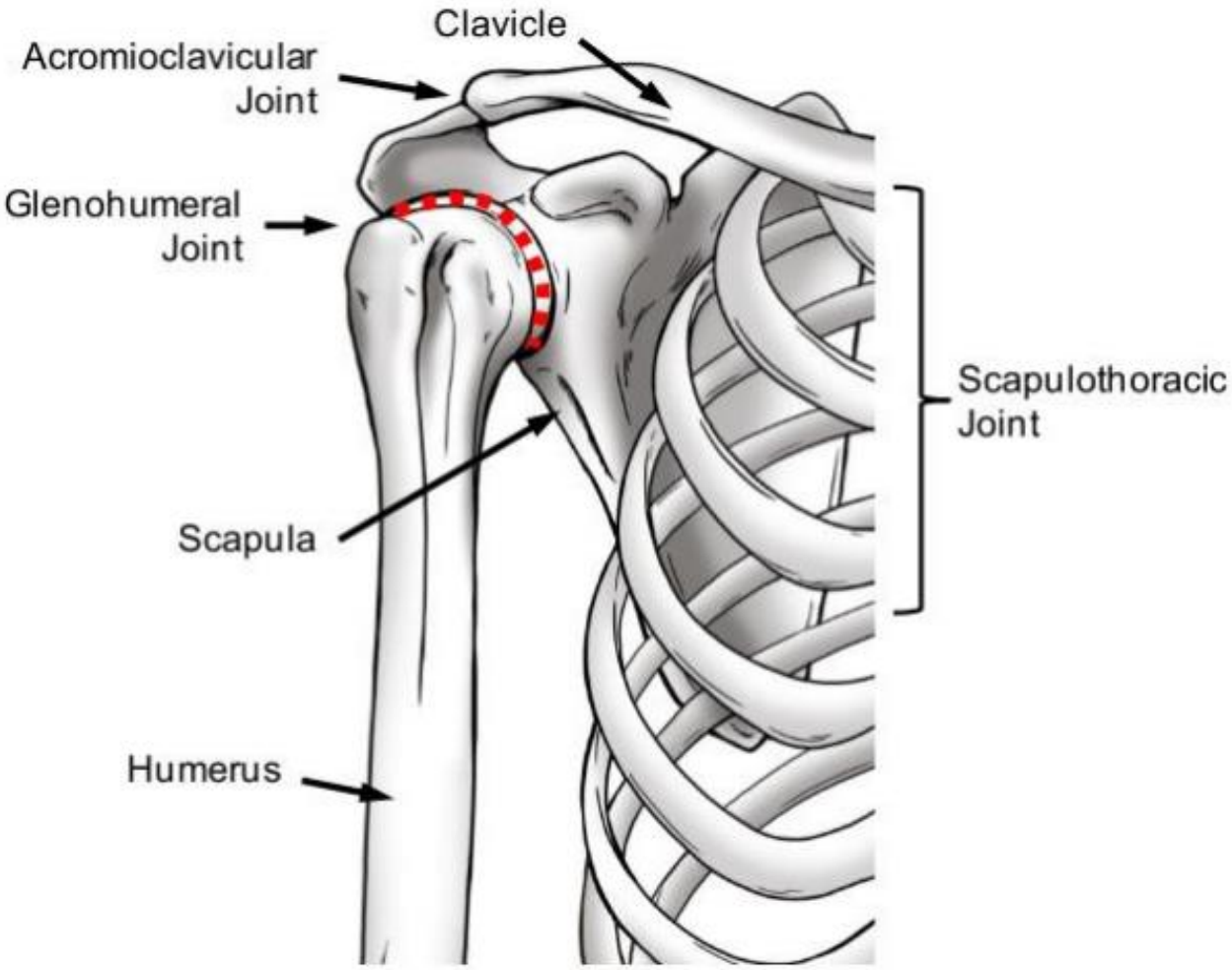

Figure 1-1: Labelled diagram of the shoulder.

Anterior view of the shoulder complex, comprising the glenohumeral joint (primary focus), acromioclavicular joint, and scapulothoracic joint (sternoclavicular joint not shown). The glenohumeral articulation is indicated by the dashed red line.

1.1.1 Osteology

1.1.1.1 Scapula

The scapula is a flat, triangular-shaped bone that connects the upper limb to the thorax and is positioned on the posterior aspect of the thorax (Figure 1-2). The scapula contributes to the glenohumeral, acromioclavicular, and scapulothoracic articulations in the shoulder. The scapula also contains several important bony features that are critical for soft tissue origin and insertion. The subscapular fossa, infraspinatus fossa, and the supraspinatus fossa are large, smooth surfaces that serve as the origins for several rotator cuff muscles. The unique shape of the scapula also gives rise to several unique bony features including the glenoid fossa, scapular spine, acromion, and coracoid, which serve as important sites for articulation or muscle attachment.

The glenoid fossa is the concave surface located on the lateral aspect of the scapula, which articulates with the humerus to comprise the glenohumeral joint. Its surface is covered in hyaline cartilage which reduces friction and improves contact mechanics at the joint surface. The shape of the glenoid articular surface is unique and is often described as pear shaped. This is due to the length of the glenoid being the greatest in the superior-inferior direction, while the anterior-posterior diameter of its inferior half is significantly greater than the anterior-posterior diameter of its superior half[95,127]. This concavity is shallow and contains only one-third to one-quarter the articulating surface area to that of the humeral head. These morphologic features prevent the glenoid from fully constraining the humerus like a true ball and socket joint, and allows for small amounts of humeral head translation to exist[130,132,149].

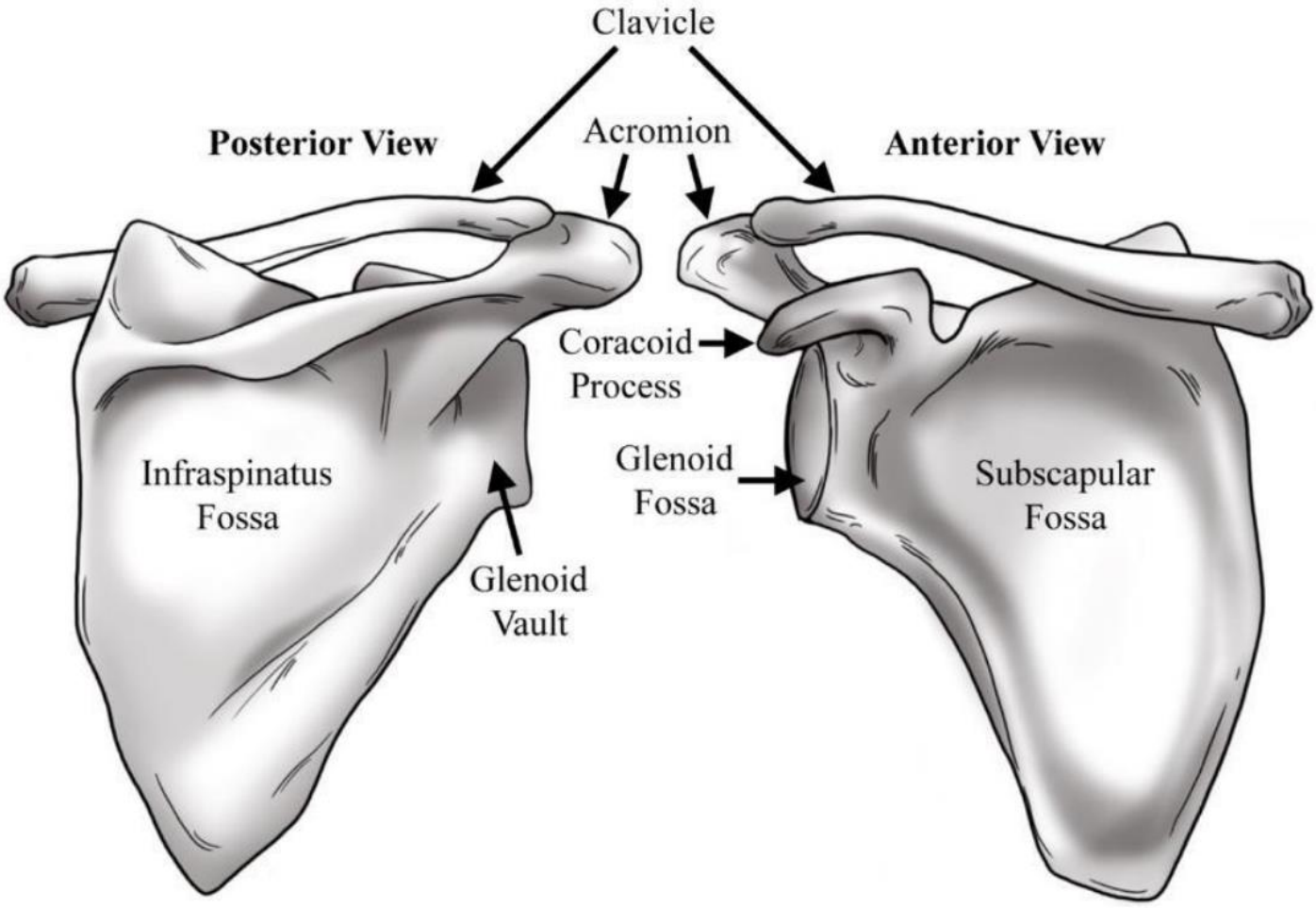

Figure 1-2: Anterior and Posterior views of the scapula and clavicle.

The scapula and clavicle form the acromioclavicular joint at the anterior edge of the acromion. Several important bony landmarks for soft tissue attachment or articulation are labelled.

The scapular spine is located on the posterior surface of the scapula and divides the supraspinatus and infraspinatus fossae. The spine starts near the medial boarder of the scapula and extends away from the surface as it projects laterally and superiorly, eventually forming the acromion. Previous literature has classified scapular spine shape into five different categories based only on the shape of the scapular spine[223]. The most prominent of these five shape classifications was identified as type 1- Fusiform shape while type 2- slender rod shape was observed the least. This structure also serves as an important attachment site for several different muscles. The trapezius attaches to the superior lip of the spine while the supraspinatus and infraspinatus muscles partly attach to the superior and inferior surfaces of the spine respectively. The scapular spine also serves as the origin for the posterior deltoid muscle that attaches to the spine's inferior lip.

The acromion is the lateral projection of the scapular spine that overhangs the glenohumeral articulation. Its anterior edge articulates with the distal clavicle forming the acromioclavicular joint, while its lateral edge and dorsal surface gives attachment to the middle deltoid. The shape of this structure is important as it increases the lever arm of the deltoid, reducing the forces exerted by this muscle during the motion of abduction or arm elevation. Previous studies have classified different categories of acromial shape due to its wide shape variance in patients (Figure 1-3). Bigliani et al.[17] classified the acromion into three shape types in the sagittal plane: type 1-flat, type 2-curved, and type 3-hooked.

The coracoid is a thick process of bone located anteriorly and slightly superiorly to the glenoid fossa and projects laterally. The tip of this structure provides attachment for the pectoralis minor, the short head of the biceps, and the coracobrachialis muscles. Additionally, this structure provides attachment for several ligaments and has a smooth concave anterior surface which the subscapularis passes over.

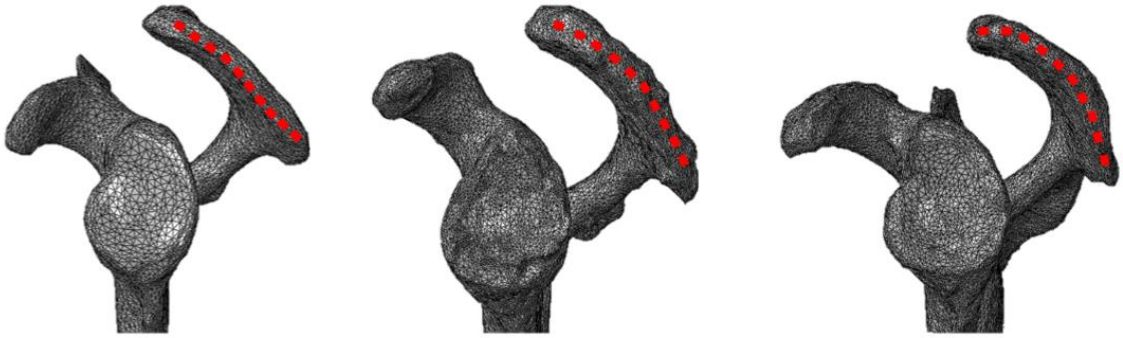

A B C

Figure 1-3: Acromion morphologic types.

The three types of acromion defined by Bigliani et al.[17] *are shown. (A) Type I Flat, (B) Type II Curved, and (C) Type III Hooked (adapted from Lockhart*[122]*).*

1.1.1.2 Humerus

The humerus is the long bone located in the proximal half of the upper limb. It contains unique bony landmarks and articular surfaces at both proximal and distal ends of a shaft roughly cylindrical in shape (Figure 1-4). Since this thesis focuses only on the glenohumeral joint, the anatomical landmarks and joint surfaces of the proximal humerus will be discussed as these are most relevant to the glenohumeral joint anatomy.

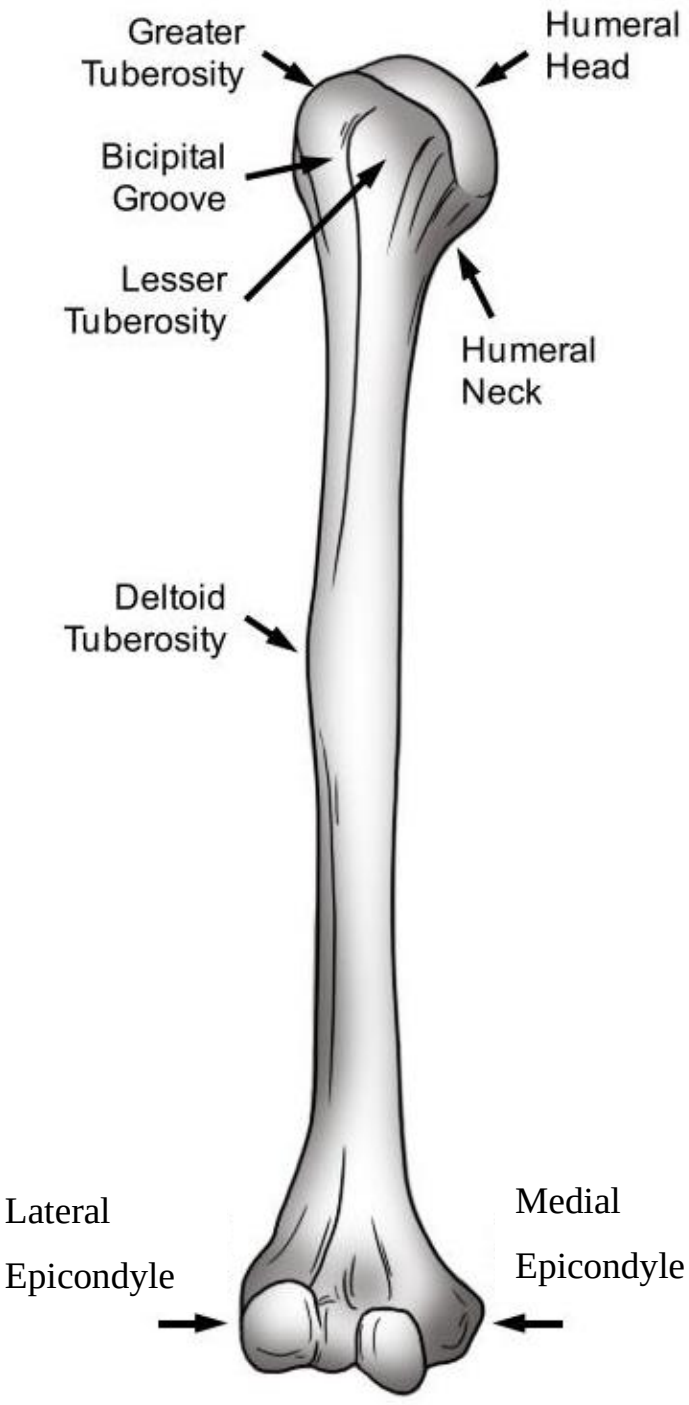

Figure 1-4: Anterior view of the humerus.

Labels are provided for important soft tissue attachment or articulation landmarks.

Arguably the most recognizable feature of the proximal humerus is the humeral head, a large nearly hemispherical surface that articulates with the glenoid. Similar to the glenoid surface, the articular surface on the humeral head is covered in cartilage, improving joint contact mechanics. The humeral head is separated from the humeral shaft by both the anatomical and surgical necks. The anatomical neck is located between the humeral head articular surface and both the lesser and greater tuberosities; while the surgical neck is located distally to these tuberosities. Both tuberosities serve as important muscle attachment sites for the rotator cuff. The lesser tuberosity is the insertion location for the subscapularis and is located on the lateral and anterior side of the humeral head. The greater tuberosity, consisting of three facets, is larger than the lesser tuberosity and is found on the lateral aspect of the humeral head. The superior facet provides insertion for the supraspinatus, the middle facet provides insertion for the infraspinatus, and the inferior and posterior facet provides insertion for the teres minor. The lesser and greater tuberosities are separated by the bicipital groove, a small groove in the humeral head for which the long head of the biceps brachii glides through. The last important bony landmark on the proximal humerus includes the deltoid tuberosity. This landmark serves as the insertion for the deltoid muscle and is located on the anterolateral surface of the humeral shaft, distal to the aforementioned humeral features.

1.1.1.3 Clavicle

The clavicle is another long bone that is subtly “S” shaped and positioned anteriorly to the thoracic cage, just above the first rib, and functions to prevent inferior and medial translation of the scapula. The medial end of the clavicle connects to the sternum to create the sternoclavicular joint and its lateral end articulates with the anterior edge of the acromion to form the acromioclavicular joint. While the clavicle provides attachment for numerus muscles, the most relevant to the glenohumeral joint is the origin of the anterior head of the deltoid. This section of muscle originates on the anterosuperior surface of the lateral third of the clavicle.

1.1.2 Passive Soft Tissue

Several passive soft tissue structures are present at the glenohumeral joint to provide stability for this articulation (Figure 1-5). These structures serve to deepen the glenohumeral joint and provide stability at end range of motion. Three passive soft tissues that will be discussed include the glenoid labrum, glenohumeral joint capsule, and the glenohumeral ligaments.

The glenoid labrum consists of fibrocartilage tissue that attaches around the periphery of the glenoid. The primary role of the labrum is to increase the stability of the glenohumeral joint by increasing the depth of the glenoid cavity. It has been found that the detachment of the labrum leads to a high incidence of glenohumeral instability[92]. The joint capsule is another passive soft tissue structure that inserts medially to the glenoid and laterally to the anatomical neck of the humerus. While the capsule remains relatively loose throughout normal range of motion, it tightens at end range motion to preserve joint stability and prevent excessive humeral head translation. The capsule is reinforced by the surrounding ligaments. These ligaments include the superior, middle, and inferior glenohumeral ligaments which increase the thickness of the anterior, inferior, and posterior joint capsule. These ligaments function to limit humeral range of motion while also providing increased stability to the joint.

1.1.3 Muscle

In order to initiate motion about the glenohumeral joint, active soft tissue, or muscle, is needed. Muscles also provide dynamic stability to the glenohumeral joint that the passive soft tissue structures are incapable of providing. Many different muscle groups are involved in shoulder motion (Figure 1-6), however, only those contributing most to the glenohumeral joint will be discussed.

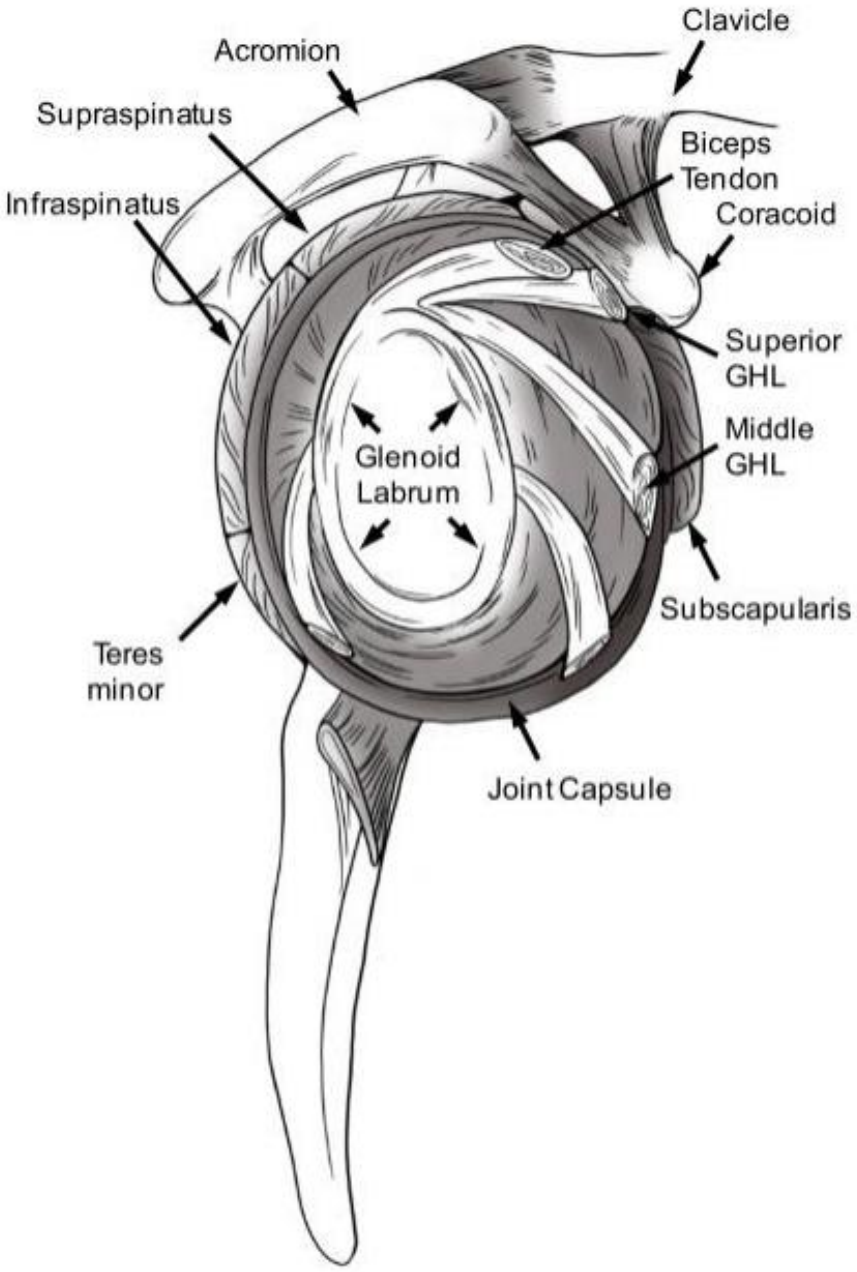

Figure 1-5: Lateral view of the glenohumeral joint with surrounding soft tissue.

This image illustrates the passive soft tissue anatomy surrounding the glenohumeral joint. The glenoid labrum is located around the periphery of the glenoid. The joint capsule envelopes the joint and is continuous with the superior, middle, and inferior glenohumeral ligaments, in addition to the biceps tendon.

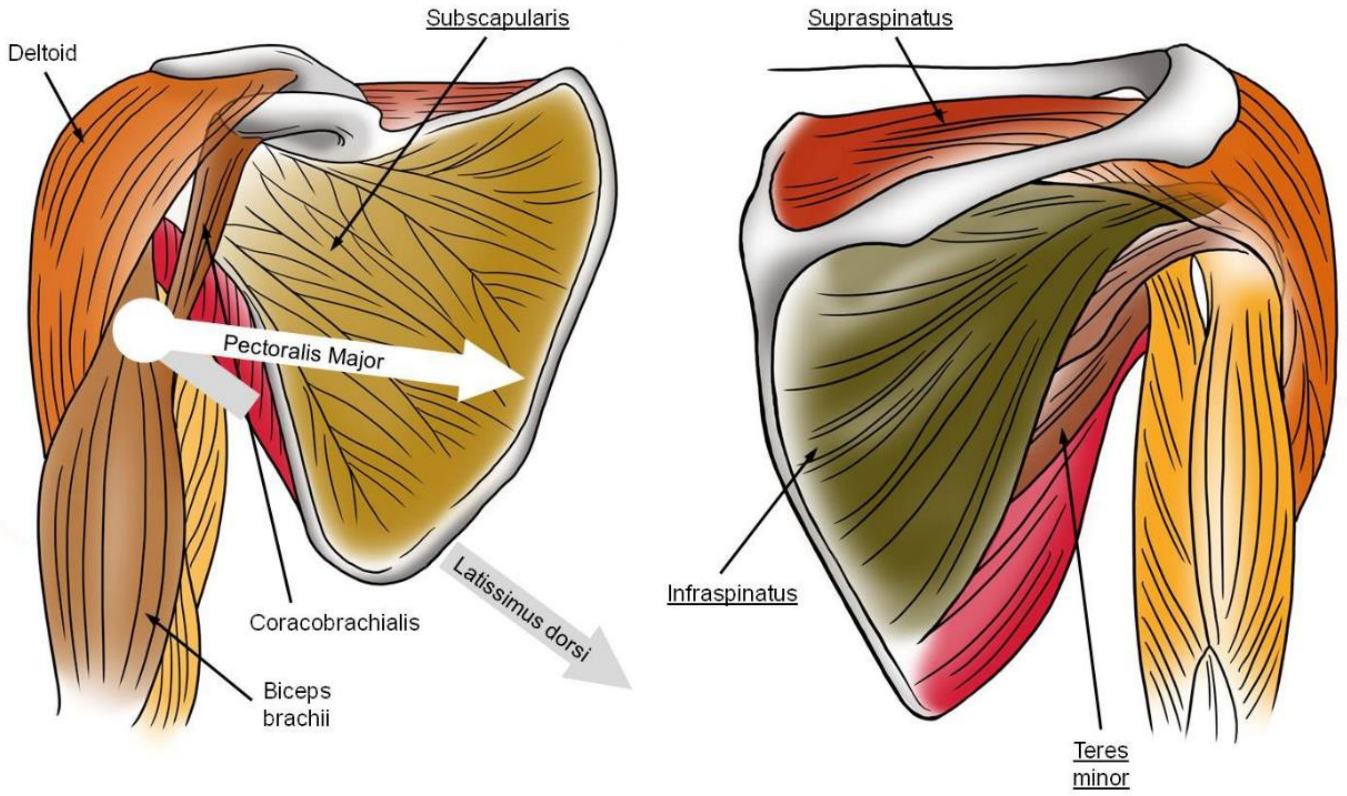

Figure 1-6:Anterior (*left*) and posterior (*right*) views of the shoulder with musculature.

The varying colours illustrates the different muscles surrounding the glenohumeral joint and their muscle paths. Arrows are provided to indicate the line of pull provided from the latissimus dorsi and pectoralis major muscles not shown.

1.1.3.1 Deltoid

The deltoid is a large, triangular-shaped muscle which consists of three distinct heads all sharing a common insertion at the deltoid tuberosity on the humerus. The anterior deltoid originates on the lateral one-third of the clavicle, the middle deltoid on the acromion, and the posterior deltoid on the spine of the scapula. As a whole, the deltoid functions primarily to abduct the arm. While the contribution of each head changes depending on the plane of elevation, the middle deltoid is believed to contribute to most to this movement. The anterior head of the deltoid, with assistance from the pectoralis major, contribute to forward elevation while the posterior deltoid, with assistance from the teres major and latissimus dorsi, contribute to extension of the arm.

1.1.3.2 The Rotator Cuff

The rotator cuff consists of a group of muscles that provide dynamic stability to the glenohumeral joint. This group of muscles consists of the subscapularis, supraspinatus, infraspinatus, and the teres minor. Individually, these muscles are not capable of producing force magnitudes such as those observed in the deltoid due to their smaller size and shorter moment arm lengths. However, the lines of action of these muscles together with their synergetic relationship provide significant dynamic stability to the glenohumeral joint.

The subscapularis originates from the subscapularis fossa on the scapula and inserts on the lesser tuberosity. The muscle wraps anteriorly around the humeral head, with bursal tissue protecting the muscle from the base of the coracoid. The primary function of the subscapularis is to internally rotate the humerus. The muscle also contributes to humeral head depression, while contributing to the prevention of anterior shoulder dislocation.

The supraspinatus originates from the supraspinatus fossa above the scapular spine. This muscle wraps superiorly over the humeral head to the superior facet of the greater tuberosity. The subacromial bursa protects the supraspinatus muscle body from gliding across the undersurface of the acromion.

The infraspinatus muscle originates from the infraspinatus fossa on the scapula and inserts onto the middle facet of the greater tuberosity. This muscle wraps over the posterosuperior

aspect of the humeral head, with bursal tissue protecting the muscle belly from the scapular spine. The infraspinatus externally rotates the humeral head while also providing support to the posterior side of the joint capsule to help prevent against posterior dislocation.

Lastly, the teres minor originates laterally to the infraspinatus muscle on the axillary boarder of the scapula. Its insertion is on the inferior facet of the greater tuberosity. Similar to the infraspinatus muscle, the teres minor's primary function is to externally rotate the humerus while also preventing against posterior dislocation.

1.1.4 Kinematics

The unique combination of osseous and soft tissue structures comprising the shoulder complex allow for a wide range of different motions to be achieved. The position of the humerus can be identified using different sequences of motion, often described according to the plane of elevation, elevation angle, and axial rotation (Figure 1-7). The plane of elevation is the plane in which the humerus is elevated in, with humeral motion described as abduction, flexion, or extension, depending on the angle of the elevation plane relative to the body. These motions describe the movement of the arm away from the body, while adduction described motion of the arm towards the body, also taking place within an elevation plane. The angle of elevation refers to the amount the arm is elevated within an elevation plane, while axial rotation refers to rotation of the humerus about its long axis. Axial rotation is often classified as either internal or external rotation.

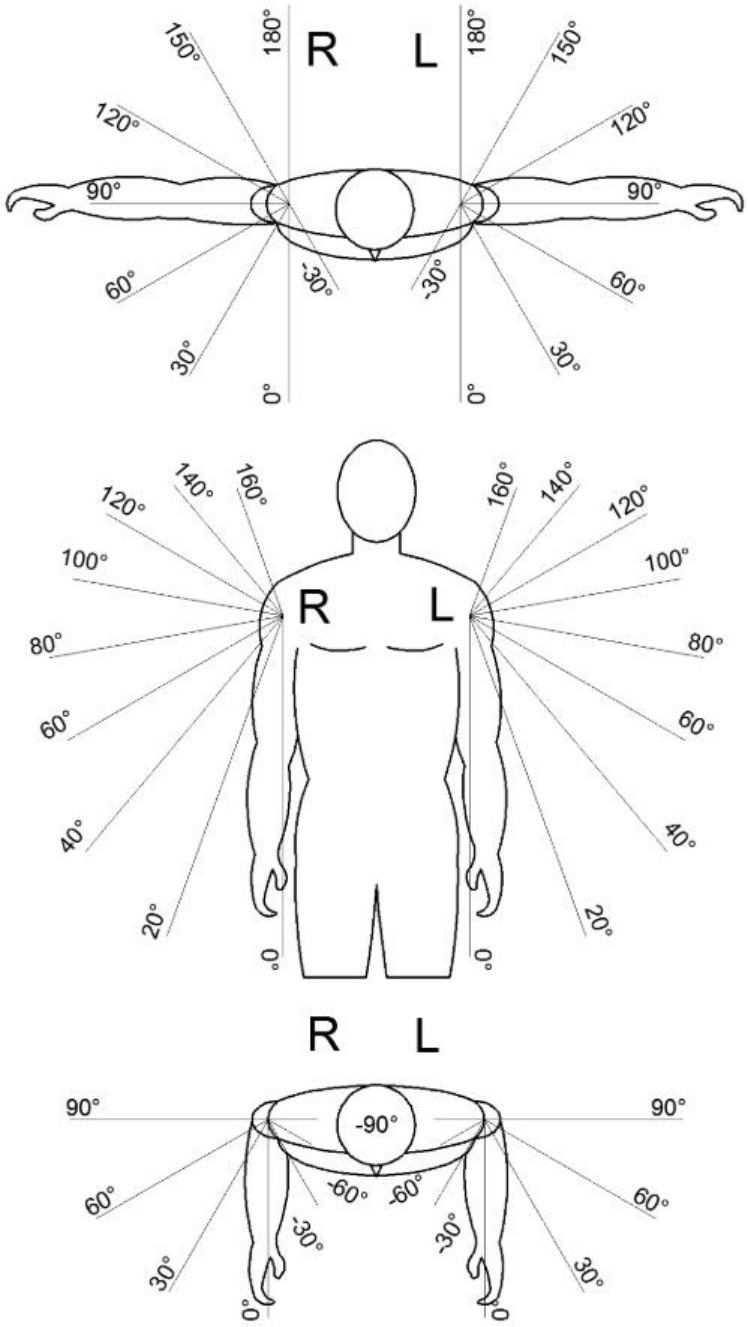

Figure 1-7: Diagram illustrating the different planes of motion.

The top image illustrates the different planes of arm elevation, with 90 degrees representing abduction in the frontal plane. The middle image shows different elevation angles while the last figure demonstrates different angles of internal and external humeral rotation.

The glenohumeral joint is not solely responsible for large variation in placement of the humerus relative to the thorax. During shoulder abduction, the scapula rotates with the humerus, in motion termed scapulohumeral rhythm (Figure 1-8). The coordination between these bones is what allows for such large upper extremity motion. Without this coordination, the greater tuberosity on the humerus would impinge against the acromion on the scapula, restricting movement of the humerus. Several studies have investigated the relative movement between the scapula and humerus during abduction to better understand the contribution each provides. It has previously been proposed that the scapula and humerus move in a constant ratio past 30 degrees of abduction, with variability in scapulothoracic contribution prior to this[97]. However, it is traditionally accepted that the relation between glenohumeral joint rotation and scapulothoracic joint rotation is 2:1 respectively.

1.2 Glenohumeral Joint Stability

As discussed previously, the glenohumeral joint has one of the largest ranges of motion in the human body. This is primarily due to the lack of constraint between the two bony articular surfaces. Unfortunately, the unconstrained nature of this joint makes it susceptible to instability and potential dislocation. To maintain stability throughout the entire range of motion, the glenohumeral joint depends on several anatomical structures surrounding the joint itself to provide stability throughout the entire range of motion. It is the synergistic relationship between these structures that maintain joint stability, preventing dislocation and allowing for such a large range of motion to be achieved. The following sections focus on the anatomical features of this joint that maintain and contribute to joint stability.

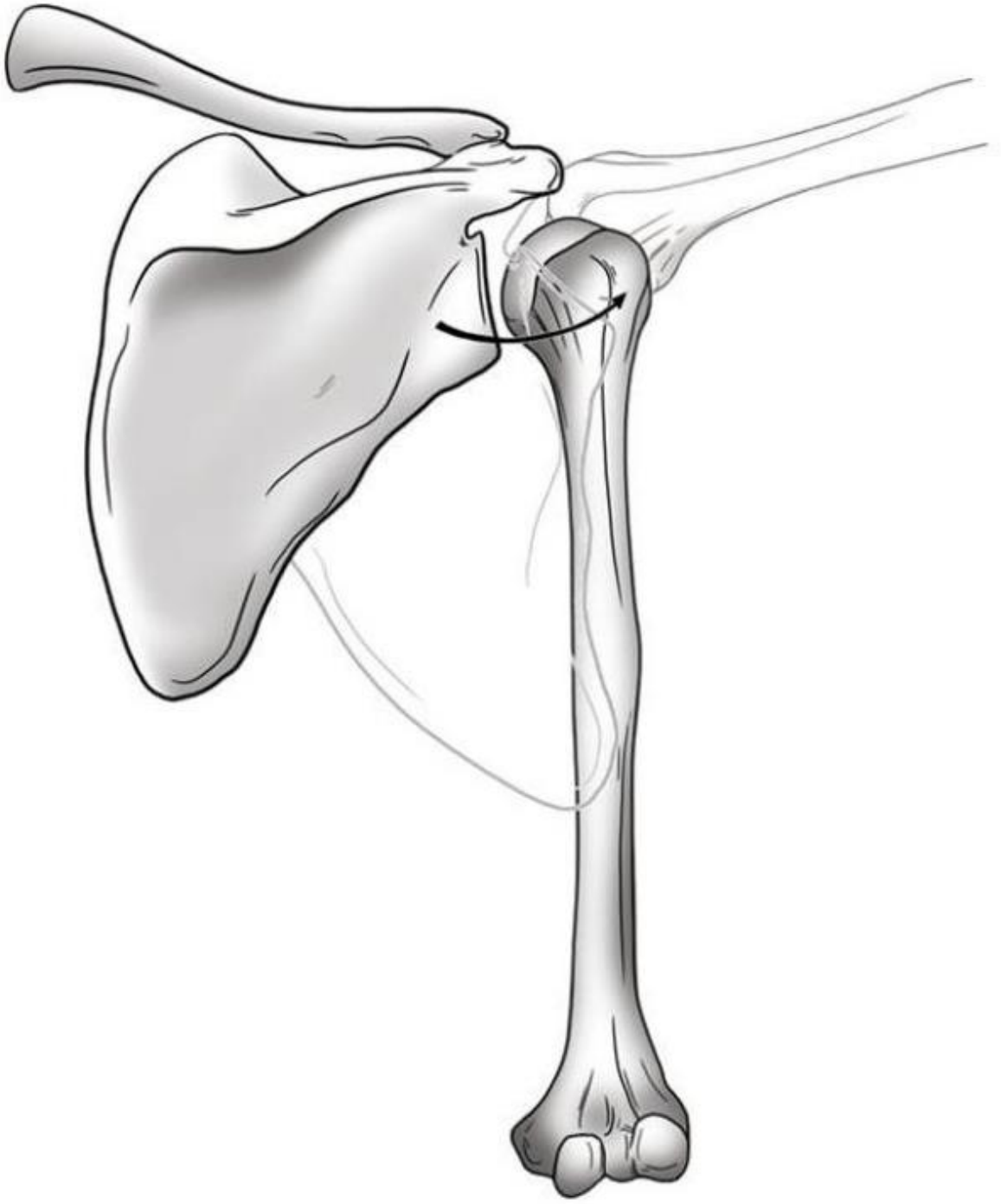

Figure 1-8: Scapulohumeral rhythm.

The scapula and humerus rotate together as the arm elevates.

1.2.1 Joint Surfaces

As noted earlier, the glenohumeral joint is comprised of the glenoid fossa on the scapula and the humeral head on the humerus. Although commonly referred to as a ball and socket joint, the glenohumeral joint is not fully constrained and allows for small amounts of translation to occur in addition to three rotations[130,132]. This small amount of translation is thought to be due to the difference in radius of curvature between the two surfaces, otherwise referred to as glenohumeral conformity. The subchondral bone of the glenoid itself is quite flat and exhibits a large radius of curvature relative to the humeral head[95]. However, the cartilage and labrum aid in increasing glenohumeral conformity, thereby increasing joint stability. Cartilage on the glenoid has previously been shown to be thicker at the periphery[95] and thinner near the center[224] of the glenoid, deepening the joint surface and decreasing its radius. The labrum, positioned at the periphery of the glenoid, has a similar affect and has been shown to increase the depth of the glenoid by 5mm in the anterior-posterior direction and by 9mm in the superior-inferior direction[94]. Although the articular cartilage and labrum increase the overall curvature of the glenoid side of the joint, 2-3mm of mismatch is commonly observed throughout the population[96].

1.2.2 Passive Soft Tissue

Several passive soft tissue structures are present within the shoulder that contribute to the stability of the glenohumeral joint. These structures include the labrum, joint capsule, and glenohumeral ligaments. The joint capsule and labrum completely envelope the glenohumeral joint from its anatomic surroundings, maintaining a pressure within the joint space known as intraarticular joint pressure. Some studies have found the intraarticular pressure to be negative relative to that of atmospheric, creating a vacuum-like environment within the joint[98,110]. At resting position, Kumar et al.[110] has shown that a puncture of the joint capsule, regardless of puncture location, resulted in inferior subluxation of the humerus. Another biomechanical study found that venting of the joint resulted in greater translation of the humeral head in both AP and SI directions relative to the intact capsule test state under static translational loading[3]. It has also been shown that the labrum helps to maintain this intraarticular pressure by creating a suction cup effect within the joint[68].

The joint capsule, glenohumeral ligaments (superior, middle, and inferior), and the coracohumeral ligament comprise the capsuloligamentous complex[226]. These structures combined are often lax within the mid-range of motion[68], but tighten and provide critical support at the end-range in order to maximize joint contact and prevent excessive humeral head translation[226]. The superior glenohumeral ligament becomes taught when the arm is externally rotated in adduction. The middle glenohumeral ligament helps to maintain joint stability in mid-range abduction and external rotation, preventing anterior humeral head subluxation[75,112]. The inferior glenohumeral joint capsule consists of an anterior and posterior band. The anterior band together with the anterior joint capsule prevent anterior dislocation in abduction and external rotation, while the posterior band prevents posterior dislocation in flexion and internal rotation. The superior capsule has also been shown to provide stability to this joint, as a tear in this structure leads to increased humeral head translation[99]. The coracohumeral ligament consists of the anterior and posterior bands. Both originate on the lateral aspect of the base of the coracoid, passing between the subscapularis and supraspinatus muscles. The anterior band inserts closer to the lesser tuberosity while the posterior band inserts closer to the greater tuberosity. While both bands of the coracohumeral ligament help prevent inferior subluxation in the adduction position, the anterior and posterior bands prevent against excessive external and internal rotation respectively[109].

Additional soft tissue structures that help to maintain glenohumeral joint stability include the coracoacromial arch and the long head of the biceps tendon. The coracoacromial arch consists of the acromion, coracoid, and the coracoacromial ligament connecting the anterior acromion and coracoid. This arch prevents anterosuperior escape, as it is located anteriorly and superiorly relative to the glenohumeral joint. However, this structure only prevents excessive anterosuperior humeral head translation in the presence of rotator cuff pathology[109]. The role of the long head of the biceps tendon in glenohumeral stability has been controversial, with disagreement arising as to whether it provides passive or dynamic stability. Studies have confirmed that it does provide passive stability to the glenohumeral joint[101,176,180], with Garg et al.[67] suggesting the effect this tendon has on glenohumeral stability is position-dependent, due to the tendon's anatomical structure. Rauch et al.[176] recently found that tensioning of this tendon reduced posterior and superior translation of

the humerus in forward flexion. Other cadaveric studies have found the long head of the biceps tendon to reduce anterior-posterior translation of the humeral head[3,101]. Rodosky et al.[180] showed greater anterior stability with the long head of the biceps tendon tensioned in the overhead (abducted and externally rotated) arm position, an arm position susceptible to anterior dislocation. McGarry et al.[134] also showed reduced range of motion and less superior humeral head translation in their cadaveric model with the long head of the biceps tendon tensioned. In-vivo studies have used electromyography to quantify muscle activation when investigating the stabilizing effect provided by the long head of the biceps tendon. Chalmers et al.[36] found increased electromyography readings in this tendon throughout motion with the forearm and elbow immobilized, suggesting this structure provides active stabilization to the glenohumeral joint. However, the results from Levy et al.[115] contradicted this as no electrical activity was recorded in the tendon throughout motion with the elbow immobilized in extension. Other in-vivo studies have used alternative measures to evaluate the contribution to joint stability provided by this tendon. Warner et al.[225] observed greater superior humeral head translation in patients with isolated loss of the proximal tendon attachment compared to the contralateral shoulder, suggesting the tendon serves as a humeral head depressor. Giphart et al.[76] however found that relocation of the proximal attachment of this tendon distally had no significant effect on superior translation of the humeral head relative to the contralateral shoulder.

1.2.3 Muscle

While the osseous and passive soft tissue anatomy discussed above serve to stabilize the glenohumeral joint, independently these structures are insufficient in providing joint stability throughout full range of motion. The primary stabilizers of the glenohumeral joint are the active soft tissues, or muscles, surrounding this joint. The muscles surrounding the glenohumeral joint provide stability through several mechanisms, such as passive muscle tensioning and indirectly tensioning passive soft tissue structures[112]. However, primary glenohumeral stability is provided by the rotator cuff muscle group and middle deltoid through concavity compression, originally investigated and proposed by Lippitt et al[119]. This study measured the degree in which compression of the humeral head into the glenoid through muscle activation stabilized the joint against shear translational forces. The results

found concavity compression to be integral for providing joint stability in the mid-range of glenohumeral motion. The authors also showed that concavity compression was further enhanced with an intact labrum. Wueler et al.[230] supported these results, further suggesting that concavity compression of the humeral head into the glenoid cavity is the primary stabilization method through the mid-range of glenohumeral motion. Lee et al.[114] illustrated that concavity compression plays a vital role in end-range glenohumeral stability as well as throughout the mid-range.

To further understand how the rotator cuff and other surrounding musculature contribute to concavity compression, the force direction of each muscle and its contribution to the different glenohumeral force couples must be considered. A force couple consists of two or more forces that act in different directions to create opposite moments about a central point. However, in equilibrium, the force magnitudes and orientations result in the moments about a common point that cancel each other out. Two integral force couples that exist about the glenohumeral joint include the transverse force couple and the coronal force couple (Figure 1-9), each named based on the anatomical plane these forces act within[26,97]. The transverse force couple primarily consists of the transverse force components produced by the subscapularis, infraspinatus, and teres minor muscles. The component from the subscapularis muscle wraps anteriorly about the joint center, while the components from the infraspinatus and teres minor pass around the joint center posteriorly. Synchronization between the two muscle groups is needed in order to provide sufficient anterior-posterior glenohumeral stability, in addition to providing axial rotation stability throughout motion. In addition, all force components in the transverse force couple contribute to concavity compression of the glenohumeral joint. Therefore, these forces also must be sufficient to provide adequate compressive force of the humeral head against the glenoid to stabilize the glenohumeral joint throughout mid-range motion.

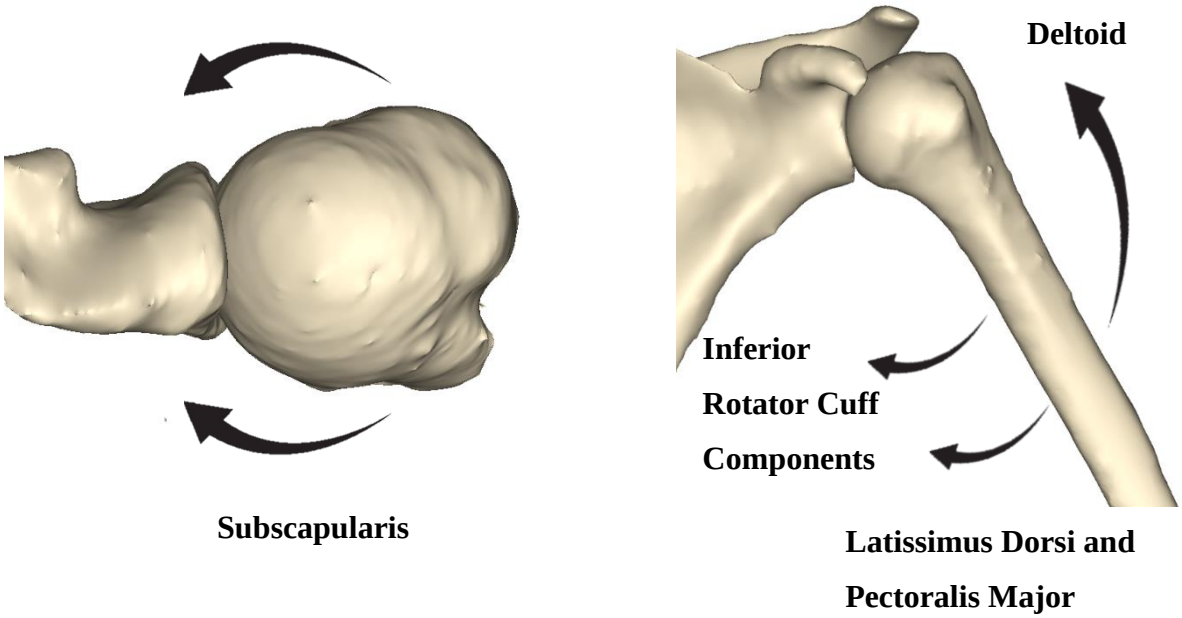

Figure 1-9: Glenohumeral force couples.

The transverse glenohumeral force couple consisting of the posterior and anterior rotator cuff muscles indicated on the left. The right image illustrates the coronal force couple, comprising the deltoid, inferior rotator cuff components, latissimus dorsi, and pectoralis major.

The coronal force couple is the second force couple that exists about the glenohumeral joint. In this mechanism, the coronal force components from the deltoid and supraspinatus act superiorly about the glenohumeral joint, while the coronal force components of the infraspinatus, subscapularis, and teres minor act inferiorly about the joint center. However, the deltoid is a powerful muscle relative to the individual rotator cuff muscles, capable of generating forces up to six times the weight of the arm [112]. Because of this, it has been previously suggested that the latissimus dorsi and pectoralis major muscles also contribute inferiorly to this coronal force couple. Although these two muscles differ in origin, they share a similar insertion site distally on the bicipital groove of the humerus and aid in adduction and internal rotation of the humerus. Previous biomechanical studies have found evidence that the latissimus dorsi and pectoralis major provide resistance to the superior pull of the deltoid[1,30]. Together they synergistically function with the rotator cuff and deltoid to maintain superior-inferior glenohumeral stability throughout motion. This is especially true near the beginning range, or initiation of abduction, as the deltoid muscle line of action is directed superiorly. This results in a significant shear force being applied to the humeral head in the superior direction, and requires the activation of the inferior cuff muscles, latissimus dorsi, and pectoralis major to provide inferior stabilizing forces. However, as the arm abducts, the deltoid muscle line of action shifts medially, contributing to concavity compression and providing additionally stability to the joint.

While the muscles surrounding the glenohumeral joint contribute to these force couples and joint stability, it is important to understand these muscle forces change throughout motion. Constant activation of these muscles would result in unbalanced force couples, leading to glenohumeral instability and possible dislocation. These muscles work synergistically to control arm motion while maintaining joint stability throughout the mid-range of glenohumeral motion[4]. For example, the supraspinatus is considered the dominant muscle during the initiation of abduction. As mentioned previously, the deltoid muscle's line of action around zero degrees of abduction acts relatively superiorly, producing more of a superior shear force then contribution to abduction. The supraspinatus however has a much more significant medial line of action and can more easily generate abduction without as significant a shear force being created. Studies have suggested that the supraspinatus muscle is more dominant in the first 30 degrees of abduction, with the deltoid

becoming more dominant past 30 degrees of abduction[4,165]. The synergistic relationship between these two muscles helps to initiate abduction in a controlled manner while maintaining joint stability. Furthermore, it has been shown that the subscapularis is additionally responsible for joint stability at the initiation of abduction, with little contribution from the posterior cuff muscles[215]. The inferior and medialized pull from the subscapularis paired with the superiorly applied force from the deltoid help to create an abduction moment about the glenohumeral joint, assisting the subscapularis in initiating abduction. The synergistic relationship between the deltoid and rotator cuff muscles also continues at mid-range and end of range glenohumeral motion. At mid-range, the deltoid becomes the primary muscle controlling abduction, as its force line of action changes to act more medially resulting in greater concavity compression. The subscapularis continues to provide critical anterior stability throughout abduction[215]. As the arm approaches the end range of motion, the subscapularis becomes less dominant compared to the infraspinatus[185], due to the external rotation required to reach the end range of abduction.

The synergistic relationship between the anatomical structures surrounding the glenohumeral joint is crucial in maintaining joint stability throughout total range of motion. Although the muscles surrounding the glenohumeral joint are considered primary stabilizers, passive soft tissue and osseous anatomy also work in conjunction with these muscles to further stabilize the joint. However, injury or soft tissue pathology to any of these structures can severely compromise the stability of the glenohumeral joint.

1.3 Rotator Cuff Tears

As discussed in the previous sections, the rotator cuff consists of a group of muscles that function to move the arm while providing critical stability to the glenohumeral joint. However, the constant usage of these muscles makes them susceptible to injury. Rotator cuff tears (RCTs) occur when a tear exists in the tendon connecting the rotator cuff muscle to the humerus (Figure 1-10). These tears can often lead to considerable pain and disability[209]. Several studies have previously reported on the prevalence of RCTs. Teunis et al.[213] found that prevalence of rotator cuff disease ranges from around 10% in patients of age 20 and up to 62% in patients 80 years of age and older. Yamamoto et al.[233] reported a rotator cuff tear incidence rate of 20.7% across the general population in a study analyzing

1366 shoulders. The prevalence of RCTs has been reported to increase with age, with Milogrom et al.[147] reporting incidence rates of 50% for those in their 70's, and 80% for those above 80 years of age. It is important to note however that RCTs are not all the same. These tears can vary in size and location, which can affect the symptoms a patient may possibly experience. The repair of the rotator cuff after a tear is a commonly performed procedure. However, in some patients, the cuff cannot be repaired and alternative treatment options need to be considered. The following sub-sections will describe the different types of RCTs that have previously been observed in literature and will discuss causes and symptoms related to these tears.

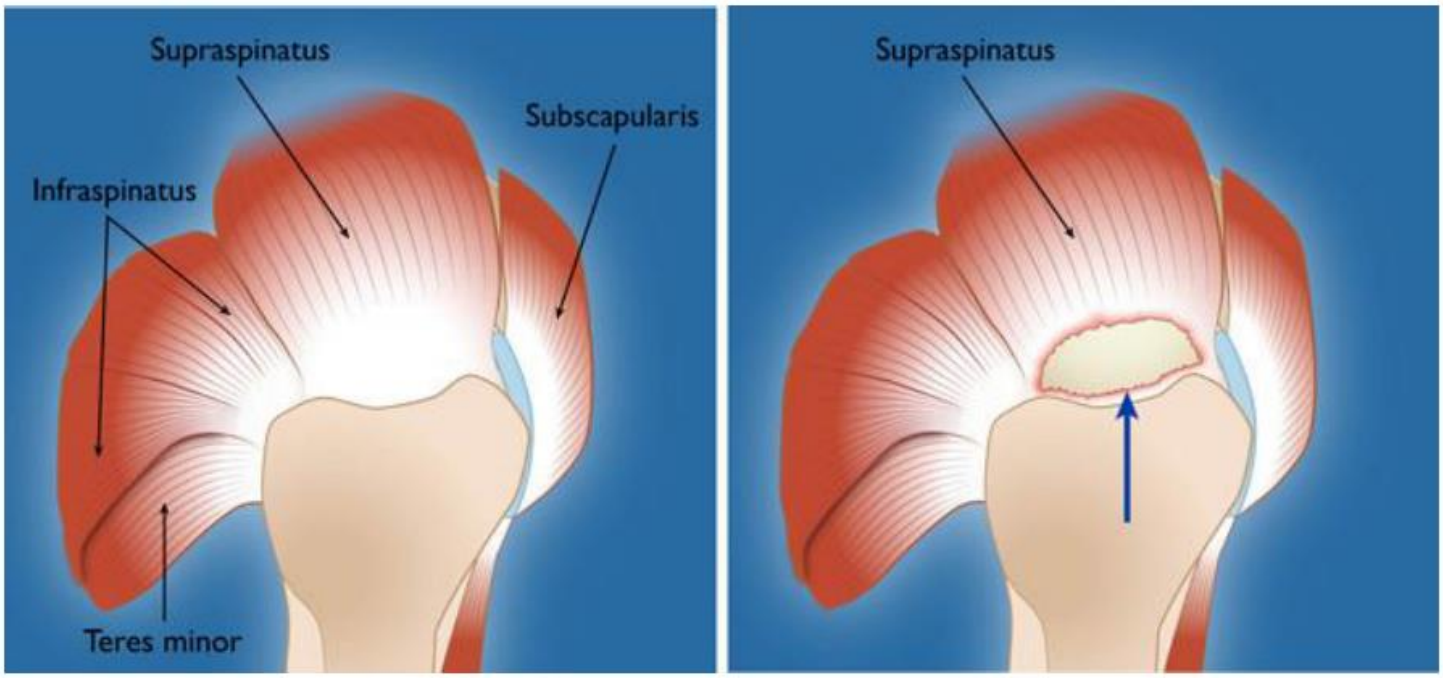

Figure 1-10: Healthy and torn rotator cuff muscles.

Left figure illustrates an intact rotator cuff, while the right image demonstrates a tear at the insertional footprint of the supraspinatus tendon indicated by the blue arrow[8].

1.3.1 Rotator Cuff Tear Types and Classifications

Numerous classifications have been developed in order to standardize the assessment of RCTs and to aid surgeons in the decision-making process as to which operative technique should be used to help treat the patient. Although there is no single classification system that has been widely accepted to cover all aspects of a rotator cuff tear, several have been widely accepted to classify specific features of a tear. Such features include aetiology, size, and location. In reference to aetiology, RCTs are commonly classified into two categories: traumatic and degenerative. Traumatic RCTs are caused by a traumatic episode which serves as a direct cause for this injury. Degenerative cuff tears are chronic and are not linked with one specific cause. Instead, it is believed that a multitude of different factors contribute to the creation and progression of these tear types.

RCTs have also been classified according to their size and location, often being defined as either a partial thickness tear or a full thickness tear. A partial thickness tear is one in which only part of the tendon is torn, meaning that the tear has not extended entirely through the thickness of the tendon. Ellman[38] proposed a classification system to differentiate partial RCTs according to their depth and size. In this classification, letter grades of A, B, and C designated the location of the tear as either articular sided, bursal sided, or interstitial. Numerical grades were used to describe the depth of the tear, with Grade 1 representing a tear less then 3mm in depth, Grade 2 representing a tear between 3-6mm in depth, and Grade 3 representing a tear greater then 6mm in depth. Synder[208] shortly after proposed their own similar classification system for partial RCTs. This system was similar to that from Ellman in that it used letter and numerical grades. However, the letter grades of A, B, and C were used to classify the location of the tear, with A indicating the articular side, B indicating the bursal side, and C indicating a complete tear. Numerical grades were used to define the severity of the tear. Grade 0 was used to indicate a normal cuff while Grade 1 identified less then 1cm of superficial bursal or synovial irritation or slight capsule fraying. Grade 2 was defined as less then 2cm of tear size with capsule fraying and synovial, bursal, or capsule injury. Grade 3 was defined as a tear of less than 3cm with more severe damage to the tendon and Grade 4 was classified as a severe tear with a sizeable flap tear, encompassing more than one tendon. Lastly, Habermeyer et al.[85]

proposed a partial rotator cuff tear classification to quantify articular sided supraspinatus tendon tears. Letter grades were used to classify sagittal tear extension while numerical grades were used to classify coronal plane tear extension.

Similar to partial RCTs, several groups have attempted to define classifications for describing full thickness RCTs. Full thickness RCTs occur when the tendon is completely torn through its full thickness. Cofield[40] and DeOrio et al.[52] developed a classification system that grouped different sized full thickness tears into four categories: small, medium, large, massive. Small tears were characterized by small fissuring and a tear size of less than 1cm in diameter, while medium tears were defined as a tear size of less than 3cm in the longest diameter. Large tears were defined as less then 5cm in diameter and massive tears were classified as greater then 5cm in tear diameter. The classification system developed by Synder[208] also specified full thickness tears according to severity. Grade 1 was used to specific small complete tears such as puncture wounds. Grade 2 described a small tear of less than 2cm while large tears were described as 3-4cm in size and minimal retraction of the torn edge. A massive tear was described to involve two or more retracted rotator cuff tendons, with scaring on the remaining tendon. This definition for massive RCTs was very similar to that originally proposed by Gerber et al.[70], defining massive as involving the detachment of two or more entire tendons. Another common classification describing the severity of RCTs includes the Patte classification. Patte[168] classified RCTs into four groups. The first group included partial and full thickness RCTs less then 1cm in size. Group 2 included full substance tears of the supraspinatus tendon and group 3 included full substance tears involving more than one tendon. Group 4 was added to include massive tears characterized by secondary osteoarthritis of the glenohumeral joint. Harryman et al.[89] also created a classification system which considered the number of tendons involved in the tear. In this classification, an intact rotator cuff was defined as Type 0, while partial thickness and full thickness tears of the supraspinatus were classified as Type 1A and 1B respectively. Type 2 classification was designated as a full thickness tear involving both the supraspinatus and infraspinatus tendons. Type 3 was defined as a full thickness tear in the supraspinatus, infraspinatus, and subscapularis. Other groups have additionally classified tears according to their three-dimensional shape. A study from Ellman et al.[62] defined full thickness cuff tears according to the following shapes: crescent, triangular

defect (grouped as either reverse L or L-shaped), trapezoidal, or massive. Furthermore, Davidson et al.[50] defined full thickness RCTs as either crescent, longitudinal (either 'L' or 'U' shaped), or massively contracted, while also recommending surgical procedures to treat each type.

Massive RCTs are of particular interest to many clinicians as these tears can lead to increased pain and disfunction. Massive tears can also be more difficult to repair and can exhibit increased retear rates after surgery[55]. It has been reported that massive RCTs can comprise as many as 40% of all RCTs[13]. While several different classifications exist for defining massive RCTs, these tears are commonly classified according to a tear greater then 5cm in diameter involving two or more rotator cuff tendons[40,52,70]. A study from Collin et al.[41] investigated the patterns of massive RCTs, categorizing five different combinations. The authors found the pattern with the highest frequency to be massive tears involving the supraspinatus and infraspinatus tendons. This type of massive tear is often referred to as a posterosuperior rotator cuff tear due to the tear location relative to the humeral anatomy. Going forward in this thesis, posterosuperior RCTs will be the primary focus.

1.3.2 Rotator Cuff Tear Aetiology and Risk Factors

The cause of RCTs depends on whether the tear is traumatic or degenerative. Traumatic tears are caused by a traumatic event which directly results in tear of the rotator cuff tendon. Degenerative RCTs are a result of gradual weakening of the tendon over time and are not linked to one specific cause. Instead, several potential factors are believed to contribute to the cause and progression of the tear. These different factors are commonly grouped into two categories: intrinsic and extrinsic.

Intrinsic factors are factors contributing to the degenerative changes of the rotator cuff tendon that occur within the tendon itself. One of the most common intrinsic theories for rotator cuff degeneration is the degenerative-microtrauma model[123,158,166]. This theory combines the degenerative effect that aging has on the tendon with the inability for the tendon to heal after repetitive microtraumas. More specifically, the microtrauma part of this theory suggests that repetitive loading of this tendon causes micro injuries to occur within the tendon. These micro injuries are not provided sufficient time to heal and also

results in the surrounding fibers to undergo increased loading[123]. This in combination with age related degenerative effects cause these tears to progressive and increase over time. It has also been suggested that the degenerative-microtrauma theory leads to inflammatory response and oxidative stress to occur within the tendon, leading to further degeneration[158].

Unlike intrinsic factors, extrinsic factors are those that occur externally to the rotator cuff tendon. This was first observed by Neer et al.[154] who reported impingement to occur between the supraspinatus and the anterior third of the acromion. Neer[157] also reported impingement to additionally occur with the coracoacromial ligament in the forward flexion position. These studies suggested that impingement between the humeral head and the anterior acromion, and between humeral head and coracoacromial ligament, significantly contribute to the formation of RCTs. There have been numerus studies since that have investigated the correlation between RCTs and acromial morphology. Bigliani et al.[17] were one of the first to study the morphology of the acromion and its relationship with RCTs. The authors from this study classified the shape of the acromion into three types: Type 1 (flat), Type 2 (curved), and Type 3 (hooked). Additionally, they found that cadavers exhibiting full thickness RCTs were associated with Type 3 acromia (69.8%), followed by Type 2 and Type 1 (24.2% and 3% respectively). Since the results from this study were published, other groups have investigated as to whether a correlation between acromion morphology and RCTs exist. A number of studies have reported results in agreement with Bigliani et al.[17], suggesting Type 3 acromion shape to be associated with RCTs[7,12,148]. However, other studies have found evidence against this[6,11]. Other extrinsic factors have also been correlated with RCTs. Nyffeler et al.[160] developed the “acromial index”, which quantifies the lateral extension of the acromion. The authors found an association to exist between larger acromial index values and RCTs, suggesting that acromia with larger acromial index values change the deltoid line of action which causes increased rotator cuff forces. Other studies have provided evidence to support the association between increased acromial index and RCTs[7,11], while evidence has also been provided against this[88]. Acromial bone spurs[88,161] and laterally sloped acromia[11] have also been correlated with RCTs. The critical shoulder angle, a metric describing the angle between the plane of the glenoid and the lateral most boarder of the acromion[193], has also been associated with RCTs[7,193]. Additionally, Cunningham et al.[48] proposed that greater tuberosity morphology

is associated with RCTs. Their study developed a measurement called the greater tuberosity angle, quantifying the position of the greater tuberosity relative to the humeral head, was implicated in RCTs. Non-anatomical factors have also been investigated for their relationship to RCTs. Such factors include age, mechanical overuse (in dominant shoulder), tobacco use, and diabetes mellitus[123,158], although some of these factors are linked with intrinsic factors.

1.3.3 Rotator Cuff Tear Symptoms

1.3.3.1 Humeral Head Translation

One of the primary symptoms a patient with a posterosuperior rotator cuff tear may experience is instability of the humeral head, resulting in superior translation, or migration, of the head (Figure 1-11). Cadaveric-based biomechanical studies have investigated the effects of RCTs on the stability of the humeral head. Also, some have investigated the effects of tear progression on the effect of joint stability using static shoulder simulators[100,153,162,182]. Stability in these studies was quantified as the difference in superior-inferior humeral head translation between the cuff deficient testing states and the intact testing state. The intact testing state replicated a healthy glenohumeral joint in which the capsule was intact, and all rotator cuff muscles were completely attached to the humeral head. Loads were applied to the different rotator cuff and deltoid muscles using electromyography (EMG) derived data in an attempt to mimic physiological conditions, while humeral head position relative to the glenoid was quantified at various positions of abduction in the scapular plane. Although the rotator cuff tear progression tested in each study differed slightly, these studies yielded similar results. Rybalko et al.[182] studied incomplete and complete supraspinatus tears, where 50% of the supraspinatus tendon was removed in the incomplete test state and 100% of the supraspinatus tendon was removed in the complete tear testing state. The authors found a significant difference in superior humeral head translation between the complete tear and intact testing states. Itami et al.[100] also tested two cuff deficient states, where the entire footprint of the supraspinatus tendon was removed in the first cuff deficient test state, followed by the removal of the anterior half of the infraspinatus tendon footprint in the second cuff deficient test state. Significant differences were found to occur in superior humeral head translation between both cuff

deficient states and the intact testing state. Mura et al.[153] and Oh et al.[162] conducted more detailed studies by comparing multiple stages of cuff tear progression. Each study found increased superior humeral translation to occur with greater rotator cuff tear progression. Superior translation of the humeral head in the presence of cuff tears have also been shown to occur in several other studies as a secondary outcome variable[14,143–146,178,183,199,200]. Another study by Berthold et al.[15] also investigated the effects of different rotator cuff tear combinations on superior translation of the humeral head. However, this study unlike the previous studies discussed, only retracted the tendon from the humeral head in the final test state, representing an irreparable rotator cuff tear. The other cuff tear progressions tested were non-retracted and non-activated, allowing the muscle to act as a passive barrier. Additionally, testing was performed using a dynamic simulator rather than a static shoulder simulator. The results illustrated that significant superior humeral migration occurred in the final retracted test state representing an irreparable posterosuperior rotator cuff tear. This suggested that the presence of the muscle-tendon units, although not active, still provide some resistance to excessive humeral head translation.

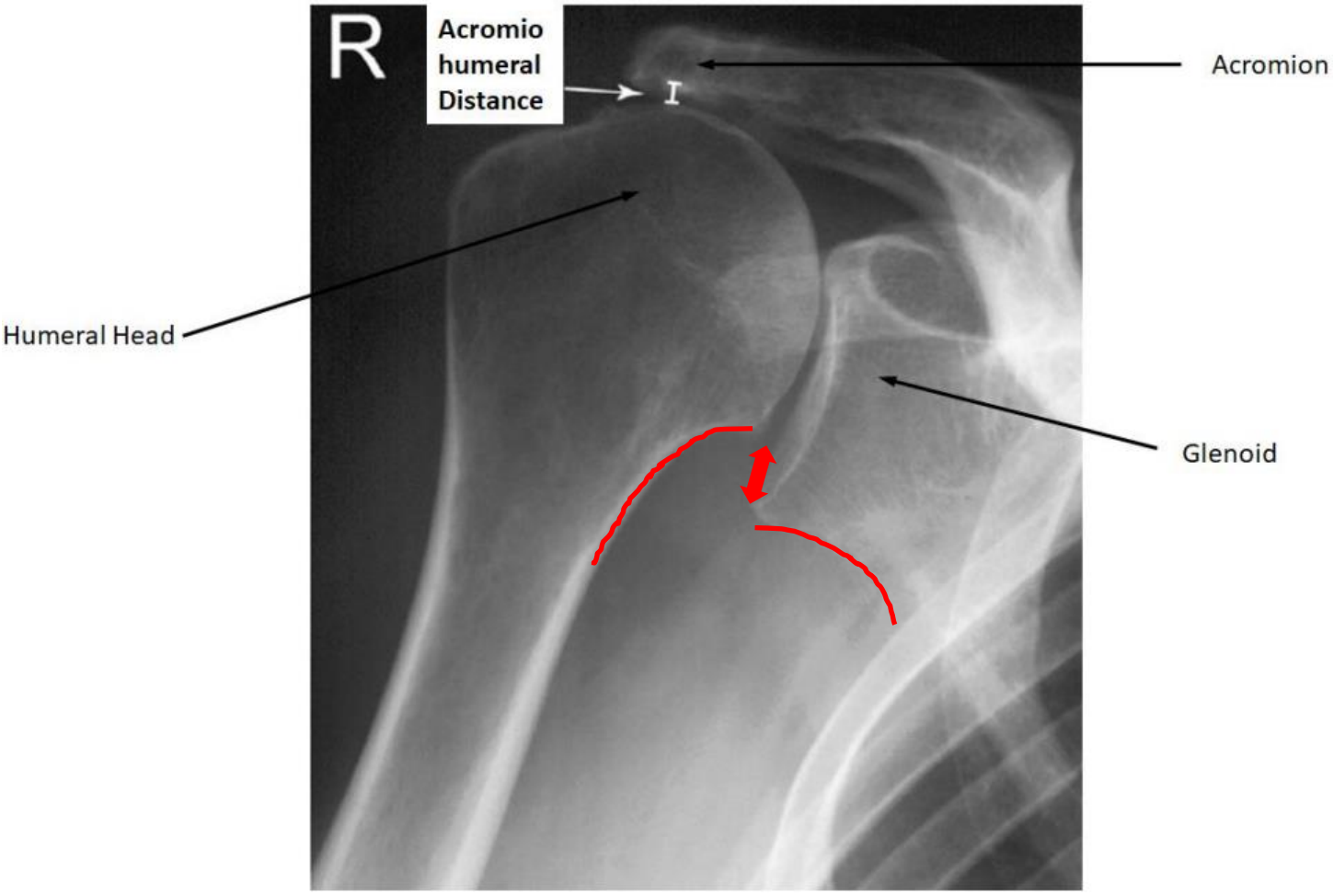

Figure 1-11: Radiograph illustrating superior humeral head migration.

Anterior radiograph illustrating decreased acromiohumeral distance and superior translation of the humeral head, as indicated by the disruption in Moloney's line shown with the red lines (adapted from Singh[198]).

Other aspects of humeral head translation in the presence of RCTs have also been studied biomechanically. Itami et al.[100] found increased superior translation in rotator cuff tear models to still occur with the humerus externally rotated in 30 degree increments up to 90 degrees of external rotation. Studies have also found the magnitude of superior humeral head translation in the presence of a rotator cuff tear to decrease at higher angles of abduction[100,178,200,199,211]. Singh et al.[200] postulated that the decrease in superior translation of the humeral head at higher angles of abduction is due to the changing deltoid muscle line of action. At higher angles of abduction, the line of action acts more medially, contributing more to concavity compression as opposed to superior shear force as seen in lower angles of abduction. Anterior-posterior translation of the humeral head has also been observed in rotator cuff tear models, with studies reporting increased posterior translation of the humeral head in the presence of RCTs[162,178,200,207]. Itami et al.[100] found increased posterior translation to occur with increased severity of RCTs at various angles of glenohumeral abduction and humeral external rotation. Oh et al.[162] reported increased posterior translation with increased rotator cuff tear progression at 30 degrees of abduction for several angles of humeral internal and external rotation, except at maximum internal rotation. Reeves et al.[178] also reported on anterior-posterior translation of the humeral head in the presence of a posterosuperior irreparable cuff tear. Their results demonstrated increased posterior humeral head translation relative to the intact testing condition. However, posterior translation was most prominent at lower angles of abduction and decreased at higher angles of glenohumeral abduction.

Humeral head translation in the presence of a rotator cuff tear has also been studied clinically. Several clinical studies have found a correlation to exist between rotator cuff tear size and narrowing of the acromiohumeral distance[78,188,201], a radiographic measure that is representative of superior humeral head translation. Tempelaere et al.[210] also investigated humeral translation using dynamic magnetic resonance imaging (MRI), allowing the range of humeral head translation to be captured throughout abduction motion. The authors reported that patients with massive cuff tears showed the greatest range of both superior-inferior and anterior-posterior humeral head translation relative to the other cuff deficient and healthy test groups. However, patient range of motion was inhibited by the scanning environment, preventing patients from completing full range of abduction

motion. Another study from Keener et al.[108] evaluated superior humeral translation radiographically in both symptomatic and asymptomatic patients with RCTs. Their findings indicated that greater superior translation occurred in patients with symptomatic RCTs. Additionally, greater translation was observed in patients with tears involving the infraspinatus muscle in addition to the supraspinatus in both symptomatic and asymptomatic test groups.

1.3.3.2 Mechanical Efficiency

RCTs have also been shown to decrease the mechanical efficiency of the glenohumeral joint. The mechanical efficiency is a general term used to describe the effort needed to abduct the arm. This can be quantified using a variety of different parameters depending on the type of study being performed. The cause of reduced mechanical efficiency of the glenohumeral joint in the setting of a rotator cuff tear is believed to be caused by reduced function or loss of the rotator cuff muscle, and a reduction in the deltoid moment arm. Reduced or complete loss of function in the supraspinatus muscle affects the mechanical efficiency as the supraspinatus contributes to abduction throughout full range of motion, especially in the early range of motion. Furthermore, the increased superior humeral head migration discussed in the previous subsection reduces the moment arm of the deltoid, thus causing the force of the deltoid to increase.

Dynra et al.[56] quantified mechanical efficiency as total deltoid force and maximum glenohumeral abduction observed throughout a programmed abduction motion. Total deltoid force was measured using loadcells connected to actuators used to apply direct loading to the different muscle tendons, while glenohumeral abduction was recorded using a motion tracking system. These variables were assessed for different rotator cuff tear progressions. Both supraspinatus tears and posterosuperior RCTs increased the total deltoid force and decreased maximum glenohumeral abduction compared to the native testing state. These results indicated that superior and posterosuperior RCTs decreased the mechanical efficiency of the glenohumeral joint and required greater forces to be generated from the deltoid in order to compensate. Studies from Berthold et al.[14,15] also used deltoid force and glenohumeral abduction range to quantify mechanical efficiency of the glenohumeral joint in different rotator cuff tear progressions. Similar findings were

reported to that from Dynra et al.[56], where the creation of an irreparable posterosuperior rotator cuff tear significantly decreased glenohumeral abduction and increased deltoid force.

Another method used to quantify the mechanical efficiency of the glenohumeral joint includes the use of a loadcell to measure the force of abduction. Several studies have utilized this method to quantify mechanical efficiency, however, the outcome variable name for the force measurement and the setup of the loadcell with respect to the humerus has varied. Studies from Mura et al.[153] and Rybalko et al.[183,182] have used a loadcell connecting the diaphysis of the humerus to a rigid support in order to measure the force generated about the center rotation of the glenohumeral joint. The force from the loadcell was referred to as the "*abduction torque"* and *"deltoid abduction force"*. Mura et al.[153] found the abduction force to decrease with increasing cuff tear progression, with the lowest abduction torque recorded in the setting of an irreparable posterosuperior rotator cuff tear. These results suggested that reduction in infraspinatus function also contributes to the reduction in mechanical efficiency. Rybalko et al.[181,182] found similar results, with complete supraspinatus tears[182] and massive irreparable posterosuperior cuff tears[183] resulting in significantly reduced deltoid abduction force compared to the intact test state. It was also reported that in all test states, the deltoid abduction force increased with glenohumeral abduction angle. Studies from Halder et al.[86] and Singh et al.[199] employed multiple degrees of freedom load cells to assess the mechanical efficiency of the glenohumeral joint. Each of these studies positioned the loadcell in the path of the humerus and measured the force generated by the distal humerus against the loadcell. Halder et al.[86] conducted testing in zero degrees of abduction as the authors believed the effect of a supraspinatus deficiency would be most observable at lower angles of abduction where this muscle contributes the most to abduction. The authors found retraction of any part of the supraspinatus tendon reduced the force recorded in the loadcell relative to the intact test state, indicating a decrease mechanical efficiency. Singh et al.[199] reported average loadcell readings, which they termed the *"functional abduction force"* across various angles of abduction for the intact and cuff deficient test states. The cuff deficient test state simulated the creation of a posterosuperior irreparable cuff tear. It was reported that the creation of

the irreparable cuff tear significantly decreased the average functional abduction force relative to the intact joint.

1.3.3.3 Joint Reaction Force

The presence of a tear in the rotator cuff can also affect the glenohumeral joint reaction force. As previously discussed, the rotator cuff provides critical glenohumeral stability through concavity compression. However, if one or more of the rotator cuff muscles is compromised by a tear, this can weaken the force generated by that particular muscle, and potentially decrease the joint reaction force. Previous in-vitro studies have reported the effects that RCTs can have on the glenohumeral joint reaction force. Parsons et al.[167] used a dynamic shoulder simulator to test several different progressions of RCTs and their effect on the joint reaction force using a six-degree freedom load cell. It was found that only cuff tears extending from the supraspinatus into the anterior or posterior rotator cuff tendons resulted in a significant decrease in joint reaction force. Furthermore, it was reported that the line of action of the joint reaction force had changed significantly in the supraspinatus and infraspinatus cuff deficient condition compared to that of the intact. The authors reasoned that only RCTs affecting the transverse force couple significantly affect the joint reaction mechanisms at the glenohumeral joint. Another in-vitro study from Loboa et al.[121] used a pressure sensing film to study joint reaction force pressure, force, and area in the presence of only an irreparable supraspinatus tear. The glenohumeral joint reaction force and contact decreased in the irreparable cuff tear state compared to the intact state at all angles of abduction tested, but differences were not significant. A computational based study from Chen et al.[39] investigated the effects of different rotator cuff tear combinations on the glenohumeral joint reaction force. It was found that slight decreases in contact force occurred for cuff tear combinations involving the supraspinatus and/or infraspinatus.

1.3.3.4 Cuff Tear Arthropathy

The term *"cuff tear arthropathy"* was first termed by Neer et al.[39] in 1983. This term was used to describe several pathologic changes observed in the glenohumeral joint in the presence of massive cuff tear (Figure 1-12). These changes included superior translation of the humerus, femoralization of the proximal humerus, collapse of the humeral head, and

erosion of the undersurface of the acromion. The author from this report proposed that the cause for cuff tear arthropathy was primarily due to mechanical and nutritional factors. Since this report was published, several groups have created additional cuff tear arthropathy classifications in an attempt to further describe and understand the physiologic changes that occur within the joint due to this pathology.

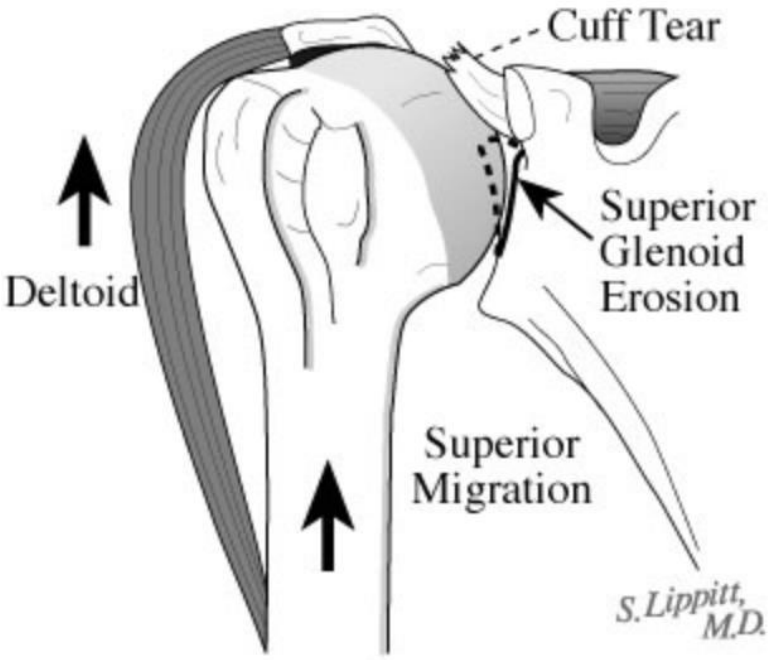

Figure 1-12: Cuff tear arthropathy progression.

Progression of cuff tear arthropathy due to rotator cuff tear. Superior humeral head migration, acetabulization of the inferior acromion, and superior glenoid erosion shown. Femoralization of the greater tuberosity not shown[131].

Hamada et al.[87] first developed a classification system describing radiographic changes observed in the glenohumeral joint in the presence of massive cuff tears. Five grades were developed with the intention of identifying early radiographic changes in the presence of massive cuff tears that eventually led to cuff tear arthropathy. Grades 1 and 2 were directly defined based on the measured acromiohumeral distance while grade 3 was defined by acetabulization, a concave deformity present on the undersurface of the acromion. Grade 4 included narrowing of the joint, indicative of glenohumeral arthritis, while grade 5 included collapse of the humeral head, characterizing cuff tear arthropathy. Furthermore, grades 2-5 also included a tear in the long head biceps tendon. The authors believed that increased stress is placed on the long head biceps tendon in the forward flexion position in the presence of a massive superior cuff tear, thus leading to eventual tear in this tissue.

Two other common classifications regarding cuff tear arthropathy were created by Sirveaux et al.[202] and Visotsky et al.[218] around 2004. The classification from Sirveaux et al.[202] developed their system from patients exhibiting massive irreparable RCTs and was primarily based on glenoid erosion pattern. Type E0 glenoid erosion was characterized as having superior migration of the humerus without any glenoid erosion. Type E1 glenoid erosion was defined according to concentric glenoid erosion while type E2 was characterized as an erosion of the superior glenoid region, leading to a biconcave glenoid. Lastly, type E3 glenoid erosion was defined as superior glenoid erosion extending to the inferior rim of the glenoid. The purpose of this classification system was to assess the Grammont reverse shoulder arthroplasty system in its effectiveness in treating patients with glenohumeral arthritis caused by massive irreparable RCTs. Visotsky et al.[218] created their classification system, referred to as the Seebauer classification, in order to aid surgeons in the decision-making process for treatments. This classification was based on biomechanics and clinical outcomes from arthroplasty surgery. The authors classified cuff tear arthropathy into four different groups. Type 1A: centered stable was classified for patients exhibiting minimal superior humeral head translation and acetabulization of the coracoacromial arch and femoralization of the humeral head. The term femoralization refers to the rounding of the humeral head caused by erosion of the greater tuberosity. This classification is also characterized by intact anterior restraints and sufficient dynamic glenohumeral stability. Type 1B: centered medialization is similar to that of type 1A,

except with compromised dynamic joint stability and erosion of the glenoid. In type 2A: decentered limited stable, superior humeral head migration is present with compromised anterior restraints and transverse force couple. Dynamic joint stability is insufficient and superior-medial glenoid erosion is present. Lastly, type 2B: decentered unstable is characterized by insufficient anterior joint restraint, resulting in anterior escape of the humeral head.

1.4 Treatment Options for Massive Irreparable RCTs

1.4.1 Overview

Various treatments are available for those with RCTs. The choice of treatment depends on both patient attributes and the extent of the rotator cuff tear. Non-operative treatment can be recommended for many rotator cuff tear patients, especially those who are older and lower functioning patients. This treatment can involve prescribed physiotherapy, anti-inflammatory medication, and corticosteroids[195]. Repair of the rotator cuff tear can also be performed. In this surgery, the torn rotator cuff tendon is reattached to its insertional footprint on the humerus, often using suture anchors. Repair of the torn rotator cuff is also a suitable treatment option, reducing pain and restoring shoulder function in patients undergoing this procedure[159]. However, the torn rotator cuff tendon cannot always be repaired to its original insertion site due to retraction of the muscle into the joint, which is more often observed in massive tears. These tears are often referred to as irreparable. Many different alternative treatments exist for patients with massive irreparable RCTs, including debridement,[117,204] subacromial decompression[133,237], biceps tenotomy/tenodesis[18], interposition grafts[116,175], partial repair[26,126], and bursal acromial reconstruction[16,177]. Other surgical interventions have also been recently proposed to more effectively restore normal shoulder function to these patients. These procedures consist of tendon transfers, the subacromial balloon spacer, superior capsule reconstruction (SCR), and arthroplasty. The following sections will discuss the details associated with each surgical procedure and its use in treating massive irreparable RCTs.

1.4.2 Tendon Transfer

Tendon transfer for the treatment of massive irreparable RCTs was first proposed by Gerber et al.[69] in 1988, detailing the technique for a latissimus dorsi tendon transfer. Since then, several other tendon transfer treatments have been proposed for this pathology. Biomechanically, tendon transfers primarily serve to restore normal glenohumeral stability by balancing the transverse force couple. Tendon transfers also contribute to humeral head depression and glenohumeral concavity compression, providing further balance to the joint. These procedures first detach part of a tendon from its original insertion site. The muscle is then rerouted around the humerus and reattached to a new insertion site on the lateral humerus. Unlike several other treatment options, tendon transfers are dynamic as the muscle that is transferred is still functional. This muscle can be trained post-operatively to be synergetic with the remaining rotator cuff muscles, thereby helping to restore the normal glenohumeral force couples[221].

The latissimus dorsi serves to adduct, internally rotate, and extend the arm. This muscle has a broad origin primarily involving the thorax and wraps anteriorly around the humerus to insert on the distal portion of the bicipital groove between the pectoralis major and teres major muscle tendons[227]. During this procedure, the latissimus dorsi tendon is detached from its original insertion and is reattached to the greater tuberosity[227]. This procedure was originally described as an open, double-incision procedure, requiring large sagittal and superior incisions to detach and reattach the tendon[69]. However, several recent studies have reported techniques that are single incision[84], arthroscopically assisted[32,82,104,107,232], or fully arthroscopic[49], minimizing the invasiveness of the surgery. This procedure changes the primary function of the latissimus dorsi muscle from an internal rotator to an external rotator to help restore normal humeral external rotation that can become compromised due to a posterosuperior massive irreparable rotator cuff tear. Studies have reported positive outcomes with this treatment, with results often showing improved clinical scores, pain relief, and function[33,71,82,170]. Furthermore, latissimus dorsi tendon transfers have also been shown to reverse pseudoparalysis in patients who showed this preoperatively[104]. The results from Kany et al.[106] also suggested that insertion of the tendon transfer to the

infraspinatus footprint, or more posteriorly on the greater tuberosity may reduce the risk of tendon rupture.

Elhassan et al.[61] more recently proposed the idea of a lower trapezius tendon transfer for the treatment of massive irreparable RCTs. Elhassan originally used this procedure to help restore external rotation in patients with a paralytic shoulder[59]. The trapezius muscle consists of three sections that function to stabilize the scapula[163]. Tendon transfer using the lower trapezius muscle more accurately restores the posterior rotator cuff line of action compared to the latissimus dorsi tendon transfer, which has a more inferior muscle force line of action (Figure 1-13). Furthermore, the lower trapezius tendon transfer can be easier and quicker to perform compared to the latissimus dorsi tendon transfer[221]. During the procedure, the insertion of the lower part of the trapezius muscle is dissected from its anatomic insertion. However, this tendon itself is not long enough to be reattached to the lateral aspect of the humerus. Therefore, an allograft is sutured to the end of the trapezius tendon. The graft is then passed through to the glenohumeral joint where its free end is arthroscopically reattached to the greater tuberosity, either using suture anchors or a transosseous cortical button[61]. Few clinical studies exist reporting on the outcomes of this procedure. In his original report, Elhassan et al.[61] showed that at mid-term follow-up, patients had improved clinical scores and range of motion. Elhassan et al.[60] later reported similar results in another clinical study, although patients with osseous pre-operative cuff tear arthropathy changes had poor outcomes.

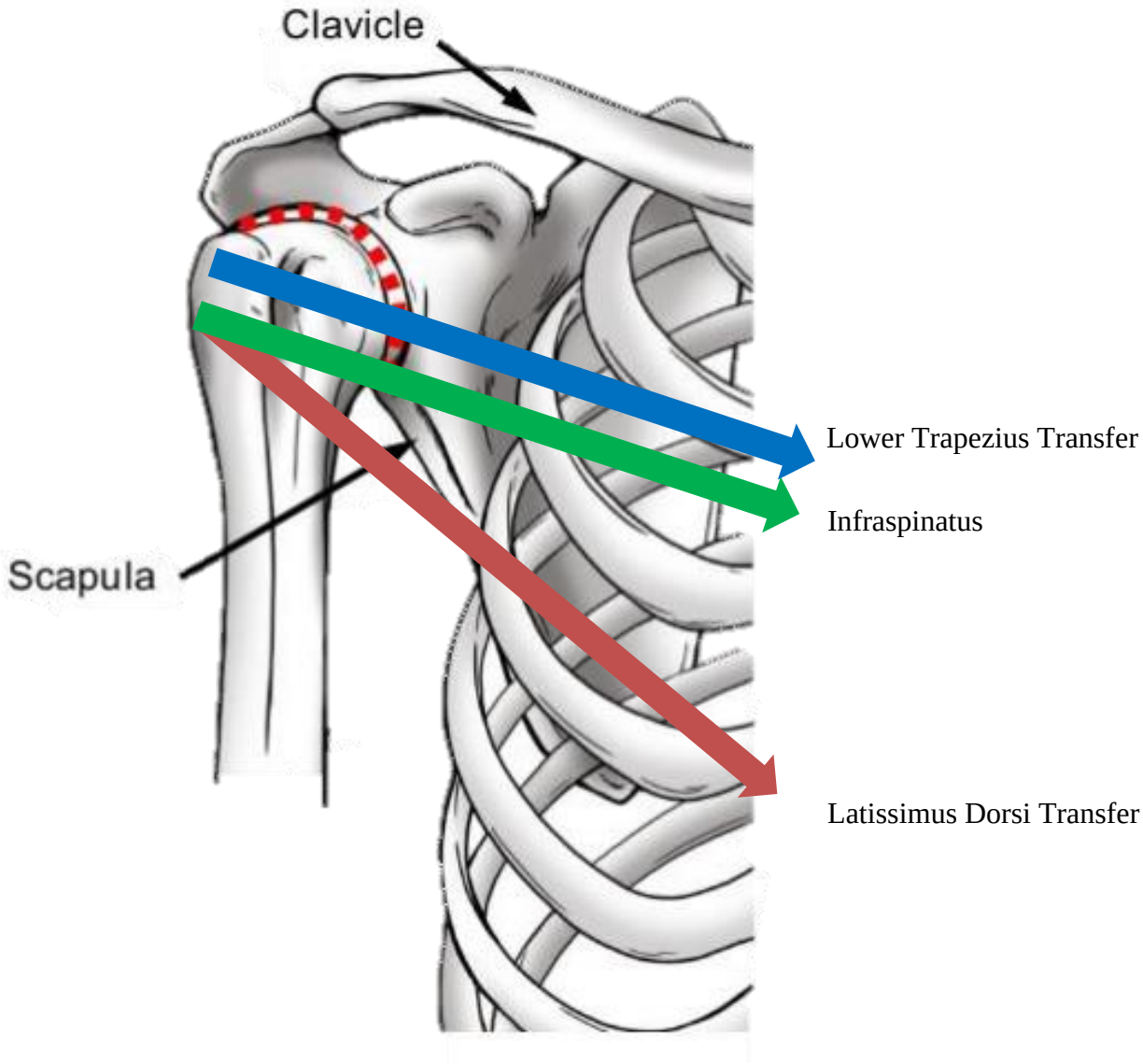

Figure 1-13: Tendon transfer and Infraspinatus muscle lines.

Arrows representing the different muscle line of actions of the latissimus dorsi and lower trapezius tendon transfer procedures compared to the native infraspinatus muscle line. Blue: lower trapezius tendon transfer line of pull; Green: Native infraspinatus muscle line of pull; Red: latissimus dorsi tendon transfer line of pull.

Limited studies have been conducted to compare latissimus dorsi and lower trapezius tendon transfer procedures in their effectiveness to restore normal shoulder function and stability. Omid et al.[164] found the trapezius to be more effective in restoring native humeral head position and normal joint reaction force. Hartzler et al.[90] also found that lower trapezius tendon transfers generate a larger external moment arm compared to latissimus dorsi tendon transfer when attached to either the infraspinatus or teres minor insertional footprint. A clinical study retrospectively compared patients who underwent tendon transfers using the latissimus dorsi and lower trapezius muscles[10]. It was reported that patients who had undergone tendon transfer using the lower trapezius muscle had better range of motion, clinical scores, and shoulder function compared to the latissimus dorsi group.

Another tendon transfer technique that can be used to help restore normal external rotation in massive irreparable cuff tear patients is the L'Episcopo tendon transfer. This was introduced by Joseph L'Episcopo in 1934 to restore external rotation in pediatric patients with obstetric palsy[10]. In this procedure, both the latissimus dorsi and teres major muscles are detached from their original insertions and transferred posteriorly and laterally on the humerus to restore normal external rotation. Boileau et al.[20] later modified this procedure so that only one incision was needed using a deltopectoral approach. The authors found this procedure to improve shoulder function in patients with external rotation deficiency. A later study from Gerhardt et al.[73] reported improved clinical scores and range of motion using this procedure to treat massive irreparable posterosuperior RCTs. However, the authors also found a high rate of cuff tear arthropathy progression in their patients. This procedure is commonly paired with reverse shoulder arthroplasty to further improve functional outcomes[19,20,23].

Although positive outcomes have been reported for these procedures, poor clinical outcomes have also been reported. Studies have previously reported latissimus dorsi tendon transfers to have a high clinical failure and complication rates[105,107,150]. Studies have also reported tendon insertion position, fatty infiltration of the teres minor muscle, subscapularis muscle weakness, and previously failed rotator cuff repair to increase the risk of tendon rupture and poor surgical outcomes[32,42,72,107]. Yamakado[232] also reported this procedure to

be technically demanding with an extensive learning period needed for this surgical technique.

1.4.3 Subacromial Balloon

A recently developed treatment for massive irreparable RCTs is the subacromial balloon spacer (Figure 1-14). This concept was first published by Savarese et al.[189] in 2012. In this study, the balloon, which is filled with saline intraoperatively, was described as a biodegradable spacer that is arthroscopically inserted into the subacromial space using a lateral arthroscopic port. This device functions as a spacer between the acromion and humeral head, restoring normal glenohumeral biomechanics while permitting a new smooth articulating surface with the humerus. The balloon is made from poly(L-lactide-co-ε-caprolactone) which biodegrades within 12 months. Three balloon sizes are available, each varying in width, length, and maximum inflation volume. However, recommended inflation volumes are also provided with each size. The balloon was originally indicated for patients with irreparable tears involving the supraspinatus and/or infraspinatus tendons. The balloon can also be used in patients with tears in the subscapularis, but it is indicated that the subscapularis must be reparable in order to use this device. Contraindications for this device primarily included glenohumeral arthropathy, in addition to infection and tissue necrosis. The study from Savarese et al.[189] also discusses surgical suggestions and tips, including that debridement and bursectomy should first be performed before inserting the balloon to aid in proper selection of the balloon size. Additionally, it was noted that displacement of this device is possible as it is not securely fixed to any surrounding tissue.

Biomechanical theory suggests the balloon helps to restore normal glenohumeral stability by preventing the humeral head from translating superiorly and posteriorly in the presence of a massive posterosuperior cuff tear. This is accomplished by positioning the balloon between the humeral head and acromion, which is located superiorly and posteriorly relative to the joint center. Prevention of superior humeral translation helps to restore the normal fulcrum of the glenohumeral joint, thereby increasing the efficiency of the deltoid as its moment arm increases.

A

B

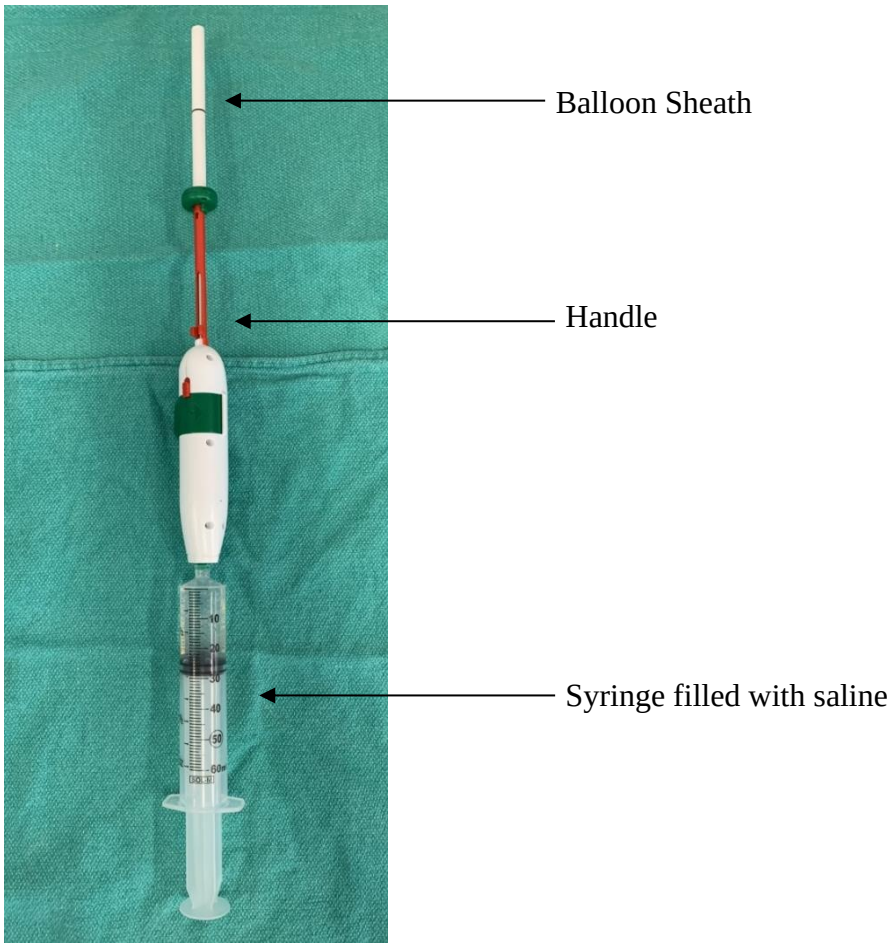

Figure 1-14: Subacromial balloon device.

(A) Placement of filled subacromial balloon within the subacromial space[197]. (B) The mechanism used to arthroscopically insert and insufflate the balloon.

Few cadaveric studies have investigated the performance of the balloon in restoring glenohumeral stability. A study from Singh et al.[200] investigated the effect of balloon fill volume on humeral head translation in a cuff deficient shoulder model. The results from this study suggested that inflation of the balloon using 25mL of saline most effectively restored native humeral head position. The authors found 10mL of balloon inflation did not restore normal humeral head position, while a fill volume of 40mL over depressed the humeral head. It was noted however that 10mL, 25mL, and 40mL balloon volumes all resulted in anterior humeral head translation relative to the intact rotator cuff model. It was reasoned that the anterior translation of the humeral head in all balloon states was due to the acromion being located posteriorly and superiorly relative to the glenoid. Since the balloon abuts the undersurface of the acromion, it not only depresses the humeral head inferiorly, but also pushes it anteriorly. This finding reiterated the need for an intact subscapularis when using this device as it was speculated the force from the subscapularis helped to prevent excessive anterior humeral head translation. Another study from this group of authors reported similar outcomes, showing the balloon caused 3mm of anterior humeral head translation relative to the intact cuff state[178]. They also reported on the balloon's ability to restore the mechanical efficiency of the glenohumeral joint by measuring the functional abduction force. Results illustrated that the average functional abduction force produced with the balloon was lower compared to that of the intact test state, suggesting that the balloon does not restore the normal mechanical efficiency of the intact arm. However, the difference between these force values was not significantly different. Furthermore, the authors reported the average functional abduction force as a single value averaged across the entire range of abduction angles tested, and did not provide insight into the effect that the balloon had on mechanical efficiency in the different stages of abduction. Another cadaveric study from Lobao et al.[121] used pressure sensitive film to measure the contact area, pressure, and force between the humeral head and glenoid in an irreparable cuff tear model with and without implantation of the subacromial balloon. The balloon restored glenohumeral contact pressure near to that of the intact test state, however, it had shifted the center of contact pressure anteriorly and inferiorly on the glenoid compared to the intact state. This resulted in decreased contact area, with the balloon primarily articulating with the anteroinferior glenoid.

There have been numerous clinical studies reporting on outcomes using the subacromial balloon spacer. The first clinical study published from Senekovic et al.[192] reported positive clinical outcomes showing significant improvement over the first one and a half years which were sustained at three-year follow-up. This study also reported that the time to implant the balloon during the procedure took between 2-20 minutes, suggesting this to be a quick and efficient surgical procedure to learn. The authors from this study again reported satisfactory clinical outcomes at five-year follow-up for this same patient group in 2017[191]. Other clinical studies have also reported similar clinical results using the subacromial balloon spacer for the treatment of irreparable RCTs[53,64,93,172,173,179,231]. These studies reported improvements in pain relief, shoulder function, and patient satisfaction. A study from Malahias et al.[125] also reported positive clinical results using this device but found no difference between patients treated with only the balloon, and patients treated with the balloon and partial rotator cuff repair or debridement. Recent studies have also reported techniques to insert this device under a local anesthesia, reducing the risks a patient may be subjected to under general anesthesia[54,74].

Although positive outcomes using the subacromial balloon spacer have been demonstrated, there is still speculation regarding the effectiveness of this procedure in treating patients with massive irreparable RCTs. Several factors from these studies have caused concern amongst surgeons, including high risk of bias, heterogeneity in patient selection and study design, lack of control, and low levels of evidence[102,205,219]. Several of these studies contained conflicts of interest involving the authors and the manufacturer[125,192,191]. Poor clinical outcomes have also been reported. Deranlot et al.[53] reported, in a study investigating 39 shoulders, that acromiohumeral distance decreased by an average of 2mm in their patients after a minimum one-year follow-up. 15% of patients in this study also progressed by one Hamada cuff tear arthropathy grade within this period. Ruiz Iban et al.[181] reported a 40% satisfaction rate within their study of 15 patients, in addition to a revision rate of 33% to a reverse shoulder arthroplasty. Prat et al.[174] also reported low patient satisfaction, a 16% complication rate, and no improvement in proximal humeral migration in a study including 22 patients. It has also been recommended this procedure be used for an older patient population with lower functional demands[174].

A common conclusion among several clinical studies investigating the subacromial balloon states the need for a randomized clinical trial to investigate the effectiveness of this device. To the delight of many clinicians, results have now been published from a recent randomized control trial. Metcalfe et al.[135] compared debridement and biceps tenotomy to the same procedure with the addition of the subacromial balloon. The authors found the results favoured debridement only and did not recommended use of the balloon for treatment of massive irreparable RCTs. It should be noted that this study included patients with poor preoperative range of motion, which has previously been correlated with low patient satisfaction[174]. Another randomized clinical study from Verma et al.[216] compared the use of the subacromial balloon to partial rotator cuff repair, however, these results have yet to be officially published.

1.4.4 Superior Capsule Reconstruction

SCR was first proposed by Teruhisa Mihata in 2012[146] as a treatment for massive irreparable RCTs. In this study, SCR was described as a procedure that uses a fascia lata allograft to reconstruct the superior capsule of the glenohumeral joint (Figure 1-15). The graft is fixed surgically to both the glenoid and greater tuberosity using suture anchors. The length of the graft is determined based on the angle of abduction the arm is positioned in during implantation. This was indicated as 45 degrees of shoulder abduction, or 30 degrees of glenohumeral abduction in this original study. Mihata et al. indicated the use of a 5mm graft thickness which was achieved by folding the graft multiple times. Graft dimensions were based on the size of the joint and supraspinatus tendon. The authors reported this reconstruction fully restored the normal position of the humeral head to that of the intact rotator cuff test state. Indications for this procedure have been reported to include younger patients, those with massive irreparable cuff tears involving the supraspinatus and infraspinatus, higher grade fatty infiltration, and lower Hamada cuff tear arthropathy grades[234].

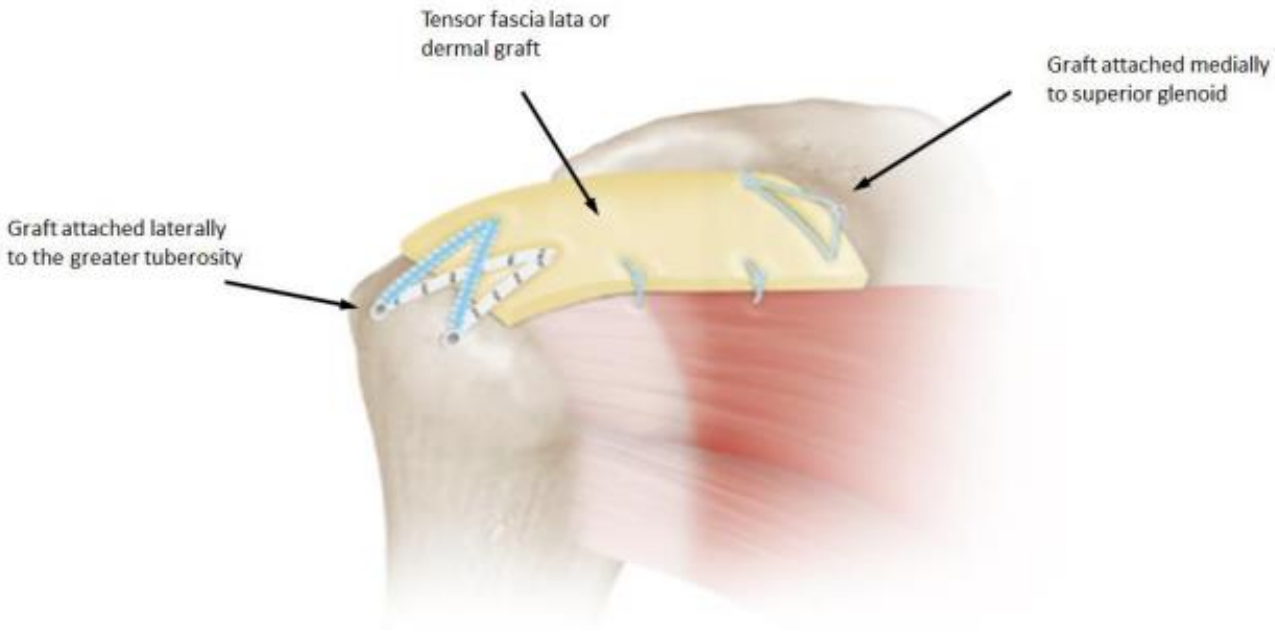

Figure 1-15: Illustration of SCR graft within the shoulder.

The graft is attached medially to the superior glenoid and laterally to the greater tuberosity of the humerus using double row repair[198].

Biomechanically, the graft is designed to act as a passive barrier to prevent superior translation of the humeral head in a shoulder with a massive irreparable cuff tear. This passive barrier is most effective in lower ranges of abduction as the graft is inserted into the shoulder at 30 degrees of glenohumeral abduction. Therefore, at angles lower than this, the tension in the graft increases as it wraps around the humeral head. This tension provides a sufficient passive barrier to superior translation of the humeral head[214]. When the arm is abducted past 30 degrees, the graft loses tension and has less of an effect on glenohumeral joint function.

Since this procedure was introduced, several biomechanical studies have attempted to improve both the procedure and graft used in this treatment. Mihata et al.[144] in 2016 investigated the effect of graft continuity, both anteriorly and posteriorly, with the rotator cuff muscles on restoring glenohumeral stability. The results illustrated posterior graft continuity, achieved by suturing the graft to the infraspinatus, improved restoration of glenohumeral stability, while the addition of anterior graft continuity with the subscapularis provided no significant benefit. In another study, Mihata et al.[145] found that the use of acromioplasty with SCR decreases the risk of graft tear against the acromion post-operatively.

Several studies have also investigated the effects of tensioning the graft at different angles of abduction on overall performance of this procedure. Tibone et al.[214] found that angles of 20 and 40 degrees of glenohumeral abduction were suitable for tensioning the graft, with each preventing superior translation without compromising range of motion. Tensioning the graft at 40 degrees was more effective at preventing superior humeral head translation at 0 degrees of abduction as more tension was present in the graft compared to the 20-degree fixation test state. However, the authors noted that tensioning at 40 degrees may increase the risk of graft tear. Adams et al.[2] also investigated tensioning the graft at 0, 15, 30, 45 and 60 degrees of glenohumeral abduction and the effect this had on maximum deltoid force observed throughout dynamic abduction. Their results yielded no significant difference in maximum deltoid force between fixation angles of 0-45 degrees but found tensioning the graft at 60 degrees resulted in a significant reduction. Furthermore, the authors found that within the 0–45 degree fixation range, only the 15 degree fixation test

state showed similar deltoid forces to that of the native test state. The thickness of the graft used in the procedure has also been studied by several groups. Scheiderer et al.[190] found a 6mm graft thickness to be more effective in restoring joint stability compared to a 3mm graft thickness, although Smith et al.[203] found no significant difference in a similar outcome between using single and double layer grafts. Mihata et al.[143] showed that an 8mm graft thickness tensioned at 10 or 30 degrees of glenohumeral abduction is more effective at restoring glenohumeral stability compared to using a 4mm graft thickness. The type of graft used is another variable that has been extensively investigated previously. Hamstring[143], patellar tendon[44], and long head biceps tendon grafts[25] have previously been studied for their potential use in this procedure. However, fascia lata allografts[145,143,144,146,220] and acellular dermal allografts[2,184,190,203,214] seem to be most commonly used in cadaveric studies, with each exhibiting good results. Two cadaveric comparative studies found fascia lata allografts provided better results compared to acellular dermal matrix allografts. Mihata et al.[136] found fascia lata allografts completely restore glenohumeral joint stability to that of the intact state, with acellular dermal allografts only partially restoring glenohumeral stability. They found that the dermal allografts elongated by up to 15% throughout testing, while the length of the fascia lata allografts remained constant. Cline et al.[57] recommended dermal allografts to be double layered as single layer grafts had inferior outcomes relative to double layer dermal grafts and fascia lata allografts.

Clinical studies have been conducted to evaluate the effectiveness of this procedure in restoring normal glenohumeral stability in the presence of massive irreparable cuff tears. Several clinical studies using fascia lata autografts were conducted by Teruhisa Mihata and his research group, who reported the SCR procedure to be effective in improving clinical scores, shoulder function, and increased pain relief in numerous clinical studies[137,138,141,140,139,142]. Furthermore, included in some of these studies, Mihata reported the procedure to be effective in reversing moderate to severe pre-operative pseudoparalysis[139] and resulted in a high rate of return to sports and physical activity post-operatively[137]. In another study, Mihata et al.[138] indicated an intact or reparable subscapularis to be an indication for performing this surgery as patients with an irreparable subscapularis tear in addition to a posterosuperior cuff tear had poor clinical outcomes.

Azevedo et al.[31] also reported on the use of fascia lata autografts for treatment of irreparable RCTs. In their study, the authors reported good clinical results using a minimally invasive harvest technique for the autograft. Although promising results have been reported with the use of this graft type, the need for a large harvesting site has caused concerns over potential donor site morbidity and increased operating room time[124]. Furthermore, a study from Lim et al.[118] reported high rates of graft failure. Other studies have expressed concern over the lack of long-term follow-up studies with this type of graft and the fair to poor quality of the short-term studies published[5,34,103].

Some studies have also reported clinical findings using a dermal allograft for SCR. Several of these studies have reported positive findings, including increased clinical scores, improved range of motion and function, and improved pain relief[27,28,111,169]. However, studies have also reported poor clinical outcomes with dermal allografts. Woodmass et al.[229] reported no significant improvement in range of motion, with a high percentage of patients suffering from pain and poor function after the procedure. Denard et al.[51] also noted low graft healing rates in their study. These findings combined with the findings from the comparative cadaveric based studies[57,136] suggest dermal allografts to be inferior to the fascia lata autografts at this time.

1.4.5 Arthroplasty

Arthroplasty, colloquially referred to as joint replacement, is a term used to describe the surgical treatment of a pathologic joint in order to improve its function. This is accomplished by replacing the damaged area of the joint with an artificial implant(s). Three main types of arthroplasties exist for the glenohumeral joint: hemiarthroplasty, anatomic total shoulder arthroplasty, and reverse shoulder arthroplasty (Figure 1-16). Hemiarthroplasty replaces one side of the joint surface with an artificial implant whereas anatomic total shoulder arthroplasty replaces both sides of the glenohumeral joint with two separate implants: one implant for the glenoid and one implant for the humeral head. Both hemiarthroplasty and anatomic total shoulder arthroplasty utilize implants that serve to recreate the native anatomy of the joint. Therefore, the humeral implant component in these procedures is hemispherical to match the native humeral head, whereas the glenoid implant component is concave to match the native anatomy of the glenoid side of the glenohumeral

joint. Reverse shoulder arthroplasty differs from these two procedures in that it reverses the natural shape of the glenohumeral joint. In this procedure, the humeral sided implant component consists of a concave ‘cup’ component, whereas the glenoid implant component is hemispherical in nature. Numerous studies have examined the implants associated with these procedures in an attempt to ultimately improve surgical and patient outcomes.

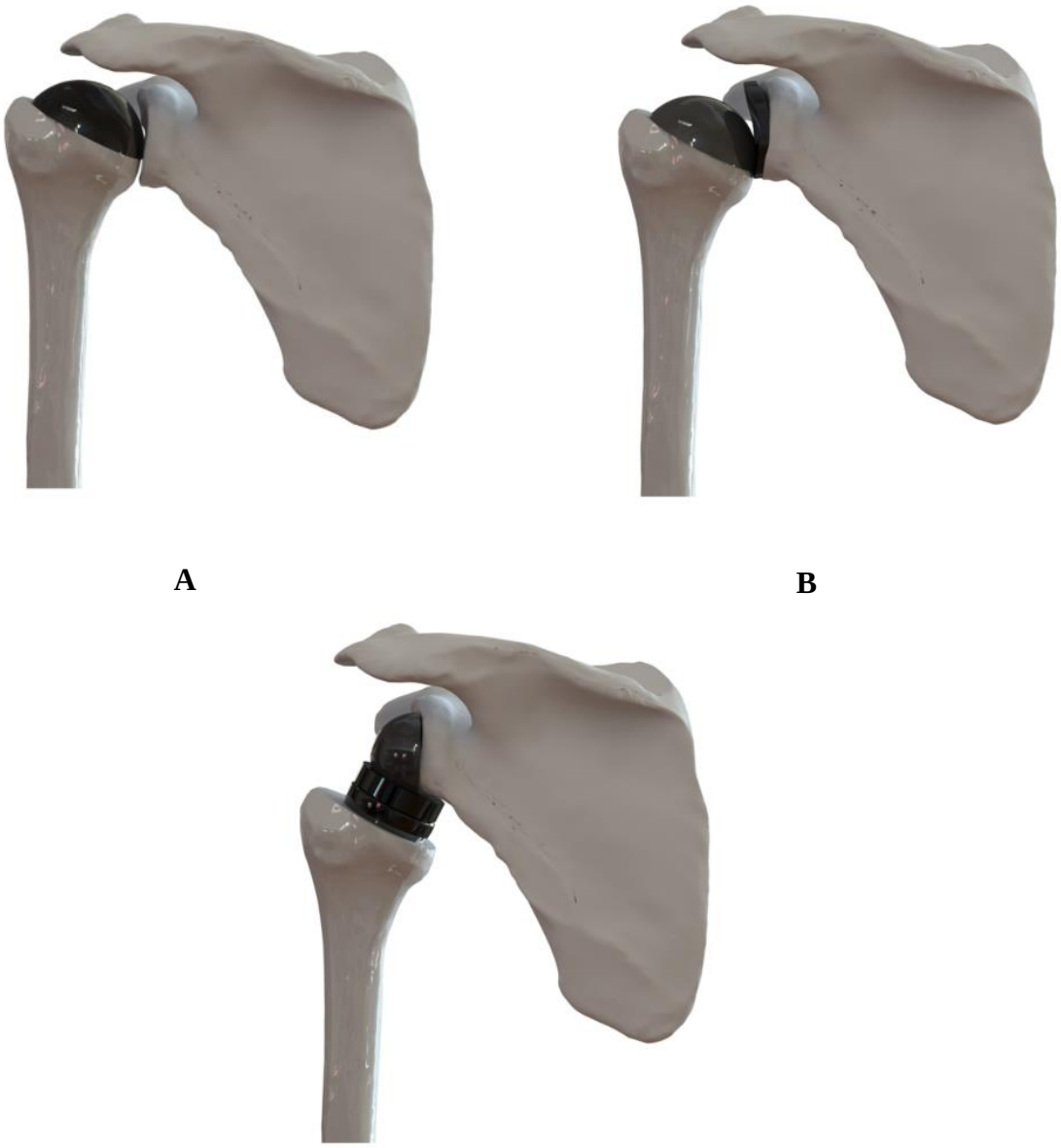

Figure 1-16: Illustration of the three types of shoulder arthroplasty.

(A) Humeral sided hemiarthroplasty, (B) Anatomic total shoulder arthroplasty, and (C) Reverse total shoulder arthroplasty (adapted from Lockhart[122]).

Although all three implant based surgical treatments have been shown to be effective for several different glenohumeral pathologies, they are not all equal when it comes to treating massive irreparable RCTs. Early studies investigating the use of anatomic total shoulder arthroplasty for the treatment of RCTs found this procedure to exhibit high rates of failure[43]. This treatment does not restore the native force couples that existed before the massive rotator cuff tear. This in part with the unconstrained design of a total shoulder arthroplasty prosthesis allows for the humerus to excessively translate as seen in the rotator cuff deficient shoulder. Furthermore, excessive translation of the humeral head can cause eccentric loading between the two implants, thereby increasing the risk for glenoid component loosening[43].

Hemiarthroplasty, as first reported by Neer[156] in 1955, is similar to anatomic total shoulder arthroplasty in that it has not had great success in the treatment of rotator cuff tear pathology. Neer[155] later observed that although humeral-sided hemiarthroplasty provided effective pain relief in patients with rotator cuff deficiency, it did not provide adequate strength to these patients. Studies have since reported mixed outcomes. While few studies have reported improvements in range of motion with hemiarthroplasty[187,228,236], instances of glenohumeral instability and pain have been reported[65,77,187]. Hemiarthroplasty has also been shown to have poor outcomes in the treatment of cuff tear arthropathy[65]. The hemiarthroplasty implant is similar to total shoulder arthroplasty in that the design of the implant is not constrained, and therefore does not restore the normal joint stability.

The optimal choice of arthroplasty for the treatment of massive irreparable RCTs has more recently been shown to be the reverse shoulder arthroplasty. Paul Grammont proposed the innovative reverse shoulder arthroplasty design of the Delta III prosthesis in the 1980's[79,80]. This prosthesis reversed the native anatomy of the joint, with a hemispherical implant inserted into the glenoid side of the joint and a concave 'cup' inserted into the humeral side of the joint. This design differed significantly from anatomic total shoulder arthroplasty implants at the time in that it was constrained, not allowing for any relative translation to occur about the two sides of the joint. Furthermore, the non-anatomic design of this prosthesis medialized the center of rotation of the glenohumeral joint, increasing the deltoid moment arm and thereby decreasing the force exerted by the deltoid (Figure 1-17). These

design changes allowed for the deltoid to compensate for the loss of rotator cuff function and helped to improve the stability of the joint relative to the cuff deficient state. Since this was introduced, many new implant variations have been proposed to further improve clinical outcomes for patients.

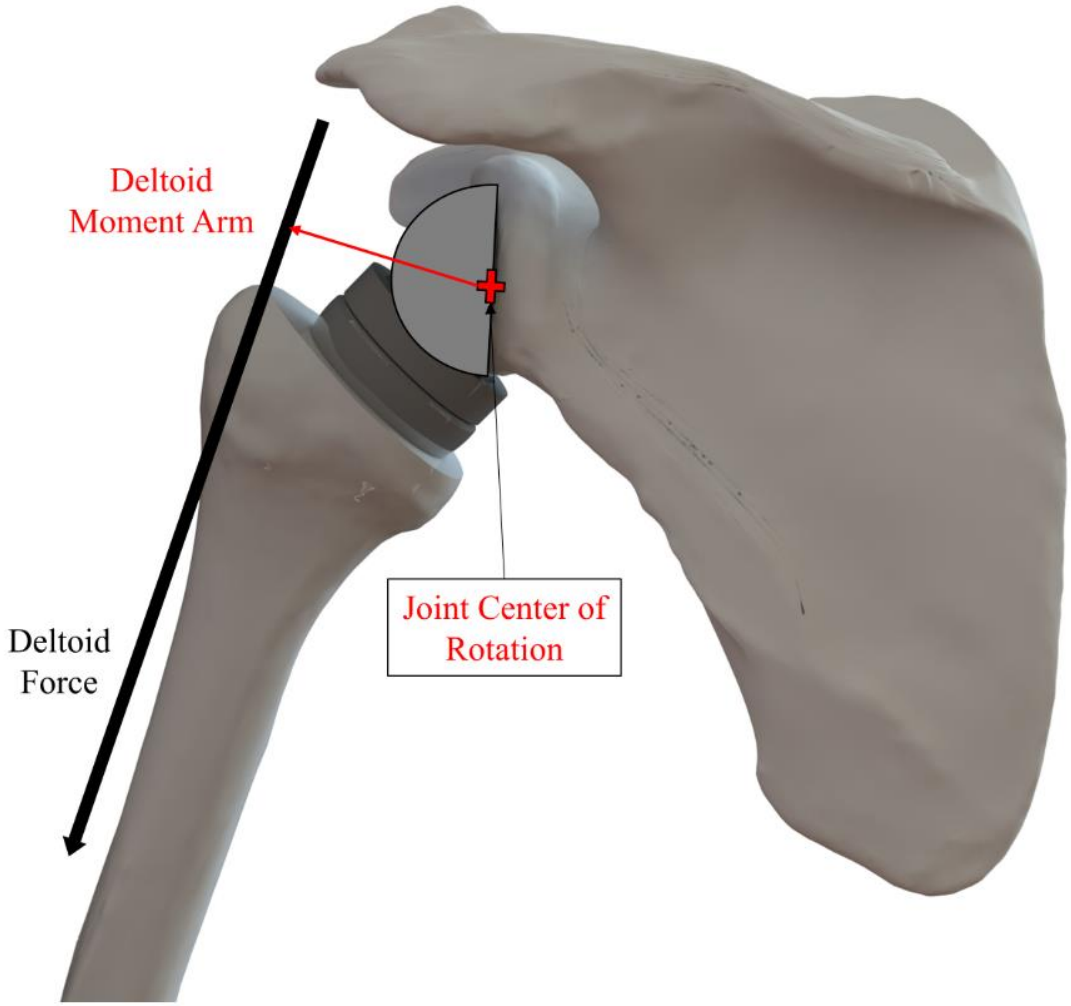

Figure 1-17: The effect of a reverse shoulder prosthesis on glenohumeral biomechanics.

The center of rotation is medialized using a reverse shoulder prosthesis. This increases the deltoid muscle moment arm relative to the anatomic state (adapted from Lockhart[122]).

The use of reverse shoulder arthroplasty for treating patients with massive irreparable RCTs has been thoroughly investigated over the past 20 years. Studies have illustrated the use of this prosthesis to be effective in relieving pain, in addition to restoring function and range of motion[171,194]. Studies have also reported positive short-term[47,152], medium-term[21,45,222], and long-term outcomes[46], with patients often experiencing less pain and improved function. Other studies have also investigated the use of reverse shoulder arthroplasty as a treatment in severe stages of cuff tear arthropathy with evidence of glenohumeral erosion. Positive outcomes have been reported using this procedure[66,222], in addition to using a metal[120] and bony[22] superior augmented with the glenoid component in this treatment. Reverse shoulder arthroplasty can also be used as an effective salvage procedure for patients with previously failed rotator cuff repair and tendon transfer procedures[21,128].

Reverse shoulder arthroplasty has also been shown to have promising results when combined with a tendon transfer procedure[9,19,24,196,235], with patients exhibiting improved external rotation and active elevation after treatment. Biomechanically, the use of the tendon transfer procedure with the latissimus dorsi and teres major tendons helps to restore the native transverse glenohumeral force couple which may be comprised by a posterosuperior rotator cuff tear and potential fatty infiltration into the infraspinatus and teres minor muscles[196]. Boileau et al.[19] showed that use of a modified L'Episcopo procedure, transferring both the latissimus dorsi and teres major tendons along with performing a reverse shoulder arthroplasty improved external rotation compared to using only the latissimus dorsi in the tendon transfer. In a biomechanical study, Chan et al.[37] found that to improve glenohumeral external rotation torque, tendon transfers should be attached to the lateral aspect of the greater tuberosity with insertion of the teres minor tendon as opposed to attachment to the lateral humeral shaft.

Although some reports have provided evidence supporting reverse shoulder arthroplasty to be an effective treatment of massive irreparable RCTs, caution is needed when considering this for a younger and more active patient demographic. Multiple studies have investigated the use of reverse shoulder arthroplasty in patients under the age of 65[58,63,186]. The results from these studies were similar, reporting good functional outcomes and improvement in

pain, but each yielded higher complication rates. Guery et al.[83] suggested that this procedure only be used for patients under 70 years of age with low functional demands, while Muh et al.[151] have reported lower patient satisfaction in patients under 60. Hartzler et al.[91] identified young age and high preoperative function to be associated with poor surgical outcomes and functional improvements in patients without osteoarthritis. Management of these higher complication rates and revision surgery in this patient demographic is a concern[217].

1.5 Thesis Motivation

RCTs are a common cause of pain and disfunction[209]. Massive irreparable RCTs can severely disrupt normal glenohumeral force couples, thereby compromising normal glenohumeral joint stability and function. As discussed in the previous section, many different treatment options exist for this pathology. Reverse shoulder arthroplasty is the definitive management for an elderly patient population with lower function demands and joint arthritis. However, in younger (age<65) more active patients with higher functional demands, the choice of treatment for this pathology is highly controversial.

The treatments that are most commonly considered for younger, active patients with massive irreparable RCTs include tendon transfer, SCR, subacromial balloon, and reverse shoulder arthroplasty. Each of these procedures employ unique solutions in attempt to restore glenohumeral stability. Tendon transfer is the only treatment that utilizes active soft tissue to restabilize the joint. Healthy muscles from elsewhere in the body are transferred to replicate the function of the pathologic rotator cuff muscle. These muscles can then be trained post-operatively to improve functionality of the transfer[221]. However, because these muscles do not completely replicate the native soft tissue anatomy of the joint, they are susceptible to tearing[105,107,150]. SCR is another treatment that utilizes soft tissue to restabilize the joint. However, unlike tendon transfers, SCR utilizes passive soft tissue to accomplish this. The graft used in a SCR serves to constrain the humeral head by preventing it from translating superiorly. This is accomplished by tensioning the graft in the early- to mid-range of abduction where translation is most significant. With sufficient tension the graft acts as a passive barrier to humeral head translation. However, similar to tendon transfers, SCR grafts are also susceptible to tearing, which usually lead to poor

clinical outcomes[51,118,229]. The subacromial balloon also serves as a passive barrier to superior humeral head motion. This treatment differs from the SCR in that it uses a foreign passive object that is freely positioned above the joint. Some studies have called into question the effectiveness of the balloon[53,174,181], with a recent randomized clinical trial reporting mixed outcomes[135]. Reverse shoulder arthroplasty significantly differs from the aforementioned treatments. This procedure involves the removal of both sides of the joint, replacing bone with metallic implants. The implants used in this procedure fully constrain the glenohumeral joint, preventing any translation from occurring. Additionally, reversing the anatomy causes the joint center to move medially, thereby lengthening the deltoid moment arm and decreasing the force through the deltoid muscle. This procedure has been well validated in the literature for several different shoulder pathologies and is considered by many to be the definitive treatment for massive irreparable RCTs in an older patient population with glenohumeral arthritis[66,222]. However, its efficacy for use in younger more active patients in absence of glenohumeral arthritis is questioned. Concerns exist for removing healthy joint surfaces in these patients and the longevity of these implants in a young patient. Higher complication rates have also been reported for this procedure when used in younger patients[58,63,186]. Although studies have compared different aspects of these all these treatments discussed, no one choice has been found to be significantly more effective than the others[29,35,113,129,183,199].

Recently, a novel solution was proposed for patients with massive irreparable RCTs, which utilizes a rigid subacromial implant to restore the native stability of the glenohumeral joint (Figure 1-18). This implant functions similarly to the subacromial balloon in that it serves as a passive barrier to superior humeral head translation. However, unlike the subacromial balloon, this implant is rigid and securely fixed to the scapula. This unique design may be capable of effectively restoring normal glenohumeral joint motion in this difficult to treat patient demographic. However, only the concept of such a device has been proposed.

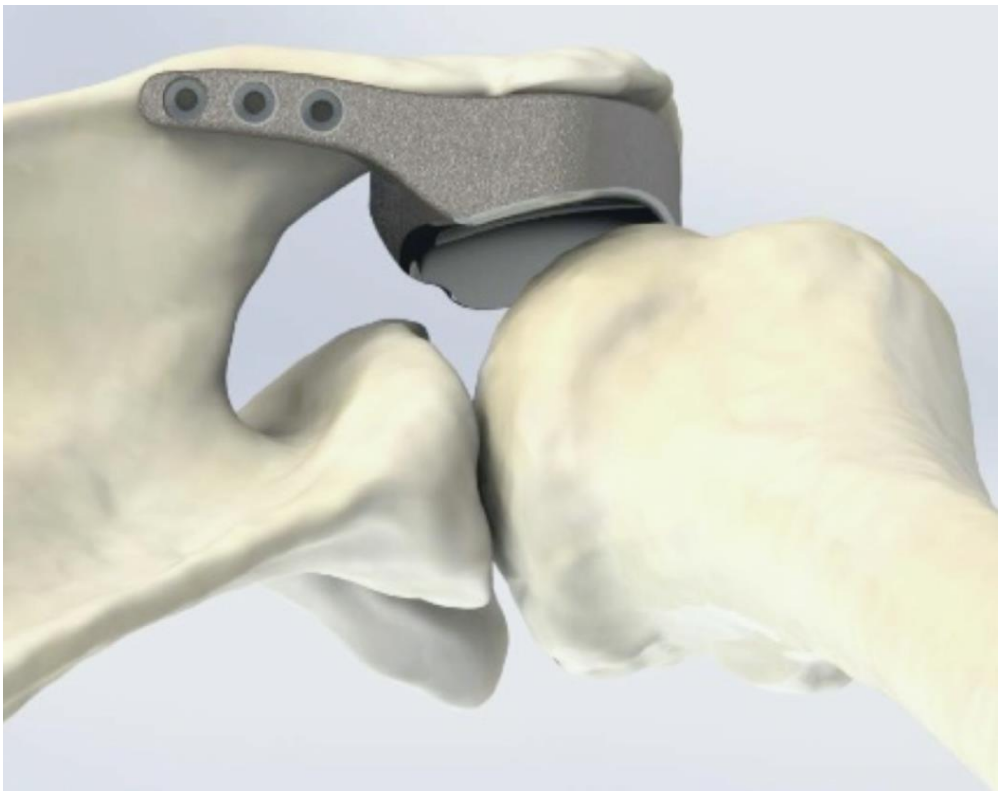

Figure 1-18: Subacromial implant design for the treatment of massive irreparable RCTs.

In light of the foregoing, this thesis focuses on the finalization of the subacromial implant design and fabrication of this device. In-vitro tests are then conducted using this device in a rotator cuff deficient cadaveric model to evaluate the implant's ability in restoring normal glenohumeral joint stability and range of motion. This in-vitro testing evaluates the implant both with and without other surgical interventions.

1.6 Objectives and Hypotheses

The overall objective of this thesis was to design and test a subacromial implant in its ability to restore normal glenohumeral joint position and range of motion in the presence of a massive irreparable rotator cuff tear. This objective was distributed across three different studies.

Chapter 2

Objective: The objective of this study was to design a subacromial implant for the purpose of restoring normal glenohumeral stability in the presence of a massive irreparable rotator cuff tear. The implant had to be designed using average scapular morphology and created as a modular device, representing different implant variables.

Hypothesis: A subacromial implant could be designed based on average scapula morphology and capture different design variables important to restoring normal humeral head position within the modularity of the implant design.

Chapter 3

Objective: The objective of this study was to investigate a rigid subacromial implant's ability to restore humeral head position from the superiorly migrated position.

Hypothesis: The implant would restore near normal humeral head position in a massive, irreparable rotator cuff tear state. Furthermore, it was predicted that different implants, characterized by different implant design variables, would be more effective in improving the implant's ability in restoring axial glenohumeral stability.

Chapter 4

Objective: The first objective of this study was to assess the effect a tuberoplasty procedure, combined with the subacromial implant placement, had on the restoration of normal humeral head position. The second objective was to investigate the difference in allowable range of motion in abduction between the subacromial implant, both with and without a tuberoplasty.

Hypothesis: Combining the insertion of the subacromial implant with a tuberoplasty procedure would more effectively restore normal joint position and increase glenohumeral range of motion compared to the use of the subacromial implant alone.

1.7 Thesis Summary

Chapter 2 describes the design process used to develop the final prototype of the subacromial implant. The original design of this device is first detailed, followed by the description of the three phases of design used to achieve the final implant prototype. The first design phase used anthropometric data to improve the conformity of the implant to both the scapula and humerus. The creation of the modular aspect of this design is also discussed. Phases 2 and 3 used observations from implanting this device into upper extremity cadavers to further improve the overall design of the implant.

Chapter 3 describes the investigation used to evaluate the effectiveness of the different implant designs in restoring normal humeral position within the glenohumeral joint. In-vitro testing using upper extremity cadavers and a static shoulder simulator was conducted with all implants compared to intact and cuff deficient rotator cuff testing states.

Chapter 4 further investigates the effectiveness of the subacromial implant in restoring normal joint position when paired with a tuberoplasty procedure. Additional testing was also performed to evaluate the change in abduction range of motion across all implant designs when used with and without a tuberoplasty.

Chapter 5 summarizes the findings from Chapters 2, 3, and 4, and revisits the original objectives and hypotheses detailed in Chapter 1. This is concluded with sections detailing future work to be conducted in order to further improve the design and function of the

implant and re-iterates the potential this implant has in treating younger, more active patients.

1.8 References

1. Ackland DC, Pandy MG. Lines of action and stabilizing potential of the shoulder musculature. *J Anat*. 2009;215(2):184-197. doi:10.1111/j.1469-7580.2009.01090.x

2. Adams CR, Comer B, Scheiderer B, et al. The Effect of Glenohumeral Fixation Angle on Deltoid Function During Superior Capsule Reconstruction: A Biomechanical Investigation. *Arthrosc - J Arthrosc Relat Surg*. 2020;36(2):400-408. doi:10.1016/j.arthro.2019.09.011

3. Alexander S, Southgate DFL, Bull AMJ, Wallace AL. The role of negative intraarticular pressure and the long head of biceps tendon on passive stability of the glenohumeral joint. *J Shoulder Elb Surg*. 2013;22(1):94-101. doi:10.1016/j.jse.2012.01.007

4. Alpert SW, Pink MM, Jobe FW, Mcmahon PJ. EMG analysis of deltoid and rotator cuff fucntion under varying loads and speeds. *J Shoulder Elb Surg*. 2000;9(Figure 1):47-58.

5. Altintas B, Scheidt M, Kremser V, et al. Superior Capsule Reconstruction for Irreparable Massive Rotator Cuff Tears: Does It Make Sense? A Systematic Review of Early Clinical Evidence. *Am J Sports Med*. 2020;48(13):3365-3375. doi:10.1177/0363546520904378

6. Amit P, Paluch AJ, Baring T. Sharpened lateral acromion morphology (SLAM sign) as an indicator of rotator cuff tear: a retrospective matched study. *JSES Int*. 2021;5(5):850-855. doi:10.1016/j.jseint.2021.05.013

7. Andrade R, Correia AL, Nunes J, et al. Is Bony Morphology and Morphometry Associated With Degenerative Full-Thickness Rotator Cuff Tears? A Systematic Review and Meta-analysis. *Arthrosc - J Arthrosc Relat Surg*. 2019;35(12):3304-3315.e2. doi:10.1016/j.arthro.2019.07.005

8. Athwal GS, Armstrong AD. Rotator Cuff Tears. OrthoInfo. Published 2022. Accessed July 26, 2022. https://orthoinfo.aaos.org/en/diseases--conditions/rotator-cuff-tears

9. Baek CH, Kim JG, Baek GR. Restoration of active internal rotation following reverse shoulder arthroplasty: anterior latissimus dorsi and teres major combined transfer. *J Shoulder Elb Surg*. 2022;31(6):1154-1165. doi:10.1016/j.jse.2021.11.008

10. Baek CH, Lee DH, Kim JG. Latissimus Dorsi Transfer versus Lower Trapezius Transfer for Posterosuperior Irreparable Rotator Cuff Tears. *J Shoulder Elb Surg*. Published online 2022. doi:10.1016/j.jse.2022.02.020

11. Balke M, Schmidt C, Dedy N, Banerjee M, Bouillon B, Liem D. Correlation of acromial morphology with impingement syndrome and rotator cuff tears. *Acta Orthop*. 2013;84(2):178-183. doi:10.3109/17453674.2013.773413

12. Banas MP, Miller RJ, Totterman S. Relationship between the lateral acromion angle and rotator cuff disease. *J Shoulder Elb Surg*. 1995;4(6):454-461. doi:10.1016/S1058-2746(05)80038-2

13. Bedi A, Dines J, Warren RF, Dines DM. Massive tears of the rotator cuff. *J Bone Jt Surg - Ser A*. 2010;92(9):1894-1908. doi:10.2106/JBJS.I.01531

14. Berthold DP, Bell R, Muench LN, et al. A new approach to superior capsular reconstruction with hamstring allograft for irreparable posterosuperior rotator cuff tears: a dynamic biomechanical evaluation. *J Shoulder Elb Surg*. 2021;30(7):S38-S47. doi:10.1016/j.jse.2021.04.002

15. Berthold DP, Muench LN, Bell R, et al. Biomechanical consequences of isolated, massive and irreparable posterosuperior rotator cuff tears on the glenohumeral joint: A dynamic biomechanical investigation of rotator cuff tears. *Obere Extrem*. 2021;16(2):120-129. doi:10.1007/s11678-021-00622-3

16. Berthold DP, Ravenscroft M, Bell R, et al. Bursal Acromial Reconstruction (BAR) Using an Acellular Dermal Allograft for Massive, Irreparable Posterosuperior Rotator Cuff Tears: A Dynamic Biomechanical Investigation. *Arthrosc J Arthrosc Relat Surg*. Published online 2021:1-10. doi:10.1016/j.arthro.2021.07.021

17. Bigliani LU, Morrison DS, April EW. The morphology of the acromion and its relationship to rotator cuff tears. *Ortho Trans*. 1986;10:228.

18. Boileau P, Baqué F, Valerio L, Ahrens P, Chuinard C, Trojani C. Isolated arthroscopic biceps tenotomy or tenodesis improves symptoms in patients with massive irreparable rotator cuff tears. *J Bone Jt Surg - Ser A*. 2007;89(4):747-757. doi:10.2106/JBJS.E.01097

19. Boileau P, Chuinard C, Roussanne Y, Bicknell RT, Rochet N, Trojani C. Reverse shoulder arthroplasty combined with a modified latissimus dorsi and teres major tendon transfer for shoulder pseudoparalysis associated with dropping arm. *Clin Orthop Relat Res*. 2008;466(3):584-593. doi:10.1007/s11999-008-0114-x

20. Boileau P, Chuinard C, Roussanne Y, Neyton L, Trojani C. Modified latissimus dorsi and teres major transfer through a single delto-pectoral approach for external rotation deficit of the shoulder: As an isolated procedure or with a reverse arthroplasty. *J Shoulder Elb Surg*. 2007;16(6):671-682. doi:10.1016/j.jse.2007.02.127

21. Boileau P, Gonzalez JF, Chuinard C, Bicknell R, Walch G. Reverse total shoulder arthroplasty after failed rotator cuff surgery. *J Shoulder Elb Surg*. 2009;18(4):600-606. doi:10.1016/j.jse.2009.03.011

22. Boileau P, Moineau G, Roussanne Y, O'Shea K. Bony Increased Offset-Reversed Shoulder Arthroplasty (BIO-RSA). *JBJS Essent Surg Tech*. 2017;7(4):e37. doi:10.2106/jbjs.st.17.00006

23. Boileau P, Rumian AP, Zumstein MA. Reversed shoulder Arthroplasty with modified L'Episcopo for combined loss of active elevation and external rotation. *J Shoulder Elb Surg*. 2010;19(2 SUPPL.):20-30. doi:10.1016/j.jse.2009.12.011

24. Boughebri O, Kilinc A, Valenti P. Reverse shoulder arthroplasty combined with a latissimus dorsi and teres major transfer for a deficit of both active elevation and external rotation. Results of 15 cases with a minimum of 2-year follow-up. *Orthop Traumatol Surg Res*. 2013;99(2):131-137. doi:10.1016/j.otsr.2012.11.014

25. Boutsiadis A, Chen S, Jiang C, Lenoir H, Delsol P, Barth J. Long Head of the Biceps as a Suitable Available Local Tissue Autograft for Superior Capsular Reconstruction: "The Chinese Way." *Arthrosc Tech*. 2017;6(5):e1559-e1566. doi:10.1016/j.eats.2017.06.030

26. Burkhart S., Nottage W., Ogilvie-Harris D., Kohn H., Pachelli A. Partial repair of irreparable rotator cuff tears. *Arthrosc J Arthrosc Relat Surg*. 1994;10(4):363-370. doi:10.1177/0363546515585122

27. Burkhart SS, Hartzler RU. Superior Capsular Reconstruction Reverses Profound Pseudoparalysis in Patients With Irreparable Rotator Cuff Tears and Minimal or No Glenohumeral Arthritis. *Arthrosc - J Arthrosc Relat Surg*. 2019;35(1):22-28. doi:10.1016/j.arthro.2018.07.023

28. Burkhart SS, Pranckun JJ, Hartzler RU. Superior Capsular Reconstruction for the Operatively Irreparable Rotator Cuff Tear: Clinical Outcomes Are Maintained 2 Years After Surgery. *Arthrosc - J Arthrosc Relat Surg*. 2020;36(2):373-380. doi:10.1016/j.arthro.2019.08.035

29. Camp CL, Elhassan B, DInes JS. Clinical faceoff: Irreparable rotator cuff tears in young, active patients: Tendon transfer versus superior capsular reconstruction? *Clin Orthop Relat Res*. 2018;476(12):2313-2317. doi:10.1097/CORR.0000000000000503

30. Campbell ST, Ecklund KJ, Chu EH, McGarry MH, Gupta R, Lee TQ. The role of pectoralis major and latissimus dorsi muscles in a biomechanical model of massive rotator cuff tear. *J Shoulder Elb Surg*. 2014;23(8):1136-1142. doi:10.1016/j.jse.2013.11.030

31. de Campos Azevedo CI, Ângelo ACLPG, Vinga S. Arthroscopic Superior Capsular Reconstruction With a Minimally Invasive Harvested Fascia Lata Autograft Produces Good Clinical Results. *Orthop J Sport Med*. 2018;6(11):1-13. doi:10.1177/2325967118808242

32. Castricini R, De Benedetto M, Familiari F, et al. Functional status and failed rotator cuff repair predict outcomes after arthroscopic-assisted latissimus dorsi transfer for irreparable massive rotator cuff tears. *J Shoulder Elb Surg*. 2016;25(4):658-665. doi:10.1016/j.jse.2015.08.043

33. Castricini R, Longo UG, De Benedetto M, et al. Arthroscopic-Assisted Latissimus Dorsi Transfer for the Management of Irreparable Rotator Cuff Tears: Short-Term Results. *J Bone Jt Surg*. 2014;96(11):e119.

34. Catapano M, de SA D, Ekhtiari S, Lin A, Bedi A, Lesniak BP. Arthroscopic Superior Capsular Reconstruction for Massive, Irreparable Rotator Cuff Tears: A Systematic Review of Modern Literature. *Arthrosc - J Arthrosc Relat Surg*. 2019;35(4):1243-1253. doi:10.1016/j.arthro.2018.09.033

35. Cavalier M, Jullion S, Kany J, et al. Management of Massive Rotator Cuff Tears: Prospective study in 218 patients. *Orthop Traumatol Surg Res*. 2018;104(8):S193-S197. doi:10.1016/j.otsr.2018.09.007

36. Chalmers PN, Cip J, Trombley R, et al. Glenohumeral function of the long head of the biceps muscle: An electromyographic analysis. *Orthop J Sport Med*. 2014;2(2):1-8. doi:10.1177/2325967114523902

37. Chan K, Langohr GDG, Athwal GS, Johnson JA. The biomechanical effectiveness of tendon transfers to restore rotation after reverse shoulder arthroplasty: latissimus versus lower trapezius. *Shoulder Elb*. 2022;14(1):48-54. doi:10.1177/1758573220946257

38. Chaudhury S, Musa A, Abdulmawjod AA, Gwilym S. Rotator cuff tears. *Orthop Trauma*. Published online 2022:1-8. doi:10.1016/j.mporth.2022.03.003

39. Chen Z, Fan X, Gao Y, et al. Effect of Rotator Cuff Deficiencies on Muscle Forces and Glenohumeral Contact Force After Anatomic Total Shoulder Arthroplasty Using Musculoskeletal Multibody Dynamics Simulation. *Front Bioeng Biotechnol*. 2021;9(July):1-8. doi:10.3389/fbioe.2021.691450

40. Cofield RH. Subscapular muscle transposition for repair of chronic rotator cuff tears. *Surg Gynecol Obstet*. 1982;154(5):667-672.

41. Collin P, Matsumura N, Lädermann A, Denard PJ, Walch G. Relationship between massive chronic rotator cuff tear pattern and loss of active shoulder range of motion. *J Shoulder Elb Surg*. 2014;23(8):1195-1202. doi:10.1016/j.jse.2013.11.019

42. Costouros JG, Espinosa N, Schmid MR, Gerber C. Teres minor integrity predicts outcome of latissimus dorsi tendon transfer for irreparable rotator cuff tears. *J Shoulder Elb Surg*. 2007;16(6):727-734. doi:10.1016/j.jse.2007.02.128

43. Craig RS, Lawrence TM. Anatomic or reverse shoulder arthroplasty: indications and decision-making. *Orthop Trauma*. 2022;36(3):166-174. doi:10.1016/j.mporth.2022.03.006

44. Croom WP, Adamson GJ, Lin CC, et al. A biomechanical cadaveric study of patellar tendon allograft as an alternative graft material for superior capsule reconstruction. *J Shoulder Elb Surg*. 2019;28(7):1241-1248. doi:10.1016/j.jse.2018.12.015

45. Cuff D, Clark R, Pupello D, Frankle M. Reverse shoulder arthroplasty for the treatment of rotator cuff deficiency: A concise follow-up,at a minimum of five years,of a previous report. *J Bone Jt Surg - Ser A*. 2012;94(21):1996-2000. doi:10.2106/JBJS.K.01206

46. Cuff D, Pupello D, Santoni BG, Clark RE, Frankle M. Reverse shoulder arthroplasty for the treatment of rotator cuff deficiency. *J Bone Jt Surg*. 2017;99:1895-1899. doi:10.2106/JBJS.G.00775

47. Cuff D, Pupello D, Virani N, Levy J, Frankle M. Reverse shoulder arthroplasty for the treatment of rotator cuff deficiency. *J Bone Jt Surg - Ser A*. 2008;90(6):1244-1251. doi:10.2106/JBJS.G.00775

48. Cunningham G, Nicodème-Paulin E, Smith MM, Holzer N, Cass B, Young AA. The greater tuberosity angle: a new predictor for rotator cuff tear. *J Shoulder Elb Surg*. 2018;27(8):1415-1421. doi:10.1016/j.jse.2018.02.051

49. Cutbush K, Peter NA, Hirpara K. All-Arthroscopic Latissimus Dorsi Transfer. *Arthrosc Tech*. 2016;5(3):e607-e613. doi:10.1016/j.eats.2016.02.007

50. Davidson J, Burkhart SS. The Geometric Classification of Rotator Cuff Tears: A System Linking Tear Pattern to Treatment and Prognosis. *Arthrosc - J Arthrosc Relat Surg*. 2010;26(3):417-424. doi:10.1016/j.arthro.2009.07.009

51. Denard PJ, Brady PC, Adams CR, Tokish JM, Burkhart SS. Preliminary Results of Arthroscopic Superior Capsule Reconstruction with Dermal Allograft. *Arthrosc - J Arthrosc Relat Surg*. 2018;34(1):93-99. doi:10.1016/j.arthro.2017.08.265

52. DeOrio JK, Cofield RH. Results of a second attempt at surgical repair of a failed initial rotator-cuff repair. *J Bone Jt Surg - Ser A*. 1984;66(4):563-567. doi:10.2106/00004623-198466040-00011

53. Deranlot J, Herisson O, Nourissat G, et al. Arthroscopic Subacromial Spacer Implantation in Patients With Massive Irreparable Rotator Cuff Tears: Clinical and Radiographic Results of 39 Retrospectives Cases. *Arthrosc - J Arthrosc Relat Surg*. 2017;33(9):1639-1644. doi:10.1016/j.arthro.2017.03.029

54. Dhir R, Prinja A, Singh J, Monga P. The Role of Biodegradable Spacer Implantation Under Local Anesthesia for Patients with Massive Rotator Cuff Tears and Significant Medical Co-morbidities. *JSES Rev Reports, Tech*. 2022;InPress. doi:10.1016/j.xrrt.2022.03.003

55. Duquin TR, Buyea C, Bisson LJ. Which Method of Rotator Cuff Repair Leads to the Highest Rate of Structural Healing? *Am J Sports Med*. 2010;38(4):835-841. doi:10.1177/0363546509359679

56. Dyrna F, Kumar NS, Obopilwe E, et al. Relationship Between Deltoid and Rotator Cuff Muscles During Dynamic Shoulder Abduction: A Biomechanical Study of

Rotator Cuff Tear Progression. *Am J Sports Med*. 2018;46(8):1919-1926. doi:10.1177/0363546518768276

57. E. Cline K, Tibone JE, Ihn H, et al. Superior Capsule Reconstruction Using Fascia Lata Allograft Compared With Double- and Single-Layer Dermal Allograft: A Biomechanical Study. *Arthrosc - J Arthrosc Relat Surg*. 2021;37(4):1117-1125. doi:10.1016/j.arthro.2020.11.054

58. Ek ETH, Neukom L, Catanzaro S, Gerber C. Reverse total shoulder arthroplasty for massive irreparable rotator cuff tears in patients younger than 65 years old: Results after five to fifteen years. *J Shoulder Elb Surg*. 2013;22(9):1199-1208. doi:10.1016/j.jse.2012.11.016

59. Elhassan B. Lower trapezius transfer for shoulder external rotation in patients with paralytic shoulder. *J Hand Surg Am*. 2014;39(3):556-562. doi:10.1016/j.jhsa.2013.12.016

60. Elhassan BT, Sanchez-Sotelo J, Wagner ER. Outcome of arthroscopically assisted lower trapezius transfer to reconstruct massive irreparable posterior-superior rotator cuff tears. *J Shoulder Elb Surg*. 2020;29(10):2135-2142. doi:10.1016/j.jse.2020.02.018

61. Elhassan BT, Wagner ER, Werthel JD. Outcome of lower trapezius transfer to reconstruct massive irreparable posterior-superior rotator cuff tear. *J Shoulder Elb Surg*. 2016;25(8):1346-1353. doi:10.1016/j.jse.2015.12.006

62. Ellman H, Gartsman GM. *Open Repair of Full Thickness Rotator Cuff Tears*. Lea and Febiger; 1993.

63. Ernstbrunner L, Suter A, Catanzaro S, Rahm S, Gerber C. Reverse Total Shoulder Arthroplasty for Massive, Irreparable Rotator Cuff Tears Before the Age of 60 Years: Long-Term Results. *J Bone Jt Surg - Am Vol*. 2017;99(20):1721-1729. doi:10.2106/JBJS.17.00095

64. Familiari F, Nayar SK, Russo R, et al. Subacromial Balloon Spacer for Massive, Irreparable Rotator Cuff Tears Is Associated With Improved Shoulder Function and High Patient Satisfaction. *Arthrosc - J Arthrosc Relat Surg*. 2021;37(2):480-486. doi:10.1016/j.arthro.2020.09.048

65. Field LD, Dines DM, Zabinski SJ, Warren RF. Hemiarthroplasty of the shoulder for rotator cuff arthropathy. *J Shoulder Elb Surg*. 1997;6(1):18-23. doi:10.1016/S1058-2746(97)90066-5

66. Frankle M, Siegal S, Pupello D, Saleem A, Mighell M, Vasey M. The Reverse Shoulder Prosthesis for Glenohumeral Arthritis Associated with Severe Rotator Cuff Deficiency: A Minimum Two-Year Follow-up Study of Sixty Patients. *J Bone Jt Surg*. 2005;87(8):1697-1705.

67. Garg R, Boydstun SM, Shafer BI, McGarry MH, Adamson GJ, Lee TQ. Role of the Biceps Tendon as a Humeral Head Depressor. In: *The Management of Biceps Pathology*. Springer Nature Switzerland; 2021:77-85. doi:10.1007/978-3-030-63019-5_5

68. Gartsman GM. *Shoulder Arthroscopy: Principles and Practice*. (Milano G, Grasso A, eds.). Springer-Verlag; 2009. doi:10.1016/B978-1-4160-4649-3.X0001-4

69. Gerber C, Vinh TS, Hertel R, Hess CW. Latissimus dorsi transfer for the treatment of massive tears of the rotator cuff. A preliminary report. *Clin Orthop Relat Res*. 1988;July(232):51-61.

70. Gerber C, Fuchs B, Hodler J. The results of repair of massive tears of the rotator cuff. *J Bone Jt Surg - Ser A*. 2000;82(4):505-515. doi:10.2106/00004623-200004000-00006

71. Gerber C, Maquieira G, Espinosa N. Latissimus dorsi transfer for the treatment of irreparable rotator cuff tears. *J Bone Jt Surg - Ser A*. 2006;88(1):113-120. doi:10.2106/JBJS.E.00282

72. Gerber C, Rahm SA, Catanzaro S, Farshad M, Moor BK. Latissimus Dorsi Tendon Transfer for Treatment of Irreparable Posterosuperior Rotator Cuff Tears. *J Bone Jt Surg*. 2013;95(21):1920-1926. http://jbjs.org.ezproxy.library.uq.edu.au/content/95/21/1920.abstract

73. Gerhardt C, Lehmann L, Lichtenberg S, Magosch P, Habermeyer P. Modified l'episcopo tendon transfers for irreparable rotator cuff tears: 5-year followup. *Clin Orthop Relat Res*. 2010;468(6):1572-1577. doi:10.1007/s11999-009-1030-4

74. Gervasi E, Cautero E, Dekel A. Fluoroscopy-guided implantation of subacromial "Biodegradable Spacer" using local anesthesia in patients with irreparable rotator cuff tear. *Arthrosc Tech*. 2014;3(4):e455-e458. doi:10.1016/j.eats.2014.05.010

75. Di Giacomo G, Piscitelli L, Pugliese M. The role of bone in glenohumeral stability. *EFORT Open Rev*. 2018;3(12):632-640. doi:10.1302/2058-5241.3.180028

76. Giphart JE, Elser F, Dewing CB, Torry MR, Millett PJ. The long head of the biceps tendon has minimal effect on in vivo glenohumeral kinematics: A biplane fluoroscopy study. *Am J Sports Med*. 2012;40(1):202-212. doi:10.1177/0363546511423629

77. Goldberg SS, Bell JE, Han JK, Bak SF, Levine WN, Bigliani LU. Hemiarthroplasty for the rotator cuff-deficient shoulder. *J Bone Jt Surg - Ser A*. 2008;90(3):554-559. doi:10.2106/JBJS.F.01029

78. Goutallier D, Le Guilloux P, Postel JM, Radier C, Bernageau J, Zilber S. Acromio humeral distance less than six millimeter: Its meaning in full-thickness rotator cuff tear. *Orthop Traumatol Surg Res*. 2011;97(3):246-251.

doi:10.1016/j.otsr.2011.01.010

79. Grammont PM, Baulot E. Delta Shoulder Prosthesis for Rotator Cuff Rupture. *Orthopedics*. 1993;16(1):65-68. doi:10.3928/0147-7447-19930101-11

80. Grammont PM, Trouilloud P, Laffay J, Deries X. Concept study and realization of a new total shoulder prosthesis. *Rhumatologie*. 1987;39:407-418.

81. Gray H. *Gray's Anatomy*. Fifteenth. (Pick TP, Howden R, eds.). Chancellor Press; 1985.

82. Grimberg J, Kany J, Valenti P, Amaravathi R, Ramalingam AT. Arthroscopic-assisted latissimus dorsi tendon transfer for irreparable posterosuperior cuff tears. *Arthrosc - J Arthrosc Relat Surg*. 2015;31(4):599-607.e1. doi:10.1016/j.arthro.2014.10.005

83. Guery J, Favard L, Sirveaux F, Oudet D, Mole D, Walch G. Reverse total shoulder arthroplasty: Survivorship Analysis of Eighty Replacements Followed for Five to Ten Years. *Bone Joint J*. 2006;88(8):1742-1747. doi:10.1302/0301-620X.103B.BJJ-2020-2101

84. Habermeyer P, Magosch P, Rudolph T, Lichtenberg S, Liem D. Transfer of the tendon of latissimus dorsi for the treatment of massive tears of the rotator cuff. A new single-incision technique. *J Bone Jt Surg - Ser B*. 2006;88(2):208-212. doi:10.1302/0301-620X.88B2.16830

85. Habermeyer P, Krieter C, Tang K lai, Lichtenberg S, Magosch P. A new arthroscopic classification of articular-sided supraspinatus footprint lesions: A prospective comparison with Snyder's and Ellman's classification. *J Shoulder Elb Surg*. 2008;17(6):909-913. doi:10.1016/j.jse.2008.06.007

86. Halder AM, O'Driscoll SW, Heers G, et al. Biomechanical comparison of effects of supraspinatus tendon detachments, tendon defects, and muscle retractions. *J Bone Jt Surg - Ser A*. 2002;84(5):780-785. doi:10.2106/00004623-200205000-00013

87. Hamada K, Fukuda H, Mikasa M, Kobayashi Y. Roentgenographic findings in massive rotator cuff tears. A long-term observation. *Clin Orthop Relat Res*. 1990;254:92-96. doi:10.1097/00003086-199005000-00014

88. Hamid N, Omid R, Yamaguchi K, Steger-May K, Stobbs G, Keener JD. Relationship of radiographic acromial characteristics and rotator cuff disease: A prospective investigation of clinical, radiographic, and sonographic findings. *J Shoulder Elb Surg*. 2012;21(10):1289-1298. doi:10.1016/j.jse.2011.09.028

89. Harryman DT, Mack LA, Wang KY, Jackins SE, Richardson ML, Matsen FA. Repairs of the Rotator Cuff. *J Bone Jt Surg*. 1991;73-A(7):982-989.

90. Hartzler RU, Barlow JD, An KN, Elhassan BT. Biomechanical effectiveness of

different types of tendon transfers to the shoulder for external rotation. *J Shoulder Elb Surg*. 2012;21(10):1370-1376. doi:10.1016/j.jse.2012.01.026

91. Hartzler RU, Steen BM, Hussey MM, et al. Reverse shoulder arthroplasty for massive rotator cuff tear: Risk factors for poor functional improvement. *J Shoulder Elb Surg*. 2015;24(11):1698-1706. doi:10.1016/j.jse.2015.04.015

92. Hess SA. Functional stability of the glenohumeral joint. *Man Ther*. 2000;5(2):63-71. doi:10.1054/math.2000.0241

93. Holschen M, Brand F, Agneskirchner JD. Subacromial spacer implantation for massive rotatorcuff tears: Clinical outcome of arthroscopically treated patients. *Obere Extrem*. 2017;12(1):38-45. doi:10.1007/s11678-016-0386-9

94. Howell SM, Galinat BJ. The Glenoid-Labral Socket: A Constrained Articular Surface. *Clin Orthop Relat Res*. 1989;243:122-125.

95. Iannotfi J, Gabriel J, Schneck S, Evans B, Misra S. The Normal Glenohumeral Relations. *J Bone Jt Surg*. 1992;74:491-500.

96. Iannotti JP, Williams GR. Total Shoulder Arthroplasty: Factors Influencing Prosthetic Design. *Orthop Clin North Am*. 1998;29(3):377-391. doi:10.1016/B978-0-323-28683-1.00041-2

97. Inman VT, Saunders JB, Abbott LC. Observations of the function of the shoulder joint. *Clin Orthop Relat Res*. 1996;330:3-12. doi:10.1097/00003086-199609000-00002

98. Inokuchi W, Olsen BS, Søjbjerg JO, Sneppen O. The relation between the position of the glenohumeral joint and the intraarticular pressure: An experimental study. *J Shoulder Elb Surg*. 1997;6(2):144-149. doi:10.1016/S1058-2746(97)90035-5

99. Ishihara Y, Mihata T, Tamboli M, et al. Role of the superior shoulder capsule in passive stability of the glenohumeral joint. *J Shoulder Elb Surg*. 2014;23(5):642-648. doi:10.1016/j.jse.2013.09.025

100. Itami Y, Park MC, Lin CC, et al. Biomechanical analysis of progressive rotator cuff tendon tears on superior stability of the shoulder. *J Shoulder Elb Surg*. 2021;30(11):2611-2619. doi:10.1016/j.jse.2021.04.012

101. Itoi E, Motzkin NE, Morrey BF, An KN. Stabilizing function of the long head of the biceps in the hanging arm position. *J Shoulder Elb Surg*. 1994;3(3):135-142. doi:10.1016/S1058-2746(09)80092-X

102. Johns WL, Ailaney N, Lacy K, Golladay GJ, Vanderbeck J, Kalore N V. Implantable Subacromial Balloon Spacers in Patients With Massive Irreparable Rotator Cuff Tears: A Systematic Review of Clinical, Biomechanical, and Financial Implications. *Arthrosc Sport Med Rehabil*. 2020;2(6):e855-e872. doi:10.1016/j.asmr.2020.06.011

103. Jordan RW, Sharma N, Daggett M, Saithna A. The role of Superior Capsule Reconstruction in the irreparable rotator cuff tear — A systematic review. *Orthop Traumatol Surg Res*. 2019;105(8):1535-1542. doi:10.1016/j.otsr.2019.07.022

104. Kanatlı U, Özer M, Ataoğlu MB, et al. Arthroscopic-Assisted Latissimus Dorsi Tendon Transfer for Massive, Irreparable Rotator Cuff Tears: Technique and Short-Term Follow-Up of Patients With Pseudoparalysis. *Arthrosc - J Arthrosc Relat Surg*. 2017;33(5):929-937. doi:10.1016/j.arthro.2016.09.023

105. Kany J, Grimberg J, Amaravathi RS, Sekaran P, Scorpie D, Werthel JD. Arthroscopically-Assisted Latissimus Dorsi Transfer for Irreparable Rotator Cuff Insufficiency: Modes of Failure and Clinical Correlation. *Arthrosc - J Arthrosc Relat Surg*. 2018;34(4):1139-1150. doi:10.1016/j.arthro.2017.10.052

106. Kany J, Sekakaran P, Amavarathi RS, et al. Posterior latissimus dorsi transfer for massive irreparable posterosuperior rotator cuff tears: does it work in the elderly population? A comparative study between 2 age groups (≤55 vs. ≥75 years old). *J Shoulder Elb Surg*. 2021;30(3):641-651. doi:10.1016/j.jse.2020.06.018

107. Kany J, Sekaran P, Grimberg J, et al. Risk of latissimus dorsi tendon rupture after arthroscopic transfer for posterior superior rotator cuff tear: a comparative analysis of 3 humeral head fixation techniques. *J Shoulder Elb Surg*. 2020;29(2):282-290. doi:10.1016/j.jse.2019.06.019

108. Keener JD, Wei AS, Kim HM, Steger-May K, Yamaguchi K. Proximal humeral migration in shoulders with symptomatic and asymptomatic rotator cuff tears. *J Bone Jt Surg - Ser A*. 2009;91(6):1405-1413. doi:10.2106/JBJS.H.00854

109. Kelkar R, Wang VM, Flatow EL, et al. Glenohumeral mechanics: A study of articular geometry, contact, and kinematics. *J Shoulder Elb Surg*. 2001;10(1):73-84. doi:10.1067/mse.2001.111959

110. Kumar VP, Balasubramaniam P. The role of atmospheric pressure in stabilising the shoulder. An experimental study. *J Bone Jt Surg - Ser B*. 1985;67(5):719-721. doi:10.1302/0301-620x.67b5.4055867

111. Lacheta L, Horan MP, Schairer WW, et al. Clinical and Imaging Outcomes After Arthroscopic Superior Capsule Reconstruction With Human Dermal Allograft for Irreparable Posterosuperior Rotator Cuff Tears: A Minimum 2-Year Follow-Up. *Arthrosc - J Arthrosc Relat Surg*. 2020;36(4):1011-1019. doi:10.1016/j.arthro.2019.12.024

112. Lam F, Bhatia DN, Mostofi SB, van Rooyen K, de Beer JF. Biomechanical considerations of the normal and rotator cuff deficient shoulders and the reverse shoulder prosthesis. *Curr Orthop*. 2007;21(1):40-46. doi:10.1016/j.cuor.2006.10.004

113. Lapner P, Henry P, Athwal GS, Moktar J, McNeil D, MacDonald P. Treatment of

rotator cuff tears: a systematic review and meta-analysis. *J Shoulder Elb Surg*. 2022;31(3):e120-e129. doi:10.1016/j.jse.2021.11.002

114. Lee SB, Kim KJ, O'Driscoll SW, Morrey BF, An KN. Dynamic glenohumeral stability provided by the rotator cuff muscles in the mid-range and end-range of motion: A study in cadavera. *J Bone Jt Surg - Ser A*. 2000;82(6):849-857. doi:10.2106/00004623-200006000-00012

115. Levy AS, Kelly BT, Lintner SA, Osbahr DC, Speer KP. Function of the long head of the biceps at the shoulder: Electromyographic analysis. *J Shoulder Elb Surg*. 2001;10(3):250-255. doi:10.1067/mse.2001.113087

116. Lewington MR, Ferguson DP, Smith TD, Burks R, Coady C, Wong IHB. Graft Utilization in the Bridging Reconstruction of Irreparable Rotator Cuff Tears: A Systematic Review. *Am J Sports Med*. 2017;45(13):3149-3157. doi:10.1177/0363546517694355

117. Liem D, Lengers N, Dedy N, Poetzl W, Steinbeck J, Marquardt B. Arthroscopic Debridement of Massive Irreparable Rotator Cuff Tears. *Arthrosc - J Arthrosc Relat Surg*. 2008;24(7):743-748. doi:10.1016/j.arthro.2008.03.007

118. Lim S, AlRamadhan H, Kwak JM, Hong H, Jeon IH. Graft tears after arthroscopic superior capsule reconstruction (ASCR): pattern of failure and its correlation with clinical outcome. *Arch Orthop Trauma Surg*. 2019;139(2):231-239. doi:10.1007/s00402-018-3025-7

119. Lippitt SB, Vanderhooft JE, Harris SL, Sidles JA, Harryman DT, Matsen FA. Glenohumeral stability from concavity-compression: A quantitative analysis. *J Shoulder Elb Surg*. 1993;2(1):27-35. doi:10.1016/S1058-2746(09)80134-1

120. Liuzza L, Mai DH, Grey S, et al. Reverse Total Shoulder Arthroplasty with a Superior Augmented Glenoid Component for Favard Type-E1, E2, and E3 Glenoids. *Jounral Bone Jt Surgury*. 2020;102:1865-1873.

121. Lobao MH, Canham RB, Melvani RT, Abboud JA, Parks BG, Murthi AM. Biomechanics of Biodegradable Subacromial Balloon Spacer for Irreparable Superior Rotator Cuff Tears. *J Bone Jt Surg*. 2019;101(11):e49.

122. Lockhart J. *A Computational Investigation Into Acromial Fractures After A Computational Investigation Into Acromial Fractures After Reverse Total Shoulder Arthroplasty Reverse Total Shoulder Arthroplasty*.; 2020. Accessed October 1, 2020. https://ir.lib.uwo.ca/etdhttps://ir.lib.uwo.ca/etd/7204

123. Maffulli N, Longo UG, Berton A, Loppini M, Denaro V. Biological factors in the pathogenesis of rotator cuff tears. *Sports Med Arthrosc*. 2011;19(3):194-201. doi:10.1097/JSA.0b013e3182250cad

124. Makovicka JL, Chung AS, Patel KA, Deckey DG, Hassebrock JD, Tokish JM.

Superior capsule reconstruction for irreparable rotator cuff tears: a systematic review of biomechanical and clinical outcomes by graft type. *J Shoulder Elb Surg*. 2020;29(2):392-401. doi:10.1016/j.jse.2019.07.005

125. Malahias MA, Brilakis E, Avramidis G, Antonogiannakis E. Satisfactory mid-term outcome of subacromial balloon spacer for the treatment of irreparable rotator cuff tears. *Knee Surgery, Sport Traumatol Arthrosc*. 2019;27(12):3890-3896. doi:10.1007/s00167-019-05485-4

126. Malahias MA, Kostretzis L, Chronopoulos E, Brilakis E, Avramidis G, Antonogiannakis E. Arthroscopic partial repair for massive rotator cuff tears: does it work? A systematic review. *Sport Med - Open*. 2019;5(1). doi:10.1186/s40798-019-0186-z

127. Mamatha T, Pai SR, Murlimanju B V., Kalthur SG, Pai MM, Kumar B. Morphometry of glenoid cavity. *Online J Heal Allied Sci*. 2011;10(3):1-4.

128. Marigi EM, Harstad C, Elhassan B, Sanchez-Sotelo J, Wieser K, Kriechling P. Reverse shoulder arthroplasty after failed tendon transfer for irreparable posterosuperior rotator cuff tears. *J Shoulder Elb Surg*. 2022;31(4):763-771. doi:10.1016/j.jse.2021.08.026

129. Marigi EM, Johnson QJ, Dholakia R, Borah BJ, Sanchez-Sotelo J, Sperling JW. Cost comparison and complication profiles of superior capsular reconstruction, lower trapezius transfer, and reverse shoulder arthroplasty for irreparable rotator cuff tears. *J Shoulder Elb Surg*. 2022;31(4):847-854. doi:10.1016/j.jse.2021.08.027

130. Massimini DF, Boyer PJ, Papannagari R, Gill TJ, Warner JP, Li G. In-vivo glenohumeral translation and ligament elongation during abduction and abduction with internal and external rotation. *J Orthop Surg Res*. 2012;7(1):1-9. doi:10.1186/1749-799X-7-29

131. Matsen III F. Rotator Cuff 2 - Clinical Considerations Relating to Shoulder Strength. Shoulder Arthritis/Causes of rotator cuff tears: causes of shoulder pain. Published 2011. Accessed July 26, 2022. http://shoulderarthritis.blogspot.com/2011/08/

132. Matsuki K, Matsuki KO, Yamaguchi S, et al. Dynamic in vivo glenohumeral kinematics during scapular plane abduction in healthy shoulders. *J Orthop Sports Phys Ther*. 2012;42(2):96-104. doi:10.2519/jospt.2012.3584

133. McClincy MP, Rodosky MW. Arthroscopic Subacromial Decompression. *Oper Tech Orthop*. 2015;25(1):10-14. doi:10.1053/j.oto.2014.10.002

134. McGarry MH, Nguyen ML, Quigley RJ, Hanypsiak B, Gupta R, Lee TQ. The effect of long and short head biceps loading on glenohumeral joint rotational range of motion and humeral head position. *Knee Surgery, Sport Traumatol Arthrosc*. 2016;24(6):1979-1987. doi:10.1007/s00167-014-3318-5

135. Metcalfe A, Parsons H, Parsons N, et al. Subacromial balloon spacer for irreparable rotator cuff tears of the shoulder (START:REACTS): a group-sequential, double-blind, multicentre randomised controlled trial. *Lancet*. 2022;6736(22):1-10. doi:10.1016/s0140-6736(22)00652-3

136. Mihata T, Bui CNH, Akeda M, et al. A biomechanical cadaveric study comparing superior capsule reconstruction using fascia lata allograft with human dermal allograft for irreparable rotator cuff tear. *J Shoulder Elb Surg*. 2017;26(12):2158-2166. doi:10.1016/j.jse.2017.07.019

137. Mihata T, Lee TQ, Fukunishi K, et al. Return to Sports and Physical Work After Arthroscopic Superior Capsule Reconstruction Among Patients With Irreparable Rotator Cuff Tears. *Am J Sports Med*. 2018;46(5):1077-1083. doi:10.1177/0363546517753387

138. Mihata T, Lee TQ, Hasegawa A, et al. Arthroscopic Superior Capsule Reconstruction for Irreparable Rotator Cuff Tears: Comparison of Clinical Outcomes With and Without Subscapularis Tear. *Am J Sports Med*. 2020;48(14):3429-3438. doi:10.1177/0363546520965993

139. Mihata T, Lee TQ, Hasegawa A, et al. Arthroscopic Superior Capsule Reconstruction Can Eliminate Pseudoparalysis in Patients With Irreparable Rotator Cuff Tears. *Am J Sports Med*. 2018;46(11):2707-2716. doi:10.1177/0363546518786489

140. Mihata T, Lee TQ, Hasegawa A, et al. Five-Year Follow-up of Arthroscopic Superior Capsule Reconstruction for Irreparable Rotator Cuff Tears. *J Bone Jt Surg - Am Vol*. 2019;101(21):1921-1930. doi:10.2106/JBJS.19.00135

141. Mihata T, Lee TQ, Hasegawa A, et al. Superior Capsule Reconstruction for Reinforcement of Arthroscopic Rotator Cuff Repair Improves Cuff Integrity. *Am J Sports Med*. 2019;47(2):379-388. doi:10.1177/0363546518816689

142. Mihata T, Lee TQ, Watanabe C, et al. Clinical results of arthroscopic superior capsule reconstruction for irreparable rotator cuff tears. *Arthrosc - J Arthrosc Relat Surg*. 2013;29(3):459-470. doi:10.1016/j.arthro.2012.10.022

143. Mihata T, McGarry MH, Kahn T, Goldberg I, Neo M, Lee TQ. Biomechanical Effect of Thickness and Tension of Fascia Lata Graft on Glenohumeral Stability for Superior Capsule Reconstruction in Irreparable Supraspinatus Tears. *Arthrosc - J Arthrosc Relat Surg*. 2016;32(3):418-426. doi:10.1016/j.arthro.2015.08.024

144. Mihata T, McGarry MH, Kahn T, Goldberg I, Neo M, Lee TQ. Biomechanical role of capsular continuity in superior capsule reconstruction for irreparable tears of the supraspinatus tendon. *Am J Sports Med*. 2016;44(6):1423-1430. doi:10.1177/0363546516631751

145. Mihata T, McGarry MH, Kahn T, Goldberg I, Neo M, Lee TQ. Biomechanical

Effects of Acromioplasty on Superior Capsule Reconstruction for Irreparable Supraspinatus Tendon Tears. *Am J Sports Med*. 2016;44(1):191-197. doi:10.1177/0363546515608652

146. Mihata T, McGarry MH, Pirolo JM, Kinoshita M, Lee TQ. Superior capsule reconstruction to restore superior stability in irreparable rotator cuff tears: A biomechanical cadaveric study. *Am J Sports Med*. 2012;40(10):2248-2255. doi:10.1177/0363546512456195

147. Milgrom C, Schaffler M, Gilbert S, Van Holsbeeck M. Rotator-cuff changes in asymptomatic adults. The effect of age, hand dominance and gender. *J Bone Jt Surg - Ser B*. 1995;77(2):296-298. doi:10.1302/0301-620x.77b2.7706351

148. Mohamed RE, Abo-Sheisha DM. Assessment of acromial morphology in association with rotator cuff tear using magnetic resonance imaging. *Egypt J Radiol Nucl Med*. 2014;45(1):169-180. doi:10.1016/j.ejrnm.2013.11.013

149. Momma D, Espinoza Orías AA, Irie T, et al. Four-dimensional computed tomography evaluation of shoulder joint motion in collegiate baseball pitchers. *Sci Rep*. 2022;12(1):1-10. doi:10.1038/s41598-022-06464-5

150. Muench LN, Kia C, Williams AA, et al. High Clinical Failure Rate After Latissimus Dorsi Transfer for Revision Massive Rotator Cuff Tears. *Arthrosc - J Arthrosc Relat Surg*. 2020;36(1):88-94. doi:10.1016/j.arthro.2019.07.034

151. Muh SJ, Streit JJ, Wanner JP, et al. Early follow-up of reverse total shoulder arthroplasty in patients sixty years of age or younger. *J Bone Jt Surg - Ser A*. 2013;95(20):1877-1883. doi:10.2106/JBJS.L.10005

152. Mulieri P, Dunning P, Klein S, Pupello D, Frankle M. Reverse shoulder arthroplasty for the treatment of irreparable rotator cuff tear without glenohumeral arthritis. *J Bone Jt Surg - Ser A*. 2010;92(15):2544-2556. doi:10.2106/JBJS.I.00912

153. Mura N, O'Driscoll SW, Zobitz ME, et al. The effect of infraspinatus disruption on glenohumeral torque and superior migration of the humeral head: A biomechanical study. *J Shoulder Elb Surg*. 2003;12(2):179-184. doi:10.1067/mse.2003.9

154. Neer, Charles S, Poppen N. Supraspinatus outlet. *Orthop Trans*. 1987;11:234.

155. Neer CS. Replacement arthroplasty for glenohumeral osteoarthritis. *J Bone Jt Surg - Ser A*. 1974;56(1):1-13. doi:10.2106/00004623-197456010-00001

156. Neer CS. Articular Replacement for the Humeral Head. *J Bone Jt Surg*. 1955;37:215-228.

157. NeerII CS. Anterior Acromioplasty for the Chronic Impingement Syndrome in the Shoulder. *J Bone Jt Surg*. 1972;87(6):1399. doi:10.2106/jbjs.8706.cl

158. Nho SJ, Yadav H, Shindle MK, MacGillivray JD. Rotator cuff degeneration: Etiology and pathogenesis. *Am J Sports Med*. 2008;36(5):987-993. doi:10.1177/0363546508317344

159. Nicholson AD, Estrada JA, Mathew JI, et al. Minimum 15-Year Follow-Up for Clinical Outcomes of Arthroscopic Rotator Cuff Repair. *J Shoulder Elb Surg*. 2022;31(8):1696-1703. doi:10.1016/j.jse.2022.01.116

160. Nyffeler RW, Werner CML, Sukthankar A, Schmid MR, Gerber C. Association of a large lateral extension of the acromion with rotator cuff tears. *J Bone Jt Surg*. 2006;88(4):800-805. doi:10.2106/00004623-200608000-00031

161. Ogawa K, Yoshida A, Inokuchi W, Naniwa T. Acromial spur: Relationship to aging and morphologic changes in the rotator cuff. *J Shoulder Elb Surg*. 2005;14(6):591-598. doi:10.1016/j.jse.2005.03.007

162. Oh JH, Jun BJ, McGarry MH, Lee TQ. Does a Critical Rotator Cuff Tear Stage Exist? *J Bone Jt Surg*. 2011;93(22):2100-2109. doi:10.2106/jbjs.j.00032

163. Omid R, Cavallero MJ, Granholm D, Villacis DC, Yi AM. Surgical anatomy of the lower trapezius tendon transfer. *J Shoulder Elb Surg*. 2015;24(9):1353-1358. doi:10.1016/j.jse.2014.12.033

164. Omid R, Heckmann N, Wang L, McGarry MH, Vangsness CT, Lee TQ. Biomechanical comparison between the trapezius transfer and latissimus transfer for irreparable posterosuperior rotator cuff tears. *J Shoulder Elb Surg*. 2015;24(10):1635-1643. doi:10.1016/j.jse.2015.02.008

165. Otis JC, Jiang CC, Wickiewicz TL, Peterson MGE, Warren RF, Santner TJ. Changes in the moment arms of the rotator cuff and deltoid muscles with abduction and rotation. *J Bone Jt Surg - Ser A*. 1994;76(5):667-676. doi:10.2106/00004623-199405000-00007

166. Pandey V, Jaap Willems W. Rotator cuff tear: A detailed update. *Asia-Pacific J Sport Med Arthrosc Rehabil Technol*. 2015;2(1):1-14. doi:10.1016/j.asmart.2014.11.003

167. Parsons IM, Apreleva M, Fu FH, Woo SLY. The effect of rotator cuff tears on reaction forces at the glenohumeral joint. *J Orthop Res*. 2002;20(3):439-446. doi:10.1016/S0736-0266(01)00137-1

168. Patte D. Classification of rotator cuff lesions. *Clin Orthop Relat Res*. 1990;254:81-86. doi:10.1097/00003086-199005000-00012

169. Pennington WT, Bartz BA, Pauli JM, Walker CE, Schmidt W. Arthroscopic Superior Capsular Reconstruction With Acellular Dermal Allograft for the Treatment of Massive Irreparable Rotator Cuff Tears: Short-Term Clinical Outcomes and the Radiographic Parameter of Superior Capsular Distance. *Arthrosc*

- *J Arthrosc Relat Surg*. 2018;34(6):1764-1773. doi:10.1016/j.arthro.2018.01.009

170. Petriccioli D, Bertone C, Marchi G. Recovery of active external rotation and elevation in young active men with irreparable posterosuperior rotator cuff tear using arthroscopically assisted latissimus dorsi transfer. *J Shoulder Elb Surg*. 2016;25(9):e265-e275. doi:10.1016/j.jse.2015.12.011

171. Petrillo S, Longo UG, Papalia R, Denaro V. Reverse shoulder arthroplasty for massive irreparable rotator cuff tears and cuff tear arthropathy: a systematic review. *Musculoskelet Surg*. 2017;101(2):105-112. doi:10.1007/s12306-017-0474-z

172. Piekaar RSM, Bouman ICE, van Kampen PM, van Eijk F, Huijsmans PE. Early promising outcome following arthroscopic implantation of the subacromial balloon spacer for treating massive rotator cuff tear. *Musculoskelet Surg*. 2018;102(3):247-255. doi:10.1007/s12306-017-0525-5

173. Piekaar RSM, Bouman ICE, van Kampen PM, van Eijk F, Huijsmans PE. The subacromial balloon spacer for massive irreparable rotator cuff tears: approximately 3 years of prospective follow-up. *Musculoskelet Surg*. 2020;104(2):207-214. doi:10.1007/s12306-019-00614-1

174. Prat D, Tenenbaum S, Pritsch M, Oran A, Vogel G. Sub-acromial balloon spacer for irreparable rotator cuff tears: Is it an appropriate salvage procedure? *J Orthop Surg*. 2018;26(2). doi:10.1177/2309499018770887

175. Ranebo MC, Björnsson Hallgren HC, Norlin R, Adolfsson LE. Long-term clinical and radiographic outcome of rotator cuff repair with a synthetic interposition graft: a consecutive case series with 17 to 20 years of follow-up. *J Shoulder Elb Surg*. 2018;27(9):1622-1628. doi:10.1016/j.jse.2018.03.011

176. Rauck RC, Jahandar A, Kontaxis A, et al. The Role of the Long Head of the Biceps Tendon in Posterior Shoulder Stabilization during Forward Flexion. *J Shoulder Elb Surg*. 2022;31:1254-1260. doi:10.1016/j.jse.2021.12.026

177. Ravenscroft M, Barnes MW, Muench LN, Mazzocca AD, Berthold DP. Bursal Acromial Reconstruction (BAR) Using an Acellular Dermal Allograft as a Surgical Solution for the Treatment of Massive Irreparable Rotator Cuff Tears. *Arthrosc Tech*. 2021;10(3):e877-e885. doi:10.1016/j.eats.2020.11.002

178. Reeves JM, Singh S, Langohr GDG, Athwal GS, Johnson JA. An in-vitro biomechanical assessment of humeral head migration following irreparable rotator cuff tear and subacromial balloon reconstruction. *Shoulder Elb*. 2020;12(4):265-271. doi:10.1177/1758573219865479

179. Ricci M, Vecchini E, Micheloni GM, et al. A clinical and radiological study of biodegradable subacromial spacer in the treatment of massive irreparable rotator cuff tears. *Acta Biomed*. 2017;88(5):75-80. doi:10.23750/abm.v88i4-S.6797

180. Rodosky MW, Harner CD, Fu FH. The Role of the Long Head of the Biceps Muscle and Superior Glenoid Labrum in Anterior Stability of the Shoulder. *Am J Sports Med*. 1994;22(1):121-130. doi:10.1177/036354659402200119

181. Ruiz Ibán MA, Lorente Moreno R, Ruiz Díaz R, et al. The absorbable subacromial spacer for irreparable posterosuperior cuff tears has inconsistent results. *Knee Surgery, Sport Traumatol Arthrosc*. 2018;26(12):3848-3854. doi:10.1007/s00167-018-5083-3

182. Rybalko D, Bobko A, Amirouche F, et al. Biomechanics in an Incomplete Versus Complete Supraspinatus Tear: A Cadaveric Study. *Orthop J Sport Med*. 2020;8(12):1-7. doi:10.1177/2325967120964476

183. Rybalko D, Bobko A, Amirouche F, et al. The biomechanics of the supraspinatus-deficient shoulder treated with superior capsular reconstruction vs. reverse total shoulder arthroplasty—experimental study. *Int Orthop*. 2020;44(11):2371-2377. doi:10.1007/s00264-020-04674-y

184. Rybalko D, Bobko A, Amirouche F, et al. Biomechanical effects of superior capsular reconstruction in a rotator cuff–deficient shoulder: a cadaveric study. *J Shoulder Elb Surg*. 2020;29(10):1959-1966. doi:10.1016/j.jse.2020.03.007

185. Saha AK. Dynamic stability of the glenohumeral joint. *Acta Orthop*. 1971;42(6):491-505. doi:10.3109/17453677108989066

186. Samuelsen BT, Wagner ER, Houdek MT, et al. Primary reverse shoulder arthroplasty in patients aged 65 years or younger. *J Shoulder Elb Surg*. 2017;26(1):e13-e17. doi:10.1016/j.jse.2016.05.026

187. Sanchez-Sotelo J, Cofield RH, Rowland CM. Shoulder hemiarthroplasty for glenohumeral arthritis associated with severe rotator cuff deficiency. *J Bone Jt Surg - Ser A*. 2001;83(12):1814-1822. doi:10.2106/00004623-200112000-00008

188. Saupe N, Pfirrmann CWA, Schmid MR, Jost B, Werner CML, Zanetti M. Association between rotator cuff abnormalities and reduced acromiohumeral distance. *Am J Roentgenol*. 2006;187(2):376-382. doi:10.2214/AJR.05.0435

189. Savarese E, Romeo R. New Solution for Massive, Irreparable Rotator Cuff Tears: The Subacromial "Biodegradable Spacer." *Arthrosc Tech*. 2012;1(1):e69-e74. doi:10.1016/j.eats.2012.02.002

190. Scheiderer B, Kia C, Obopilwe E, et al. Biomechanical Effect of Superior Capsule Reconstruction Using a 3-mm and 6-mm Thick Acellular Dermal Allograft in a Dynamic Shoulder Model. *Arthrosc - J Arthrosc Relat Surg*. 2020;36(2):355-364. doi:10.1016/j.arthro.2019.08.026

191. Senekovic V, Poberaj B, Kovacic L, et al. The biodegradable spacer as a novel treatment modality for massive rotator cuff tears: a prospective study with 5-year

follow-up. *Arch Orthop Trauma Surg*. 2017;137(1):95-103. doi:10.1007/s00402-016-2603-9

192. Senekovic V, Poberaj B, Kovacic L, Mikek M, Adar E, Dekel A. Prospective clinical study of a novel biodegradable sub-acromial spacer in treatment of massive irreparable rotator cuff tears. *Eur J Orthop Surg Traumatol*. 2013;23(3):311-316. doi:10.1007/s00590-012-0981-4

193. Seo J, Heo K, Kwon S, Yoo J. Critical shoulder angle and greater tuberosity angle according to the partial thickness rotator cuff tear patterns. *Orthop Traumatol Surg Res*. 2019;105(8):1543-1548. doi:10.1016/j.otsr.2019.05.005

194. Sevivas N, Ferreira N, Andrade R, et al. Reverse shoulder arthroplasty for irreparable massive rotator cuff tears: a systematic review with meta-analysis and meta-regression. *J Shoulder Elb Surg*. 2017;26(9):e265-e277. doi:10.1016/j.jse.2017.03.039

195. Shepet KH, Liechti DJ, Kuhn JE. Nonoperative treatment of chronic, massive irreparable rotator cuff tears: a systematic review with synthesis of a standardized rehabilitation protocol. *J Shoulder Elb Surg*. 2021;30(6):1431-1444. doi:10.1016/j.jse.2020.11.002

196. Shi LL, Cahill KE, Ek ET, Tompson JD, Higgins LD, Warner JJP. Latissimus Dorsi and Teres Major Transfer With Reverse Shoulder Arthroplasty Restores Active Motion and Reduces Pain for Posterosuperior Cuff Dysfunction. *Clin Orthop Relat Res*. 2015;473(10):3212-3217. doi:10.1007/s11999-015-4433-4

197. Shoulderdoc.co.uk. InSpace Balloon for Massive Rotator Cuff Tears. Published 2022. https://www.shoulderdoc.co.uk/article/1642

198. Singh S. A Biomechanical Study Examining The Subacromial Balloon Spacer and Superior Capsular Reconstruction in the Treatment of Massive, Irrepa. Published online 2017. Accessed November 12, 2020. https://ir.lib.uwo.ca/etdhttps://ir.lib.uwo.ca/etd/5134

199. Singh S, Reeves J, Langohr GDG, Johnson JA, Athwal GS. The Subacromial Balloon Spacer Versus Superior Capsular Reconstruction in the Treatment of Irreparable Rotator Cuff Tears: A Biomechanical Assessment. *Arthrosc - J Arthrosc Relat Surg*. 2019;35(2):382-389. doi:10.1016/j.arthro.2018.09.016

200. Singh S, Reeves J, Langohr GDG, Johnson JA, Athwal GS. The effect of the subacromial balloon spacer on humeral head translation in the treatment of massive, irreparable rotator cuff tears: a biomechanical assessment. *J Shoulder Elb Surg*. 2019;28(10):1841-1847. doi:10.1016/j.jse.2019.03.036

201. Siow MY, Mitchell BC, Hachadorian M, et al. Association Between Rotator Cuff Tears and Superior Migration of the Humeral Head: An MRI-Based Anatomic Study. *Orthop J Sport Med*. 2021;9(6):1-7. doi:10.1177/23259671211009846

202. Sirveaux F, Favard L, Oudet D, Huquet D, Walch G, Molé D. Grammont inverted total shoulder arthroplasty in the treatment of glenohumeral osteoarthritis with massive rupture of the cuff. Results of a multicentre study of 80 shoulders. *J Bone Jt Surg*. 2004;86(3):388-395. doi:10.1302/0301-620X.86B3.14024

203. Smith GCS, Im HY, Lam PH. Effect of human dermal allograft thickness on glenohumeral stability for superior capsular reconstruction in irreparable supraspinatus tears: A biomechanical analysis of the superior capsular reconstruction – A cadaveric study. *Shoulder Elb*. 2022;14(1):31-37. doi:10.1177/1758573220925086

204. Soderlund M, Boren M, O'Reilly A, San Juan A, Mahylis JM. Arthroscopic debridement for management of massive, irreparable rotator cuff tears: a systematic review of outcomes. *JSES Rev Reports, Tech*. 2022;2(1):1-7. doi:10.1016/j.xrrt.2021.08.012

205. Stewart RK, Kaplin L, Parada SA, Graves BR, Verma NN, Waterman BR. Outcomes of Subacromial Balloon Spacer Implantation for Massive and Irreparable Rotator Cuff Tears: A Systematic Review. *Orthop J Sport Med*. 2019;7(10):1-10. doi:10.1177/2325967119875717

206. Su Cho N, Jeong WK, McGarry MH, Lee T. Biomechanics and Clinical Function of the Rotator Cuff. In: Provencher M, Cole B, Romeo A, Boileau P, Verma N, eds. *Disorders of the Rotator Cuff and Biceps Tendon: The Surgeon's Guide to Comprehensive Management*. 1st ed. Elsevier. https://books.google.ca/books?hl=en&lr=&id=ZRWbDwAAQBAJ&oi=fnd&pg=PA16&dq=info:CzE2MyGUWf0J:scholar.google.com&ots=nHf4B6uTUl&sig=wy5bKvmisslc8u-r1jswWxjDjog&redir_esc=y#v=onepage&q&f=false

207. Su WR, Budoff JE, Luo ZP. Posterosuperior displacement due to rotator cuff tears. *Arthrosc - J Arthrosc Relat Surg*. 2011;27(11):1472-1477. doi:10.1016/j.arthro.2011.06.018

208. Synder S. *Arthroscopic Classification of Rotator Cuff Lesions and Surgical Decision Making*. Lippincott Williams, and Wilkins; 2003.

209. Tashjian RZ. The Natural History of Rotator Cuff Disease: Evidence in 2016. *Tech Shoulder Elb Surg*. 2016;17(4):132-138. doi:10.1097/BTE.0000000000000109

210. Tempelaere C, Pierrart J, Lefèvre-Colau MM, et al. Dynamic three-dimensional shoulder Mri during active motion for investigation of rotator cuff diseases. *PLoS One*. 2016;11(7):1-12. doi:10.1371/journal.pone.0158563

211. Terrier A, Reist A, Vogel A, Farron A. Effect of supraspinatus deficiency on humerus translation and glenohumeral contact force during abduction. *Clin Biomech*. 2007;22(6):645-651. doi:10.1016/j.clinbiomech.2007.01.015

212. Terry GC, Chopp TM. Functional Anatomy of the Shoulder. *J Athl Train*.

2000;35(3):248-255. doi:10.1093/ptj/46.10.1043

213. Teunis T, Lubberts B, Reilly BT, Ring D. A systematic review and pooled analysis of the prevalence of rotator cuff disease with increasing age. *J Shoulder Elb Surg*. 2014;23(12):1913-1921. doi:10.1016/j.jse.2014.08.001

214. Tibone JE, Mansfield C, Kantor A, et al. Human Dermal Allograft Superior Capsule Reconstruction With Graft Length Determined at Glenohumeral Abduction Angles of 20° and 40° Decreases Joint Translation and Subacromial Pressure Without Compromising Range of Motion: A Cadaveric Biomechanical Study. *Arthrosc J Arthrosc Relat Surg*. 2022;38(5):1398-1407. doi:10.1016/j.arthro.2021.11.007

215. Turkel SJ, Panio MW, Marshall JL, Girgis FG. Stabilizing mechanisms preventing anterior dislocation of the glenohumeral joint. *J Bone Jt Surg*. 1981;63(A):1208-1217. doi:10.1007/978-1-4471-5451-8_76

216. Verma N, Srikumaran U, Roden C, et al. InSpace Implant Compared with Partial Repair for the Treatment of Full-Thickness Massive Rotator Cuff Tears. *J Bone Jt Surg*. 2022;0:1250-1262. https://jbjs.org/reader.php?rsuite_id=3282610&native=1&source=The_Journal_of_Bone_and_Joint_Surgery/Publish Ahead of Print//10.2106/JBJS.21.00667/abstract&topics=sh#info

217. Virk MS, Nicholson GP, Romeo AA. Irreparable Rotator Cuff Tears Without Arthritis Treated With Reverse Total Shoulder Arthroplasty. *Open Orthop J*. 2018;10(1):296-308. doi:10.2174/1874325001610010296

218. Visotsky JL, Basamania C, Seebauer L, Rockwood CA, Jensen KL. Cuff Tear Arthropathy: Pathogenesis, Classification, and Algorithm for Treatment. *J Bone Jt Surg*. 2004;86:35-40. doi:10.2106/00004623-200412002-00007

219. Viswanath A, Drew S. Subacromial balloon spacer – Where are we now? *J Clin Orthop Trauma*. 2021;17:223-232. doi:10.1016/j.jcot.2021.03.017

220. Vredenburgh ZD, Prodromo JP, Tibone JE, et al. Biomechanics of tensor fascia lata allograft for superior capsular reconstruction. *J Shoulder Elb Surg*. 2021;30(1):178-187. doi:10.1016/j.jse.2020.04.025

221. Wagner ER, Elhassan BT. Surgical Management of Massive Irreparable Posterosuperior Rotator Cuff Tears: Arthroscopic-Assisted Lower Trapezius Transfer. *Curr Rev Musculoskelet Med*. 2020;13(5):592-604. doi:10.1007/s12178-020-09657-5

222. Wall B, Nové-Josserand L, O'Connor DP, Edwards TB, Walch G. Reverse total shoulder arthroplasty: A review of results according to etiology. *J Bone Jt Surg - Ser A*. 2007;89(7):1476-1485. doi:10.2106/JBJS.F.00666

223. Wang HJ, Giambini H, Hou DB, et al. Classification and Morphological Parameters

of the Scapular Spine. *Med (United States)*. 2015;94(45):e1986. doi:10.1097/MD.0000000000001986

224. Warner JJP, Bowen MK, Deng XH, Hannafin JA, Arnoczky SP, Warren RF. Articular contact patterns of the normal glenohumeral joint. *J Shoulder Elb Surg*. 1998;7(4):381-388. doi:10.1016/S1058-2746(98)90027-1

225. Warner JJP, McMahon PJ. The role of the long head of the biceps brachii in superior stability of the glenohumeral joint. *J Bone Jt Surg - Ser A*. 1995;77(3):366-372. doi:10.2106/00004623-199503000-00006

226. Warth RJ, Millett PJ. Glenohumeral Instability. In: *Physical Examination of the Shoulder: An Evidence-Based Approach*. 1st ed. Springer Science+Business Media; 2015:139-181. doi:10.1007/978-1-4939-2593-3

227. Wieser K, Ernstbrunner L, Zumstein MA. Surgical Management of Massive Irreparable Cuff Tears: Latissimus Dorsi Transfer for Posterosuperior Tears. *Curr Rev Musculoskelet Med*. 2020;13(5):605-611. doi:10.1007/s12178-020-09659-3

228. Williams GR, Rockwood CA. Hemiarthroplasty in rotator cuff-deficient shoulders. *J Shoulder Elbow Surg*. 1996;5(5):362-367. doi:10.1016/s1058-2746(96)80067-x

229. Woodmass JM, Wagner ER, Borque KA, Chang MJ, Welp KM, Warner JJP. Superior capsule reconstruction using dermal allograft: early outcomes and survival. *J Shoulder Elb Surg*. 2019;28(6):S100-S109. doi:10.1016/j.jse.2019.04.011

230. Wueler N, Korell M, Thren K. Dynamic glenohumeral joint stability. *J Shoulder Elb Surg*. 1998;7(1):43-52.

231. Yallapragada RK, Apostolopoulos A, Katsougrakis I, Selvan TP. The use of a subacromial spacer-inspace balloon in managing patients with irreparable rotator cuff tears. *J Orthop*. 2018;15(3):862-868. doi:10.1016/j.jor.2018.08.004

232. Yamakado K. Clinical and Radiographic Outcomes With Assessment of the Learning Curve in Arthroscopically Assisted Latissimus Dorsi Tendon Transfer for Irreparable Posterosuperior Rotator Cuff Tears. *Arthrosc - J Arthrosc Relat Surg*. 2017;33(12):2144-2151. doi:10.1016/j.arthro.2017.06.015

233. Yamamoto A, Takagishi K, Osawa T, et al. Prevalence and risk factors of a rotator cuff tear in the general population. *J Shoulder Elb Surg*. 2010;19(1):116-120. doi:10.1016/j.jse.2009.04.006

234. Yamamoto N, Itoi E. Treatment of irreparable rotator cuff tears with superior capsular reconstruction. *J Exp Orthop*. 2021;8(1):4-9. doi:10.1186/s40634-021-00342-1

235. Young BL, Connor PM, Schiffern SC, Roberts KM, Hamid N. Reverse shoulder arthroplasty with and without latissimus and teres major transfer for patients with

combined loss of elevation and external rotation: a prospective, randomized investigation. *J Shoulder Elb Surg*. 2020;29(5):874-881. doi:10.1016/j.jse.2019.12.024

236. Zuckerman JD, Scott AJ, Gallagher MA. Hemiarthroplasty for cuff tear arthropathy. *J Shoulder Elb Surg*. 2000;9(3):169-172. doi:10.1067/mse.2000.105138

237. Zvijac JE, Levy HJ, Lemak LJ. Arthroscopic subacromial decompression in the treatment of full thickness rotator cuff tears: A 3- to 6-year follow-up. *Arthroscopy*. 1994;10(5):518-523. doi:10.1016/S0749-8063(05)80006-4

Chapter 2

2 Design and Fabrication of a Subacromial Implant

This chapter describes the process of designing and fabricating a subacromial implant for the purpose of restoring normal glenohumeral joint stability in patients with massive irreparable posterosuperior rotator cuff tears. The chapter begins by reviewing the symptoms of this pathology and the treatment options currently available. The idea of a rigid subacromial implant for restoring normal joint stability in these patients is then introduced, outlining how this concept differs from current treatment options and the potential advantages it may provide. This is followed by a description of the original subacromial implant design and the changes made to this design in order to improve function and also fixation to bone. This chapter concludes by detailing the fabrication process used to create the final design of the subacromial implant (that is tested in Chapter 3 and 4).

2.1 Introduction[2]

Rotator cuff tears (RCTs) are one of the most common shoulder injuries observed clinically and can be a significant source of pain and disfunction[36]. These tears occur in the tendons connecting the rotator cuff muscles to the humeral head. Tears in the rotator cuff can exist in several different configurations and sizes, although massive posterosuperior RCTs are of concern to many clinicians due to their disruptive influence on normal glenohumeral stability. Massive tears are commonly classified as tears greater then 5cm in length and involving two or more tendons[3,6,10], while posterosuperior tears make reference to the tear location relative to the humeral head. Posterosuperior tears often involve tears of the supraspinatus and part of the infraspinatus muscles. These massive posterosuperior RCTs disrupt the synergetic relationship between rotator cuff muscles and deltoid, thereby affecting the normal fulcrum of the glenohumeral joint. Disruption of this normal joint

[2] This review is similar to that covered in Chapter 1 but is provided here for completeness.

stability is often observed through superior and posterior translation of the humeral head[13]. This translation can also contribute to decreased mechanical efficiency of the glenohumeral joint[8], and the potential onset of cuff tear arthropathy[24]. Although massive RCTs can sometimes be surgically repaired in patients, there are instances where the muscle has retracted too far into the joint. This makes repair of the tendon to its original insertion site very difficult or impossible. These types of tears are often referred to as irreparable and require alternative treatment options.

Four common surgical interventions used for treating massive irreparable posterosuperior RCTs include tendon transfers, the insertion of a subacromial balloon, superior capsule reconstruction (SCR), and reverse shoulder arthroplasty. All of these procedures are designed to restore the normal stability of the glenohumeral joint, with each intervention utilizing different methods to do so. Tendon transfers involve transferring an active muscle unit from elsewhere in the body to the glenohumeral joint to best replicate the native function of the posterior rotator cuff. This transferred muscle unit can be trained post-operatively to depress the humeral head and aid in external rotation, thereby helping to restore normal joint stability[37]. These procedures however can be technically demanding[40] and can exhibit high complication rates[14,15,22]. The subacromial balloon is a passive, biodegradable device that is positioned between the humeral head and undersurface of the acromion arthroscopically. This balloon functions as a spacer to prevent superior and posterior translation of the humeral head when inflated[32]. Several studies have reported positive clinical outcomes using this device[9,27,33], while others have called into question the effectiveness of this treatment as a long-term solution for these patients[7,28,30]. SCR is another surgical procedure that utilizes a passive technique to prevent the humeral head from translating superiorly. This procedure however uses a graft that is tensioned to both medial and lateral sides of the joint to prevent superior translation of the humerus[21]. Furthermore, since the graft is inserted with the arm slightly abducted, the tension within the graft contributes to early abduction. Although studies have reported SCR to relieve pain and improve shoulder function[2,20,19,25], high rates of graft failure and poor clinical outcomes have also been reported[5,17,38]. Reverse shoulder arthroplasty is a well-established procedure that involves the replacement of both medial and lateral glenohumeral joint surfaces with implants. The design of these implants reverses the native anatomy of the glenohumeral

joint, which serves to medialize the joint center of rotation and increase the mechanical efficiency of the shoulder. Reverse shoulder arthroplasty has been reported to have good clinical outcomes when treating massive irreparable RCTs[4,26,34]. However, usage in younger, more active patients is still questioned with evidence of higher complication rates[11,12,23].

The optimal treatment for younger and higher functioning patients with massive irreparable RCTs is still unclear. While the surgical interventions discussed above all demonstrate the ability to restore normal glenohumeral joint stability, their efficacy is called into question for meeting the long-term needs of these higher functioning patients. These treatments do not utilize the concept of a rigid spacer device securely fixed within the glenohumeral joint to prevent superior and posterior translation of the humeral head. Such a device could be advantageous to this specific patient demographic in that it could serve as a durable solution, with rigid fixation allowing for long-term use. Recently, the concept of a subacromial implant (REACH Orthopaedics, Halifax, N.S., Canada) was proposed which includes these unique features. However, this device has yet to be thoroughly designed and tested for its ability to restore normal glenohumeral joint stability.

The objective of this study was to design a subacromial implant for the purpose of restoring normal glenohumeral stability in the presence of a massive irreparable rotator cuff tear. The implant had to be designed using average scapular morphology and created as a modular device, representing different implant variables.

2.2 Original Implant Design

The original design for the subacromial implant was proposed by REACH Orthopaedics (Figure 2-1). The implant was designed to be positioned along the undersurface of the acromion and posterior aspect of the scapular spine (Figure 2-2). This device consists of two distinct features: a spacer and a fixation plate. The spacer of the implant comprises the volumetric majority of this device. The shape of the spacer viewed in the transverse plane mimics that of the acromion to reduce the overhang of the implant beyond this osseous structure. An important aspect of the spacer region is its inferior surface, which serves to articulate with the humeral head. This surface is concave in nature with large fillets

surrounding the periphery of this surface to reduce potential impingement with the humerus. The spacer's superior surface is curved to match the undersurface of the acromion to which it is positioned against. The fixation plate of the implant is a long narrow structure that extends medially along the posterior surface of the scapular spine. This plate was designed with three countersunk holes along its length for 3.5mm cortical compression screws used to fix the implant to the scapula along the scapula spine.

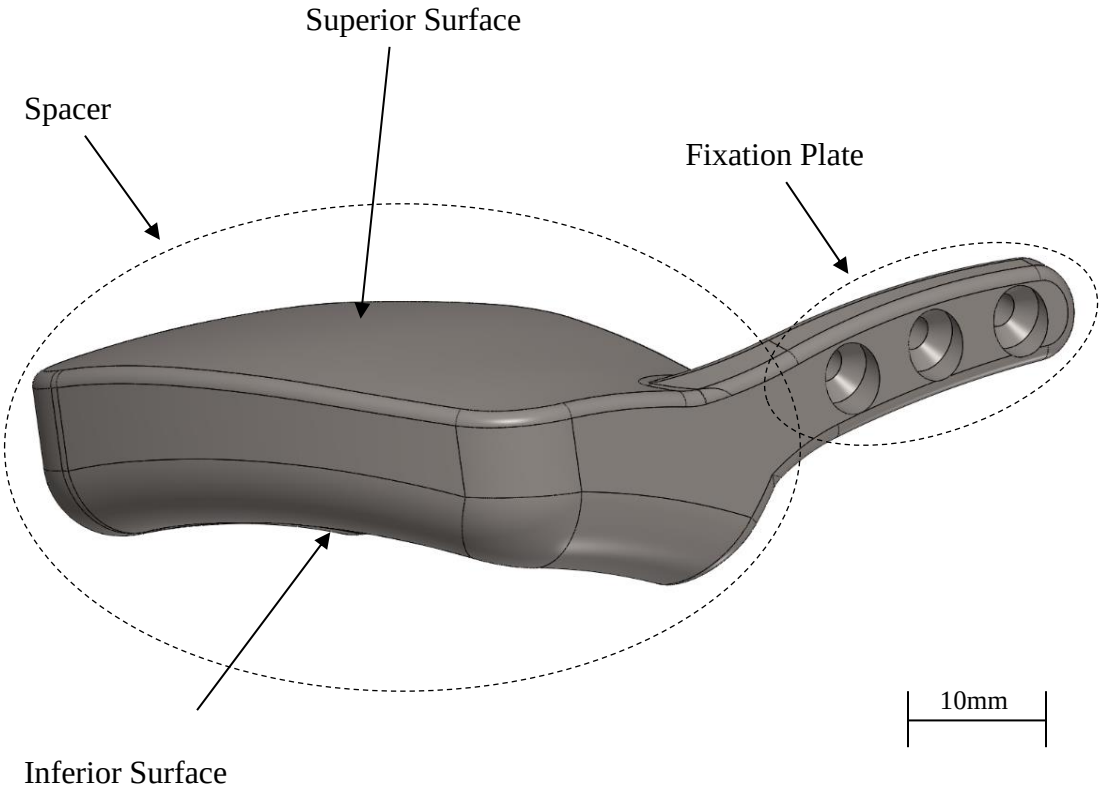

Figure 2-1: Originally proposed implant design.

The design consists of two primary features: the spacer and the fixation plate. Scale shown for reference.

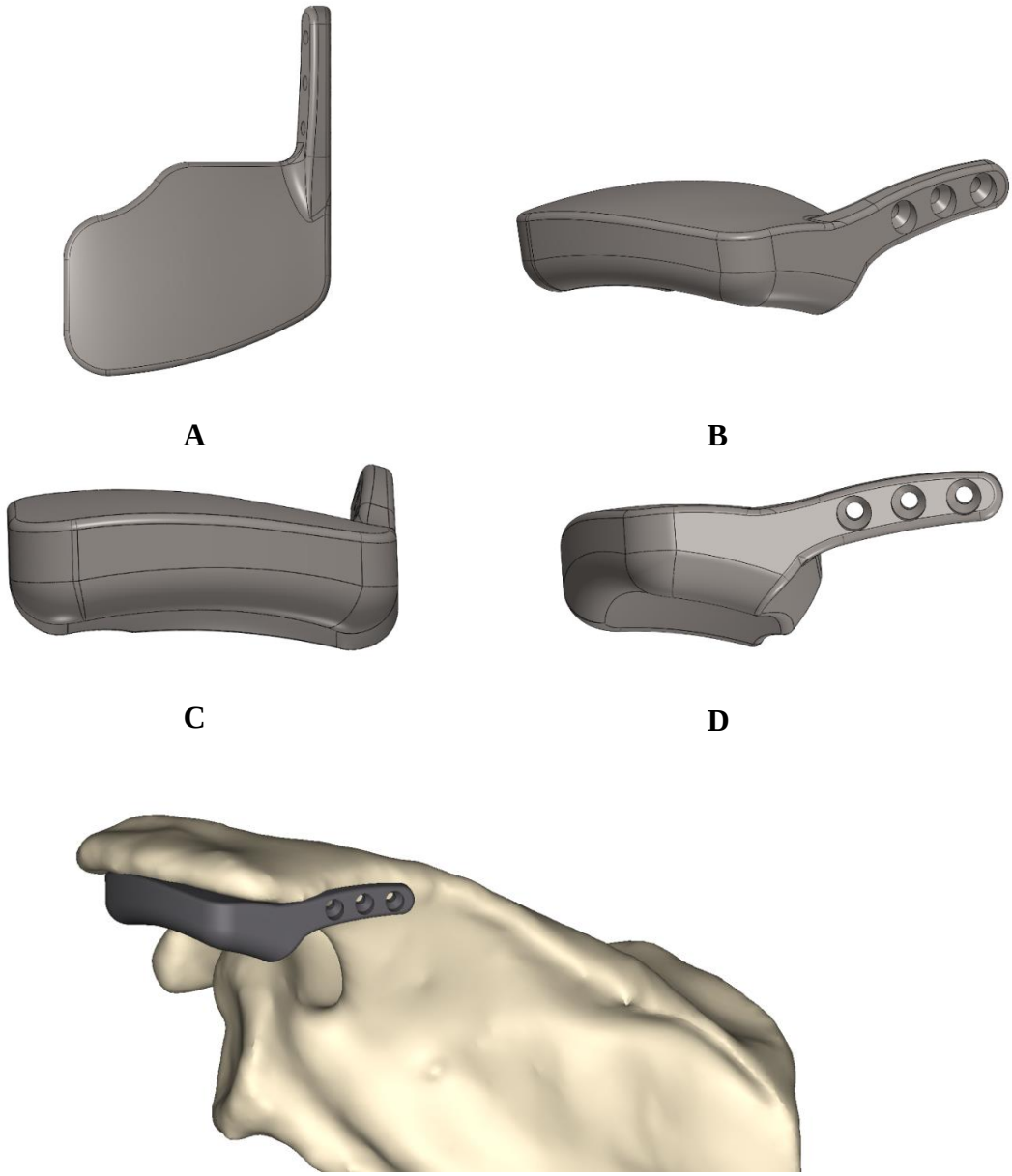

Figure 2-2: Different views of the original subacromial implant design.

(A) Superior view, (B) Lateral-posterior view, (C) Lateral View, (D) Posterior view, (E) Image illustrating implant positioning relative to scapular spine and acromion.

As stated, the purpose of this subacromial implant is to prevent superior and posterior translation of the humerus in the presence of a massive irreparable posterosuperior RCT. The implant prevents translation of the humerus in these directions as it is positioned superiorly and posteriorly relative to the glenohumeral joint. The thickness of the spacer clearly influences the extent to which translation of the humerus is reduced, while the inferior surface of the implant's spacer region serves to smoothly articulate with the superior aspect of the humeral head. The fixation plate of the implant meanwhile serves to securely fix the implant to the scapula. This device is similar to the subacromial balloon in that it shares the same position relative to the glenohumeral joint and that it passively serves as a barrier to humeral head translation. However, the rigid and fixed aspects of this implant suggest this device may be more advantageous to a younger, more active patient demographic for providing long term glenohumeral stability. This implant may also have a long lifespan if made from a rigid material, such as metal similar to other hemiarthroplasty implants. Furthermore, it does not require removal of bone at the joint as opposed to other arthroplasty procedures. This may be advantageous to a younger patient demographic without glenohumeral arthritis.

2.3 Subacromial Implant Design Modifications

The original design of the subacromial implant, as shown in Figure 2-1, conveys the general features of the desired implant appearance. It was decided that design modifications were needed for the implant to improve its compliance with average scapula morphology. Design modifications were performed in three phases. Phase 1 utilized anthropometric measurements obtained from computer tomography (CT) scans of ten upper extremity cadavers. These measurements were used to improve the implant's articulation with both the scapula and humerus. Additionally, changes were applied to convert the original implant design to that of a modular subacromial implant, allowing for multiple implant designs to be tested in-vitro at a later time. Phases 2 and 3 utilized observations from implanting three-dimensional (3D) printed prototypes of the subacromial implant into different cadaver arms to further improve the design of the implant. Implantation of the device also allowed for a surgical technique to be developed for this device which would be used in later testing and also assist in the eventual planning of clinical protocols.

2.3.1 Phase 1 - Initial Modifications to the Original Implant Design

2.3.1.1 Anthropometric Measurements

CT scans were obtained from ten male upper extremity cadavers with an average age of 71±17 years using a Canon Aquilion ONE scanner (Canon Medial Systems Corporation, Otawara, Japan) using 120kV and 0.5mm slice thickness. The average height and weight of these cadavers were 175.8 ± 14.6 cm (range: 170.1-182.9 cm) and 67.1 ± 10.1 kg (range: 54.4-85.3 kg) respectively. All scans were then reviewed to ensure no signs of glenohumeral osteoarthritis or cuff tear arthropathy were present in any of the cadavers. All scans were uploaded as Digital Imaging and Communications in Medicine (DICOM) files into an imaging visualization software (Mimics, version 21.0, Materialise, Belgium). Standard segmentation techniques previously validated by Bryce et al.[1] were used to isolate the scapula and humerus on each left arm using a minimum threshold value of 226 Hounsfield units (HU). The acromion was isolated from the scapula to gain better perspective of the acromial undersurface. The 3D mask viewer in the software viewing window was then used for subsequent acromial and humeral head measurements.

Measurements of the acromion and humeral head were obtained using internal software features to improve the subacromial implant's articulation with both these osseous structures (Figure 2-3). For analysis of the acromion, points were plotted along its undersurface in both anterior-posterior and medial-lateral directions and spanned the full length of the acromion in each respective direction. These points approximated the acromion's curvature in both anterior-posterior and medial-lateral directions and were used to modify the curvature of the implant's superior surface. Points were also plotted across the humeral head articular surface to approximate the diameter of the humeral head to improve the subacromial implant's inferior articular surface. All point locations were exported as text files and imported into MATLAB (MathWorks, Natick, MA, USA). A custom MATLAB code was developed to approximate the radius of a best fit 3D circle to both acromial point curves and the radius of a best fit sphere to the humeral plotted points.

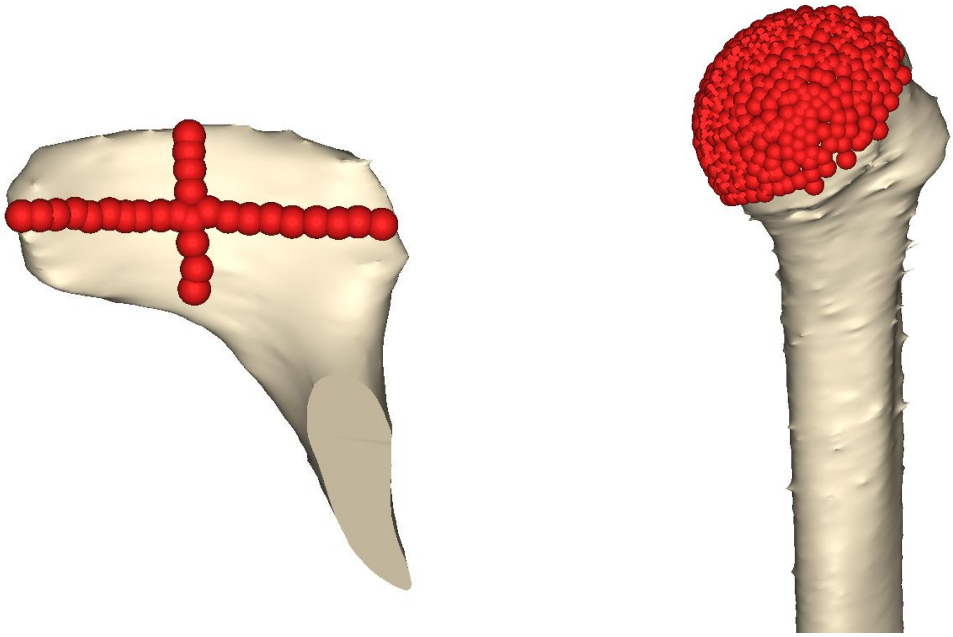

Figure 2-3: Computational acromial and proximal humeral models.

Red dots represent points collected along the surfaces of each model.

The average radii for the anterior-posterior and medial-lateral points were 164.2 ± 222.3mm and 34.4 ± 11.7mm respectively. Points plotted in the anterior-posterior direction produced a concave curve while points plotted in the medial-lateral direction were convex in nature. These curves suggest that the undersurface of the acromion is shaped similar to that of a saddle, with the top of the saddle facing towards the glenohumeral joint. Modifications to the original implant shape were applied using a computer-aided design (CAD) software (SOLIDWORKS, Dassault Systèmes, Vélizy-Villacoublay, France) to reflect these observations. Additionally, the curvature of the anterior aspect of the implant in the anterior-posterior direction was increased. This design modification was applied for the implant to be compliant with all types of acromion shapes.

The average radius of a best fit sphere, applied to the humeral head plotted points, was 25.5±1.2mm. The influence this value had on the changes made to the implant's inferior articulating surface was dictated by the modular design of the implant and is described in more detail in the following section.

2.3.1.2 Modular Design

The term modularity, when used in design, refers to the concept of subdividing an object into multiple different parts called modules, or components. When objects are designed as modular, individual components are created with slight variation in shape or size. These slight variations are then captured in the overall design of the object when the components are fully assembled. This concept of modularity has been extensively used in the design of orthopaedic implants. Modular implants in shoulder arthroplasty allow surgeons the ability to select different sized or shaped components that best suit the native anatomy of the patient, which is important for proper implant functioning and longevity. Modular implant designs are also important in orthopaedic research as they allow different implant variables to be tested with relative ease and lower cost.

It was decided that the design of the subacromial implant would be created as modular. This was to ensure different implant design variations could later be studied in their ability to restore normal glenohumeral joint stability. To minimize both cost of fabrication and the time testing, two implant design parameters were captured by the modular design of the

implant. These parameters included the thickness of the implant and the constraint of the implants inferior surface that articulates with the humeral head (Figure 2-4). These variables were selected as it was believed that they would have the greatest effect on the implant's ability to restore normal joint stability.

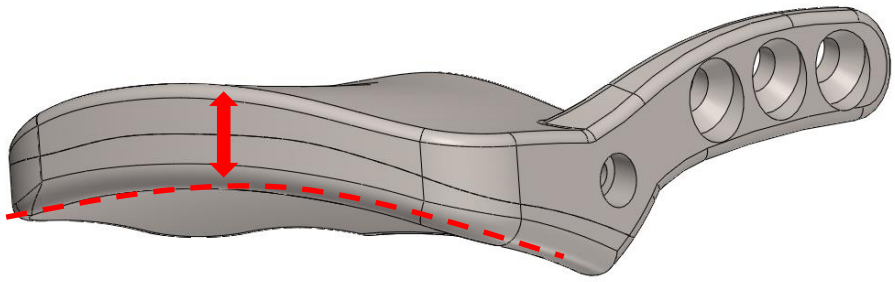

Figure 2-4: Illustration of the two implant design parameters.

The red arrow represents the implant thickness while the dashed red line represents the constraint of the implant's articulator surface.

Both implant thickness and constraint variables first had to be defined. The thickness of the implant was defined at the junction of the middle (medial-lateral direction) and anterior third (anterior-posterior direction) of the implant's spacer feature. This was decided due to the location of this area being located superior to the glenohumeral joint when the scapula is tilted 10 degrees in forward inclination[39]. The constraint of the implant's inferior articulating surface was categorized based on this surface's radius in the sagittal plane. It was determined that thickness values of 5mm and 8mm would be used with high constrained and low constrained inferior implant surfaces. Thicknesses were selected based on general values of superior humeral translation previously reported in literature[13,31,35]. Constraint categorizations were representative of different surface radius values. The high constraint surface was defined by a 25mm inferior surface radius based on the average value of the humeral head size calculated in the anthropometric analysis. The high constraint surface therefore served to fully constrain the humeral head. The low constraint surface was created by increasing the radius of this surface to 55mm.

To create the modular implant designs, an implant was first created to capture each combination of thickness and constraint, leading to the creation of six unique implant designs (two thicknesses and three constraints). These models were created using the same CAD software previously used. To simplify the modular design of the implant, it was decided that each implant would be split into two components. Since both implant design variables being assessed only influenced the shape of the spacer feature, all implants were split transversely into superior and inferior components using the same curved plane (Figure 2-5). The superior component consisted of the fixation plate and the top portion of the spacer, while the inferior component comprised the inferior aspect of the implant spacer feature and captured the specified design parameters (thickness and surface constraint). The same curved plane was used to split each implant design into superior and inferior components, which resulted in each implant design sharing a common superior implant component. This superior implant component was compatible with all inferior components, each of which represented a different implant thickness and constraint value. Furthermore, this required the fabrication of only one superior component. It was postulated this modular design would permit the inferior implant components to be easily changed easy when implanted into a shoulder, as the superior component could first be inserted and fixed

within the shoulder. The inferior components could then be tested sequentially without requiring the removal of the superior implant component, thereby preserving the fixation of the implant to the scapular spine.

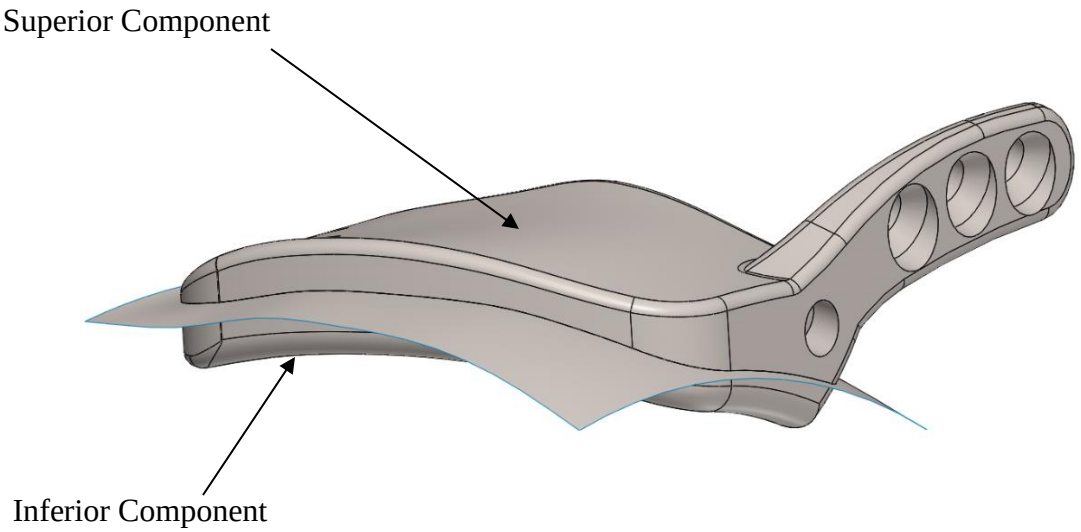

Figure 2-5: Cut plane used to divide the implant into superior and inferior components.

The superior component consists of the fixation plate and the upper half of the spacer feature. The inferior component comprises the lower portion of the spacer feature. All implant models shared a common superior component, as the variations in implant shape were captured in the design of the inferior implant components.

Two design concepts were considered for the fixation of the inferior components to the superior component during in-vitro testing. These concepts included a sliding dove tail design and a set screw design. The sliding dove tail concept utilized a sliding dove tail groove designed onto the inferior surface of the superior component, and the superior surface of the inferior components. This design would have allowed each inferior component to be fixed to the superior component through the connection between the dove tail grooves. However, this design did not constrain translation of the inferior component in the direction of the dove tails during testing, which could have resulted in displacement of the inferior implant components relative to the superior component. Furthermore, the volume comprising both inferior and superior components would have made fabrication of this design difficult. Therefore, it was decided that the set screw design would be used. This design entailed the use of a 5mm square hole designed into the bottom surface of the superior implant component. It also contained a 2.5mm diameter through-hole between the square hole and the flat posterior surface of the implant (Figure 2-6). The through-hole was designed with a diameter of 2.5mm to allow for a M3X0.5mm thread to be created through this channel post-fabrication. A square extrusion was designed at the appropriate location on the top surface of each inferior component. This square extrusion contained a 3.2mm hole designed into the posterior side of the extruded feature for the insertion of a M3X0.5mm set screw. The dimension of this square extrusion was specified as 4.94mm, similar to a free running fit used for a circular hole with a 5mm diameter. This dimension was selected to allow for the two components to be assembled with relative ease and minimal clearance to minimize potential looseness between these two constructs. When assembled, a set screw was inserted into the threaded channel from the posterior surface of the implant and tightened to provide sufficient compressive force, preventing the inferior component from loosening. This design not only provided a secure method of fixation between superior and inferior implant components but was postulated to facilitate an efficient transfer of different implant designs during later in-vitro testing.

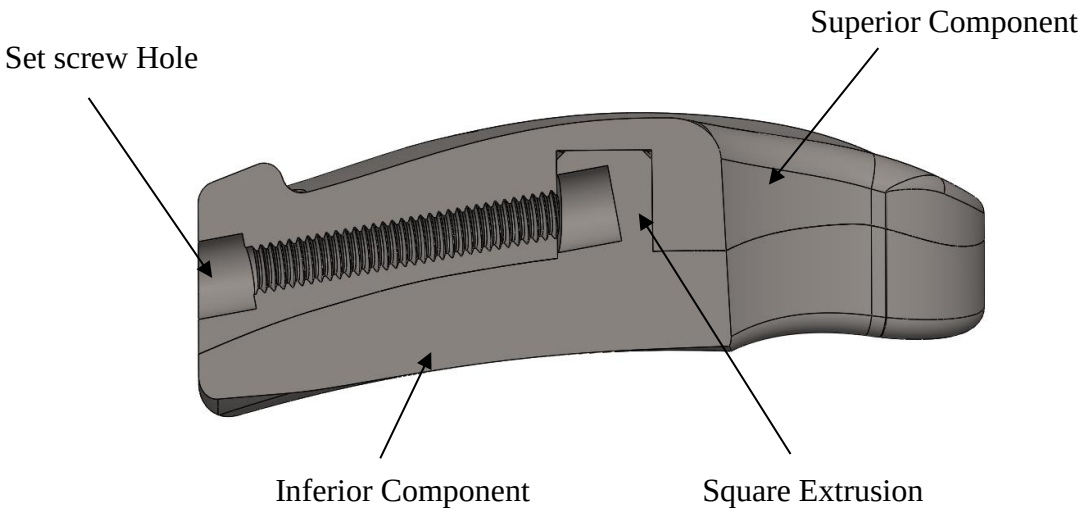

Figure 2-6: Cross-sectional view of the implant.

The inferior component inserts into the square hole located in the superior component. A set screw is inserted through the posterior side of the superior component to fix the two components together.

2.3.2 Phase 2 – Design Modifications

To evaluate the design changes made in Phase 1, the implant was 3D printed for the purpose of inserting and evaluating its fit within a shoulder cadaver. All subacromial implant components (one superior component and six inferior components corresponding to the different thickness and constraint values) were 3D printed (Prusa i3Mk3S, Prusa Research, Partyzánská, Czech Republic) from Polylactic acid with a 40% infill and gyroid fill pattern (Figure 2-7). It was decided to 3D print the implant using Polylactic acid as opposed to a medical approved metallic material as this was the most cost-efficient option for the purpose of evaluating the fit of the implant to the shape of a cadaveric scapula. The through-hole was tapped after 3D printing was completed to create the internal threads.

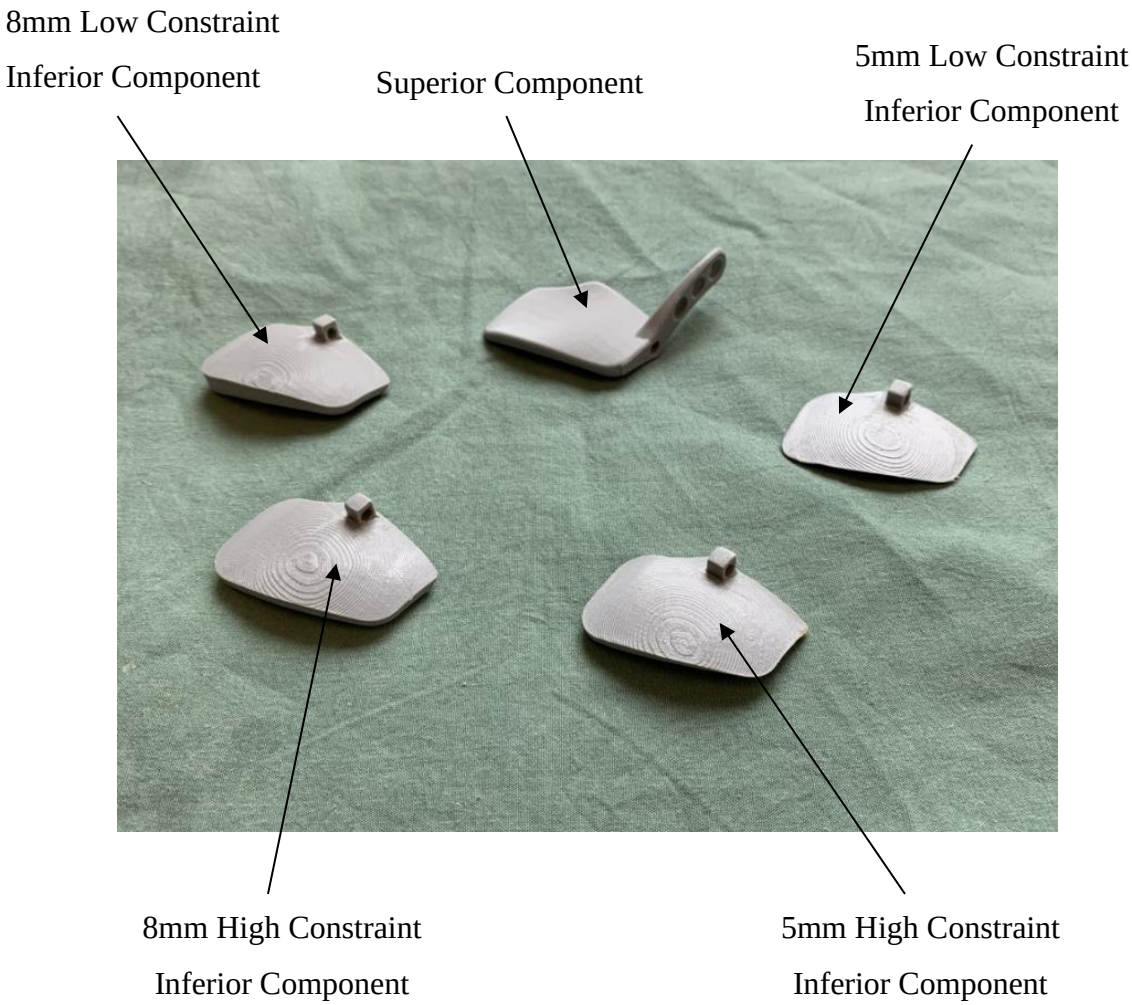

Figure 2-7: Implant models used for insertion into a cadaveric shoulder during Phase 2.

The superior implant component is shown at the top, with all four inferior components representing the different implant thicknesses and constraint shown surrounding it.

All implants were inserted into an upper extremity cadaver (age: 85 years; gender: male) to assess the compatibility of the implant design with both the scapula and humeral head. Insertion of the implant was conducted by a board-certified orthopaedic surgeon (D.M.) for these and all subsequent trials. This also allowed for the development of an in-vitro technique for implant insertion that will later be used to develop a clinical procedure. Throughout trial testing, observations were documented on the technique used to insert and position the implant, in addition to the conformity of the implant to the acromion and scapular spine surfaces. Furthermore, observations were made regarding the articulation between the implant and humeral head.

It was found that the most efficient technique for insertion of the implant into the subacromial space first involved the creation of a small lateral incision for which both superior and inferior components were inserted through (Figure 2-8). The creation of this incision was necessary for later in-vitro testing of the implant to create a massive irreparable RCT test state. The implant was then positioned to maximize seating on the undersurface of the acromion, with adequate positioning of the fixation arm along the scapular spine. Visualization of the fixation plate along the scapular spine required a small, transverse, posterior incision to be created with a deltoid split to gain access to the scapular spine (Figure 2-9). The incision also allowed for the cortical screws to be inserted in order to fix the implant. Furthermore, the inferior components of the implant were efficiently inserted and interchanged through this posterior incision without further disrupting the joint capsule in the cuff deficient shoulder model.

Figure 2-8: Lateral incision created on an upper extremity cadaver.

This incision was used to create the massive irreparable rotator cuff tear as shown here by evidence of the visible humeral articular surface. This incision was also used for insertion of the subacromial implant.

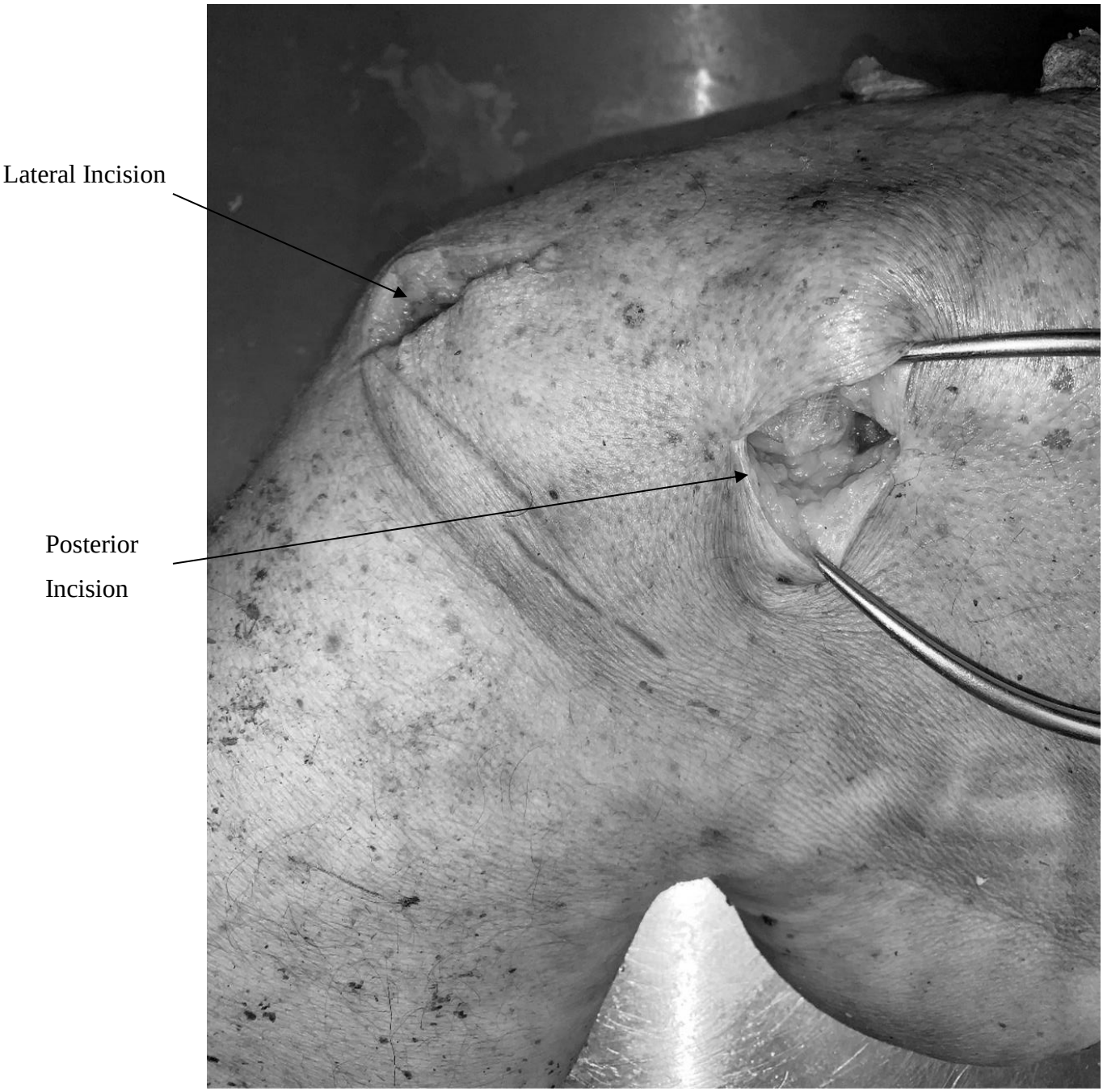

Figure 2-9: Posterior incision created on upper extremity cadaver.

A small posterior incision with a deltoid split is created on the posterior aspect of the shoulder to position the fixation plate against the scapular spine and to insert the locking screws.

Several important observations were made regarding the design of the implant models created in Phase 1. It was observed that the inferior implant shim of the 5mm, high constraint implant design exhibited regions of near zero thickness geometry. The cause of this thin geometry was multifactorial. The design of the implant's high constraint articulating surface caused the middle region of this inferior shim to approach a thickness value of nearly zero. The curvature of the superior implant surface also contributed to this thin geometry as this surface was designed to match the shape of the undersurface of the acromion. This caused the medial-lateral curvature of this surface to be concave and required the curved plane dividing the superior and inferior implant components to be translated inferiorly. This allowed for sufficient volume to exist within the superior implant module needed to support the setscrew protruding into this component. This thin inferior shim geometry could pose difficulty in future fabrication of this implant and may also weaken the design of the inferior implant components. For these reasons, it was decided that further design changes were necessary.

To increase the thickness of the inferior components, the radius value defining the high constraint implant design was no longer considered. Furthermore, the medial-lateral curvature of the superior components top surface was reduced. These decisions were made as reducing the medial-lateral curvature of the superior surface allowed for the curved surface splitting the superior and inferior implant components to be translated superiorly, thereby increasing the volume and thickness of all inferior components. Removal of the high constraint implant design also increased the allowable thickness of the other implant components. This was also decided since this design fully constrained the humeral head. Therefore, perfect implant positioning relative to the glenohumeral joint was needed to restore normal joint position. Imperfect positioning of the implant with this design may have constrained the humeral head in a position outside of joint center. Slight modifications were then made to the remaining implant constraint definitions. The high constraint model was reclassified to contain an articular surface radius of 40mm. Although this surface does not entirely constrain the position of the humeral head, it was observed that it significantly reduced the translation of the humeral head in the anterior-posterior direction when inserted in the cadaveric shoulder. Furthermore, the radius of the inferior surface in the low

constraint implant design was increased from 55mm to 80mm to more accurately represent a low constraint articular surface.

It was also observed during insertion of this device into a cadaveric shoulder that the implant did not span the entire anterior-posterior length of the acromion (Figure 2-10), and therefore provided little resistance to direct superior humeral head translation. To correct this, the computational acromion models from Phase 1 were revisited. Internal measuring tools within the imaging software were used to measure the length of the ten acromion models in the anterior-posterior direction. The average anterior-posterior acromion length was found to equal 48.0 ± 6.7mm. Therefore, an additional inferior shim for the 5mm low constraint implant design was created with an anterior-posterior length of 48mm, compared to the original 41mm length implant design. Furthermore, this new shim was designed with a rounded anterior edge as opposed to a flat anterior face to maximize coverage of the acromion (Figure 2-11). This additional shim was compatible with the original 41mm long superior component to allow for direct comparison with the other implant designs.

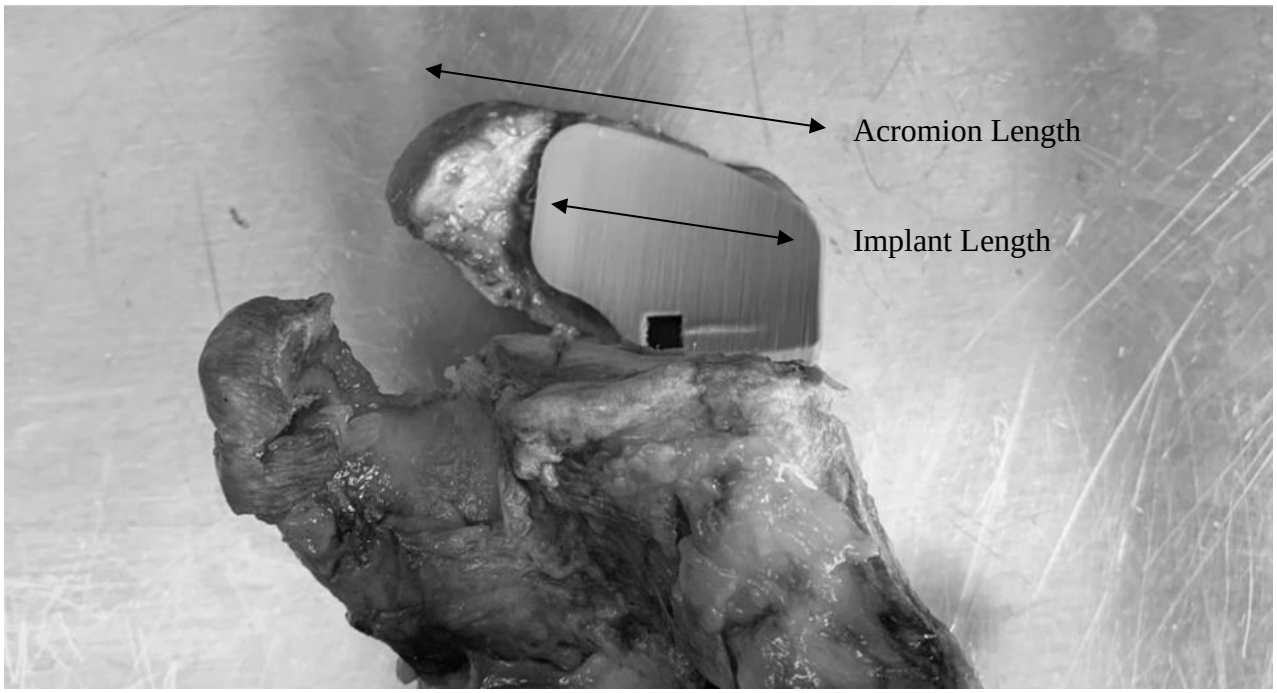

Figure 2-10: Inferior view of implant positioned against acromion.

The figure illustrates that the implant model designed in Phase 1 did not cover the entire AP length of the acromion.

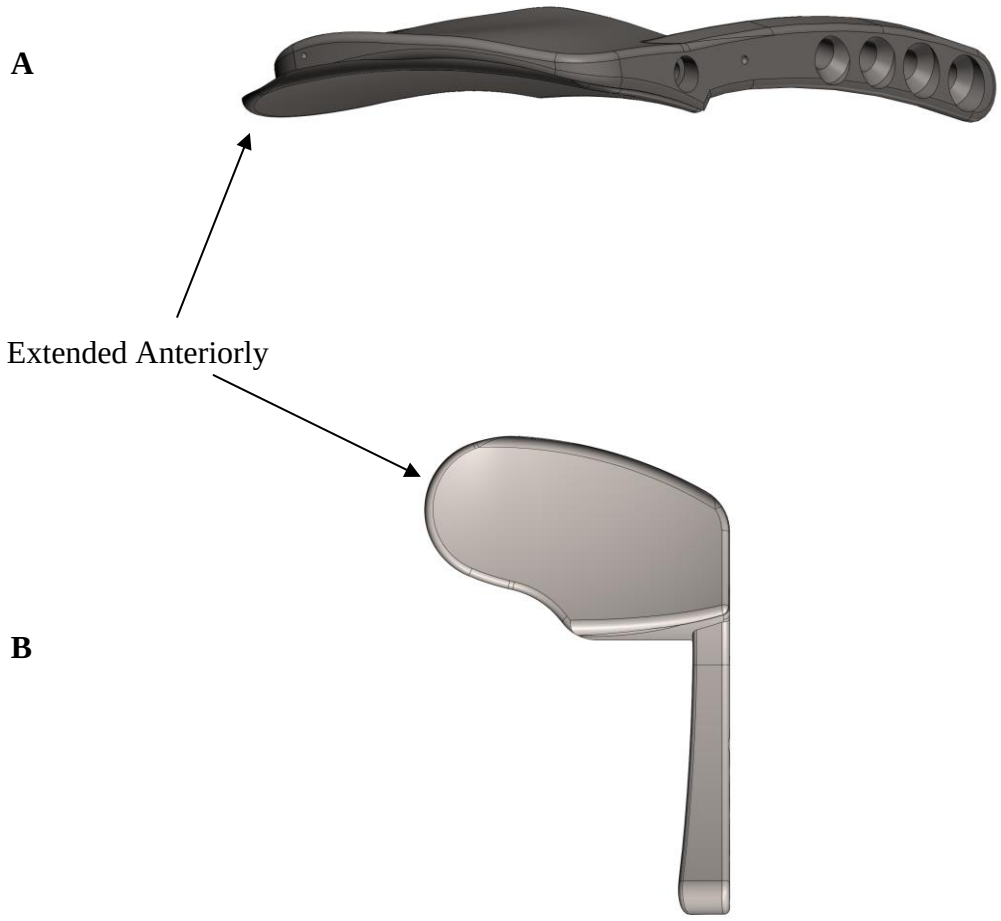

Figure 2-11: 5mm low constraint extended implant design.

The inferior component is extended anteriorly with a rounded anterior edge to mimic the shape of the acromion more accurately. (A) Lateral-posterior view and (B) Inferior view.

Another observation included the inferior articulating surface of the implant to be angled too posteriorly. This was in part due to the increased curvature of the anterior aspect of the acromion to account for hooked, or type 3 acromion. It was also observed that when the implant was positioned underneath the acromion, the fixation plate was angled too superiorly as opposed to following the slope of the scapular spine. This complicated the fixation of this device to the scapular spine and reduced the number of holes that could be used for screw fixation. To address these problems, the curvature of the anterior aspect of the implant in the sagittal plane was reduced, which allowed for the inferior articular surface to be angled towards the joint center. The angle of the fixation plate was also angled more inferiorly in addition to its length being extended. These changes were based upon a visual and iterative approach of computationally fitting 3D implant models to ten scapula bone models in the previously used CAD software. The curvature of the anterior aspect of the implant was reduced while ensuring proper fit between the implant and posterior acromion. The angle of the fixation plate relative to the spacer was decreased to ensure an appropriate articulation with the posterior surface of the scapular spine was achieved on all scapula models. The length of the fixation plate and the number of screw holes were also increased to allow for greater medial fixation.

All changes to the implant design discussed were applied using the same CAD modeling software as previously used.

2.3.3 Phase 3 – Final Implant Design Modifications

The implant designs were again 3D printed using the same material and settings as previously used to evaluate the design modifications made in Phase 2. This involved the printing of one superior component and five inferior components, capturing the different implant thickness and constraint values, in addition to the extended inferior 5mm low constraint trial component (Figure 2-12). A male cadaveric shoulder (age: 101 years) was used for evaluating the effect the new design changes had on the fit of the implant with both the scapula and humerus.

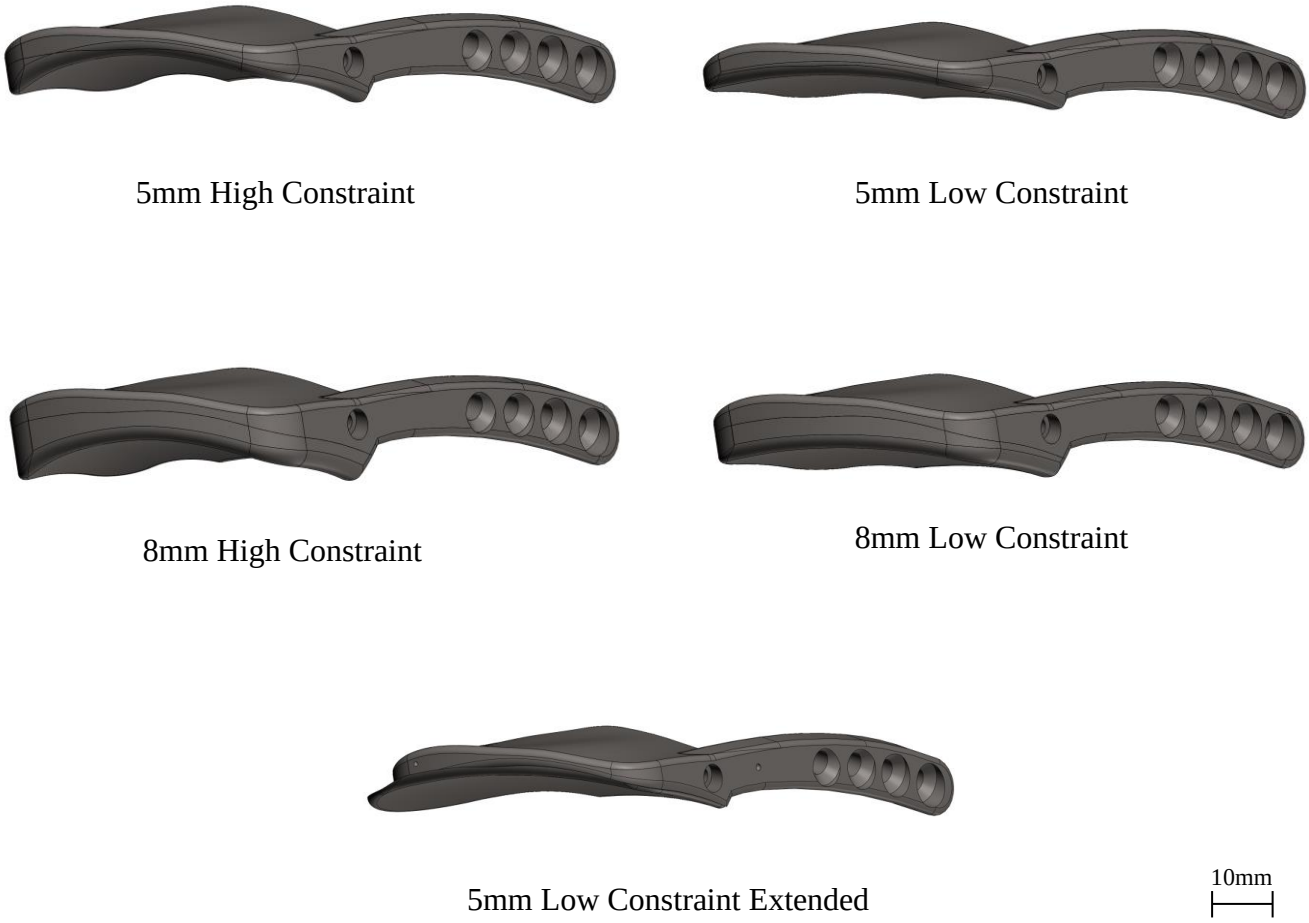

Figure 2-12: Implant designs inserted into the upper extremity cadaver in Phase 3.

Scale shown for reference.

The improvements made to the design of the subacromial implant in Phase 2 were found to visually improve the conformity of the implant to both the acromion and scapular spine. The extended 5mm low constraint implant design showed improved superior coverage of the glenohumeral joint, suggesting this to potentially be more effective in preventing direct superior humeral head translation. The rounded nature of the anterior aspect of this implant design also improved the coverage of this implant with the undersurface of the acromion. Furthermore, the decreased angle of the fixation plate visually improved the fit of the implant to the scapular spine (Figure 2-13), while the increased length of this fixation plate allowed for more screws to be used for implant fixation.

Figure 2-13: Position of the fixation plate along the posterior surface of the scapular spine.

The new fixation plate design improves the articulation between this implant feature and the posterior surface of the scapular spine.

All implant designs were extended to 48mm in anterior-posterior length with a rounded anterior edge. The shape of the fixation plate was slightly modified to further improve its conformity with the slope of the scapular spine. The angle of the lateral aspect of the fixation plate was slightly decreased compared to the implants created in Phase 2 to further improve its fit with the scapular spine and prevent any impingement with the posterior aspect of the acromion. Changes were also made to the curvature of the fixation plate to improve its conformity with different scapular spine shapes (Figure 2-14). The medial-lateral curvature of the superior surface of the implant was further reduced to increase the thickness of the inferior implant components for future fabrication.

Figure 2-14: Posterior view of final fixation plate design.

The new, curved fixation plate design is illustrated with a decreased angle laterally to improve articulation with the scapular spine.

Additional modifications to the implant design were performed to improve osseous fixation (Figure 2-15). The countersunk holes designed for the compression screws were changed to locking screw holes which utilize a threaded connection with the implant to secure to the plate at a fixed angle. It was decided that locking screws would be used with this implant to reduce the stress applied to the scapular spine as would occur with non-locking screws that employ the lag effect[16]. Small spikes were also added to the superior surface of the implant to increase the friction between the implant and acromion. These spikes were designed to mimic a porous superior implant surface, potentially allowing for bony in-growth with the undersurface of the acromion. While these changes do not significantly affect the implant's ability to restore normal joint stability in a cadaveric model, they will be useful for improving implant fixation and function for future implant testing. Additional features, also illustrated in Figure 2-15, were added for the purpose of testing this implant in-vitro at a later time. Small spherical indents were created along the sides of the implant to serve as landmarks for digitization in order to quantify the position of the implant relative to bone post-testing. An additional locking screw hole and two small angled through-holes were added to the lateral aspect of the implant's fixation plate. These features, while not used in this thesis, were designed for the attachment of a device that could be used to aid in percutaneous screw fixation to minimize the invasiveness of this surgery.

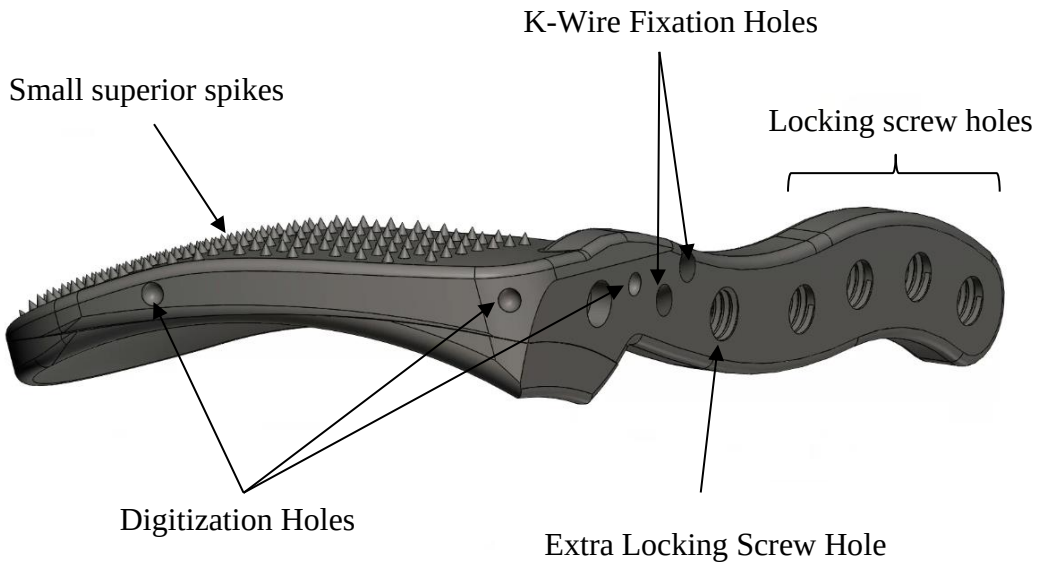

Figure 2-15: Lateral-posterior view of final implant design.

Compression screw holes were changed to locking screw holes to improve implant fixation to the scapular spine. Additional features added to the implant include the small spikes located on the superior surface of the spacer feature, three digitization holes along the lateral and posterior edge of the spacer feature, and an extra locking screw hole and K-wire fixation holes located on the posterior fixation plate surface.

The final design of the modular subacromial implant consisted of one superior component and four inferior components (Figure 2-16). These inferior components varied in design to capture 5mm and 8mm implant thicknesses, in addition to high constraint and low constraint inferior articular surfaces characterized by a 40mm and 80mm radius respectively.

5mm High Constraint

5mm Low Constraint

8mm High Constraint

8mm Low Constraint

10mm

Figure 2-16: Final implant designs.

Scale shown for reference.

2.4 Implant Fabrication

The final design of the subacromial implant for full testing (Chapter 3 and 4) was 3D printed from medical grade titanium, with printing being performed at a local facility (ADEISS, London, ON, Canada). Printing was performed with a Renishaw AM400 printer (Renishaw Ltd., Mississauga, ON, Canada), using a 200-400W laser and 70 μm spot size. Medical grade titanium (Ti-6Al-4V, grade 5) was chosen for its advantageous mechanical properties, and has also extensively been used in hemiarthroplasty implants[29]. These material properties are advantageous to ensure that implant deformation and failure do not occur during testing given the predicted load magnitudes the implant will be subjected to[18].

Metal 3D printing was selected as the method of fabrication due to its high precision and accuracy. Additional machining was required post-printing in order to create the threads in both the screw holes and setscrew channel in the superior implant component. M5X0.8mm course thread was machined for each locking screw hole while M3X0.5mm thread was used in the set screw channel.

2.5 Conclusion

This chapter presented the design process used to develop a metallic 3D printed prototype of a subacromial implant. Several design modifications were made based on anthropometric data obtained from CT scans from ten cadavers, in addition to observations made when inserting different implant designs into upper extremity cadaveric models. The subacromial implant was configured as a modular design allowing for different implant thicknesses and articular constraints to be fabricated. The next study focuses on assessing this implant in a series of cadaver arms to assess the influence of implant thickness and constraint on restoration of normal joint stability in a massive RCT model.

2.6 References

1. Bryce CD, Pennypacker JL, Kulkarni N, et al. Validation of three-dimensional models of in situ scapulae. *J Shoulder Elb Surg*. 2008;17(5):825-832. doi:10.1016/j.jse.2008.01.141

2. Burkhart SS, Hartzler RU. Superior Capsular Reconstruction Reverses Profound Pseudoparalysis in Patients With Irreparable Rotator Cuff Tears and Minimal or No Glenohumeral Arthritis. *Arthrosc - J Arthrosc Relat Surg*. 2019;35(1):22-28. doi:10.1016/j.arthro.2018.07.023

3. Cofield RH. Subscapular muscle transposition for repair of chronic rotator cuff tears. *Surg Gynecol Obstet*. 1982;154(5):667-672.

4. Cuff D, Pupello D, Santoni BG, Clark RE, Frankle M. Reverse shoulder arthroplasty for the treatment of rotator cuff deficiency. *J Bone Jt Surg*. 2017;99:1895-1899. doi:10.2106/JBJS.G.00775

5. Denard PJ, Brady PC, Adams CR, Tokish JM, Burkhart SS. Preliminary Results of Arthroscopic Superior Capsule Reconstruction with Dermal Allograft. *Arthrosc - J Arthrosc Relat Surg*. 2018;34(1):93-99. doi:10.1016/j.arthro.2017.08.265

6. DeOrio JK, Cofield RH. Results of a second attempt at surgical repair of a failed initial rotator-cuff repair. *J Bone Jt Surg - Ser A*. 1984;66(4):563-567. doi:10.2106/00004623-198466040-00011

7. Deranlot J, Herisson O, Nourissat G, et al. Arthroscopic Subacromial Spacer Implantation in Patients With Massive Irreparable Rotator Cuff Tears: Clinical and Radiographic Results of 39 Retrospectives Cases. *Arthrosc - J Arthrosc Relat Surg*. 2017;33(9):1639-1644. doi:10.1016/j.arthro.2017.03.029

8. Dyrna F, Kumar NS, Obopilwe E, et al. Relationship Between Deltoid and Rotator Cuff Muscles During Dynamic Shoulder Abduction: A Biomechanical Study of Rotator Cuff Tear Progression. *Am J Sports Med*. 2018;46(8):1919-1926. doi:10.1177/0363546518768276

9. Familiari F, Nayar SK, Russo R, et al. Subacromial Balloon Spacer for Massive, Irreparable Rotator Cuff Tears Is Associated With Improved Shoulder Function and High Patient Satisfaction. *Arthrosc - J Arthrosc Relat Surg*. 2021;37(2):480-486. doi:10.1016/j.arthro.2020.09.048

10. Gerber C, Fuchs B, Hodler J. The results of repair of massive tears of the rotator cuff. *J Bone Jt Surg - Ser A*. 2000;82(4):505-515. doi:10.2106/00004623-200004000-00006

11. Guery J, Favard L, Sirveaux F, Oudet D, Mole D, Walch G. Reverse total shoulder arthroplasty: Survivorship Analysis of Eighty Replacements Followed for Five to Ten Years. *Bone Joint J*. 2006;88(8):1742-1747. doi:10.1302/0301-

620X.103B.BJJ-2020-2101

12. Hartzler RU, Steen BM, Hussey MM, et al. Reverse shoulder arthroplasty for massive rotator cuff tear: Risk factors for poor functional improvement. *J Shoulder Elb Surg*. 2015;24(11):1698-1706. doi:10.1016/j.jse.2015.04.015

13. Itami Y, Park MC, Lin CC, et al. Biomechanical analysis of progressive rotator cuff tendon tears on superior stability of the shoulder. *J Shoulder Elb Surg*. 2021;30(11):2611-2619. doi:10.1016/j.jse.2021.04.012

14. Kany J, Grimberg J, Amaravathi RS, Sekaran P, Scorpie D, Werthel JD. Arthroscopically-Assisted Latissimus Dorsi Transfer for Irreparable Rotator Cuff Insufficiency: Modes of Failure and Clinical Correlation. *Arthrosc - J Arthrosc Relat Surg*. 2018;34(4):1139-1150. doi:10.1016/j.arthro.2017.10.052

15. Kany J, Sekaran P, Grimberg J, et al. Risk of latissimus dorsi tendon rupture after arthroscopic transfer for posterior superior rotator cuff tear: a comparative analysis of 3 humeral head fixation techniques. *J Shoulder Elb Surg*. 2020;29(2):282-290. doi:10.1016/j.jse.2019.06.019

16. Kicinski M, Puskas GJ, Zdravkovic V, Jost B. Osteosynthesis of type III acromial fractures with locking compression plate, lateral clavicular plate, and reconstruction plate: a biomechanical analysis of load to failure and strain distribution. *J Shoulder Elb Surg*. 2018;27(11):2093-2098. doi:10.1016/j.jse.2018.05.031

17. Lim S, AlRamadhan H, Kwak JM, Hong H, Jeon IH. Graft tears after arthroscopic superior capsule reconstruction (ASCR): pattern of failure and its correlation with clinical outcome. *Arch Orthop Trauma Surg*. 2019;139(2):231-239. doi:10.1007/s00402-018-3025-7

18. Lobao MH, Canham RB, Melvani RT, Abboud JA, Parks BG, Murthi AM. Biomechanics of Biodegradable Subacromial Balloon Spacer for Irreparable Superior Rotator Cuff Tears. *J Bone Jt Surg*. 2019;101(11):e49.

19. Mihata T, Lee TQ, Hasegawa A, et al. Arthroscopic Superior Capsule Reconstruction Can Eliminate Pseudoparalysis in Patients With Irreparable Rotator Cuff Tears. *Am J Sports Med*. 2018;46(11):2707-2716. doi:10.1177/0363546518786489

20. Mihata T, Lee TQ, Hasegawa A, et al. Five-Year Follow-up of Arthroscopic Superior Capsule Reconstruction for Irreparable Rotator Cuff Tears. *J Bone Jt Surg - Am Vol*. 2019;101(21):1921-1930. doi:10.2106/JBJS.19.00135

21. Mihata T, McGarry MH, Pirolo JM, Kinoshita M, Lee TQ. Superior capsule reconstruction to restore superior stability in irreparable rotator cuff tears: A biomechanical cadaveric study. *Am J Sports Med*. 2012;40(10):2248-2255. doi:10.1177/0363546512456195

22. Muench LN, Kia C, Williams AA, et al. High Clinical Failure Rate After Latissimus Dorsi Transfer for Revision Massive Rotator Cuff Tears. *Arthrosc - J Arthrosc Relat Surg*. 2020;36(1):88-94. doi:10.1016/j.arthro.2019.07.034

23. Muh SJ, Streit JJ, Wanner JP, et al. Early follow-up of reverse total shoulder arthroplasty in patients sixty years of age or younger. *J Bone Jt Surg - Ser A*. 2013;95(20):1877-1883. doi:10.2106/JBJS.L.10005

24. Neer CS, Craig E V., Fukuda H. Cuff-Tear Arthropathy. *J Bone Jt Surg*. 1983;65:1232-1244.

25. Pennington WT, Bartz BA, Pauli JM, Walker CE, Schmidt W. Arthroscopic Superior Capsular Reconstruction With Acellular Dermal Allograft for the Treatment of Massive Irreparable Rotator Cuff Tears: Short-Term Clinical Outcomes and the Radiographic Parameter of Superior Capsular Distance. *Arthrosc - J Arthrosc Relat Surg*. 2018;34(6):1764-1773. doi:10.1016/j.arthro.2018.01.009

26. Petrillo S, Longo UG, Papalia R, Denaro V. Reverse shoulder arthroplasty for massive irreparable rotator cuff tears and cuff tear arthropathy: a systematic review. *Musculoskelet Surg*. 2017;101(2):105-112. doi:10.1007/s12306-017-0474-z

27. Piekaar RSM, Bouman ICE, van Kampen PM, van Eijk F, Huijsmans PE. The subacromial balloon spacer for massive irreparable rotator cuff tears: approximately 3 years of prospective follow-up. *Musculoskelet Surg*. 2020;104(2):207-214. doi:10.1007/s12306-019-00614-1

28. Prat D, Tenenbaum S, Pritsch M, Oran A, Vogel G. Sub-acromial balloon spacer for irreparable rotator cuff tears: Is it an appropriate salvage procedure? *J Orthop Surg*. 2018;26(2). doi:10.1177/2309499018770887

29. Ronoh K, Mwema F, Dabees S, Sobola D. Biomedical Engineering Advances Advances in sustainable grinding of different types of the titanium biomaterials for medical applications : A review. *Biomed Eng Adv*. 2022;4(May):100047. doi:10.1016/j.bea.2022.100047

30. Ruiz Ibán MA, Lorente Moreno R, Ruiz Díaz R, et al. The absorbable subacromial spacer for irreparable posterosuperior cuff tears has inconsistent results. *Knee Surgery, Sport Traumatol Arthrosc*. 2018;26(12):3848-3854. doi:10.1007/s00167-018-5083-3

31. Rybalko D, Bobko A, Amirouche F, et al. Biomechanics in an Incomplete Versus Complete Supraspinatus Tear: A Cadaveric Study. *Orthop J Sport Med*. 2020;8(12):1-7. doi:10.1177/2325967120964476

32. Savarese E, Romeo R. New Solution for Massive, Irreparable Rotator Cuff Tears: The Subacromial "Biodegradable Spacer." *Arthrosc Tech*. 2012;1(1):e69-e74. doi:10.1016/j.eats.2012.02.002

33. Senekovic V, Poberaj B, Kovacic L, et al. The biodegradable spacer as a novel treatment modality for massive rotator cuff tears: a prospective study with 5-year follow-up. *Arch Orthop Trauma Surg*. 2017;137(1):95-103. doi:10.1007/s00402-016-2603-9

34. Sevivas N, Ferreira N, Andrade R, et al. Reverse shoulder arthroplasty for irreparable massive rotator cuff tears: a systematic review with meta-analysis and meta-regression. *J Shoulder Elb Surg*. 2017;26(9):e265-e277. doi:10.1016/j.jse.2017.03.039

35. Singh S, Reeves J, Langohr GDG, Johnson JA, Athwal GS. The effect of the subacromial balloon spacer on humeral head translation in the treatment of massive, irreparable rotator cuff tears: a biomechanical assessment. *J Shoulder Elb Surg*. 2019;28(10):1841-1847. doi:10.1016/j.jse.2019.03.036

36. Tashjian RZ. The Natural History of Rotator Cuff Disease: Evidence in 2016. *Tech Shoulder Elb Surg*. 2016;17(4):132-138. doi:10.1097/BTE.0000000000000109

37. Wagner ER, Elhassan BT. Surgical Management of Massive Irreparable Posterosuperior Rotator Cuff Tears: Arthroscopic-Assisted Lower Trapezius Transfer. *Curr Rev Musculoskelet Med*. 2020;13(5):592-604. doi:10.1007/s12178-020-09657-5

38. Woodmass JM, Wagner ER, Borque KA, Chang MJ, Welp KM, Warner JJP. Superior capsule reconstruction using dermal allograft: early outcomes and survival. *J Shoulder Elb Surg*. 2019;28(6):S100-S109. doi:10.1016/j.jse.2019.04.011

39. Wuelker N, Wirth CJ, Plitz W, Roetman B. A dynamic shoulder model: Reliability testing and muscle force study. *J Biomech*. 1995;28(5). doi:10.1016/0021-9290(94)E0006-O

40. Yamakado K. Clinical and Radiographic Outcomes With Assessment of the Learning Curve in Arthroscopically Assisted Latissimus Dorsi Tendon Transfer for Irreparable Posterosuperior Rotator Cuff Tears. *Arthrosc - J Arthrosc Relat Surg*. 2017;33(12):2144-2151. doi:10.1016/j.arthro.2017.06.015

Chapter 3

3 In-vitro Testing of a Subacromial Implant to Restore Normal Glenohumeral Joint Kinematics

This chapter describes the testing conducted to evaluate the effectiveness of the subacromial implant designed in Chapter 2 in restoring normal glenohumeral joint position in a massive irreparable rotator cuff tear model. Testing was conducted on all four implant designs using a previously developed shoulder testing apparatus. Static muscle loading was employed at varying angles of glenohumeral abduction, with translation of the humerus relative to the glenoid recorded in both anterior-posterior, and superior-inferior directions[3].

3.1 Introduction

Rotator cuff tears are a considerable source of pain and dysfunction[31] and have a prevalence rate of up to 23% in patients over 50 years of age[33]. When a tear is greater than 5cm and involves two or more tendons, it may be classified as massive, and possibly, irreparable[8]. These larger tears can be difficult to repair due to the decreased cuff mobility and muscle atrophy[10]. Massive, irreparable rotator tears have been shown to cause posterosuperior migration of the humeral head when subjected to superiorly directed deltoid loads[13,25]. Humeral head superior migration can produce eccentric loading on the glenoid, leading to irregular wear patterns and thereby increasing the patient's risk of developing arthritis[4,15,28].

Reverse shoulder arthroplasty is a common procedure used for treating massive, irreparable rotator cuff tears[3,9]. However, it is a relatively invasive surgical procedure with a finite survivability. Additionally, reverse shoulder arthroplasty used to treat younger patients and patients with massive rotator cuff tears without arthritis have generally poorer outcomes than for cuff tear arthropathy[7,12]. Another surgical technique used to treat

[3] A copy of this chapter has been submitted to a peer reviewed journal for publication.

massive irreparable tears is the superior capsule reconstruction (SCR)[21]. This technique utilizes autograft or allograft tissue to reconstruct the superior capsule of the glenohumeral joint in order to limit superior humeral migration. Although several studies have shown positive results for this procedure[5,19,20], other reports have exhibited higher complication rates calling into question early to medium term clinical results[1,35]. The subacromial balloon spacer (InSpace; Stryker, Kalamazoo, MI, USA) is a more recent treatment option that uses a biodegradable spacer to translate the humeral head inferiorly to restore shoulder function[27]. This balloon is inserted arthroscopically and is then insufflated with saline to fill the subacromial space and depress the humeral head. Studies have found this procedure to decrease pain, increase range of motion, and to have a sustained effect[23,29], however, some conflicting literature does exist[24,26]. Additionally, at the present time, this product is only indicated for patients 65 years of age and older.

Currently, no optimal treatment option exists for the management of massive, irreparable rotator cuff tears. We postulated that development of a space occupying implant affixed to the inferior aspect of the acromion and scapular spine would minimize superior humeral head migration and hence restore native glenohumeral kinematics. The objective of this study was to investigate a rigid subacromial implant's ability to restore humeral head position from the superiorly migrated position. It was hypothesized that the implant would restore near normal humeral head position in the presence of a massive, irreparable rotator cuff tear state. Furthermore, it was predicted that different implants, characterized by different implant design variables, would be more effective in improving the implant's ability in restoring axial glenohumeral stability.

3.2 Methods

Eight male left cadaver shoulders with a mean age of 64 ± 13 years (age range: 49-79) were used for testing. All cadavers were scanned prior to testing using Computer Tomography (CT) and inspected by an orthopaedic surgeon (D.M.) to ensure no rotator cuff or glenohumeral joint pathology was present. Specimens were transected mid-humerus and thawed for 18 hours prior to testing. Soft tissues were maintained on the specimen throughout testing. Each rotator cuff tendon was identified and tagged at the musculotendinous junction using #5 Ethibond sutures (Ethicon, Johnson&Johnson, New

Brunswick, NJ). The three heads of the deltoid muscle were tagged with transosseous sutures placed at the humeral insertions.

Each specimen was affixed to a previously developed shoulder testing apparatus[11]. The scapula was clamped to the base of the testing apparatus using two transosseous bolts, while an intramedullary humeral rod assembly was cemented in to the diaphyseal humeral canal (Figure 3-1). The humeral rod assembly was mounted to an abduction arc to allow for 0-90 degrees of glenohumeral rotation in the scapular plane. The humerus was secured in 0 degrees of internal/external rotation. The humeral head was free to translate in the sagittal plane with minimal resistance. Braided line was used to connect each sutured tendon to pneumatic actuators controlled by a custom LabVIEW (National Instruments, Austin, Texas, USA) program. Supraspinatus, infraspinatus, teres minor, superior subscapularis, and inferior subscapularis tendon lines were physiologically positioned along the apparatus base, while the deltoid wires were guided over the acromion. Optical tracking markers attached to the humerus and scapula (Certus, Northern Digital, Ontario, Canada) were used to track the relative position of each bone throughout testing. Normal saline was employed to keep the joint and adjacent tissues hydrated throughout testing.

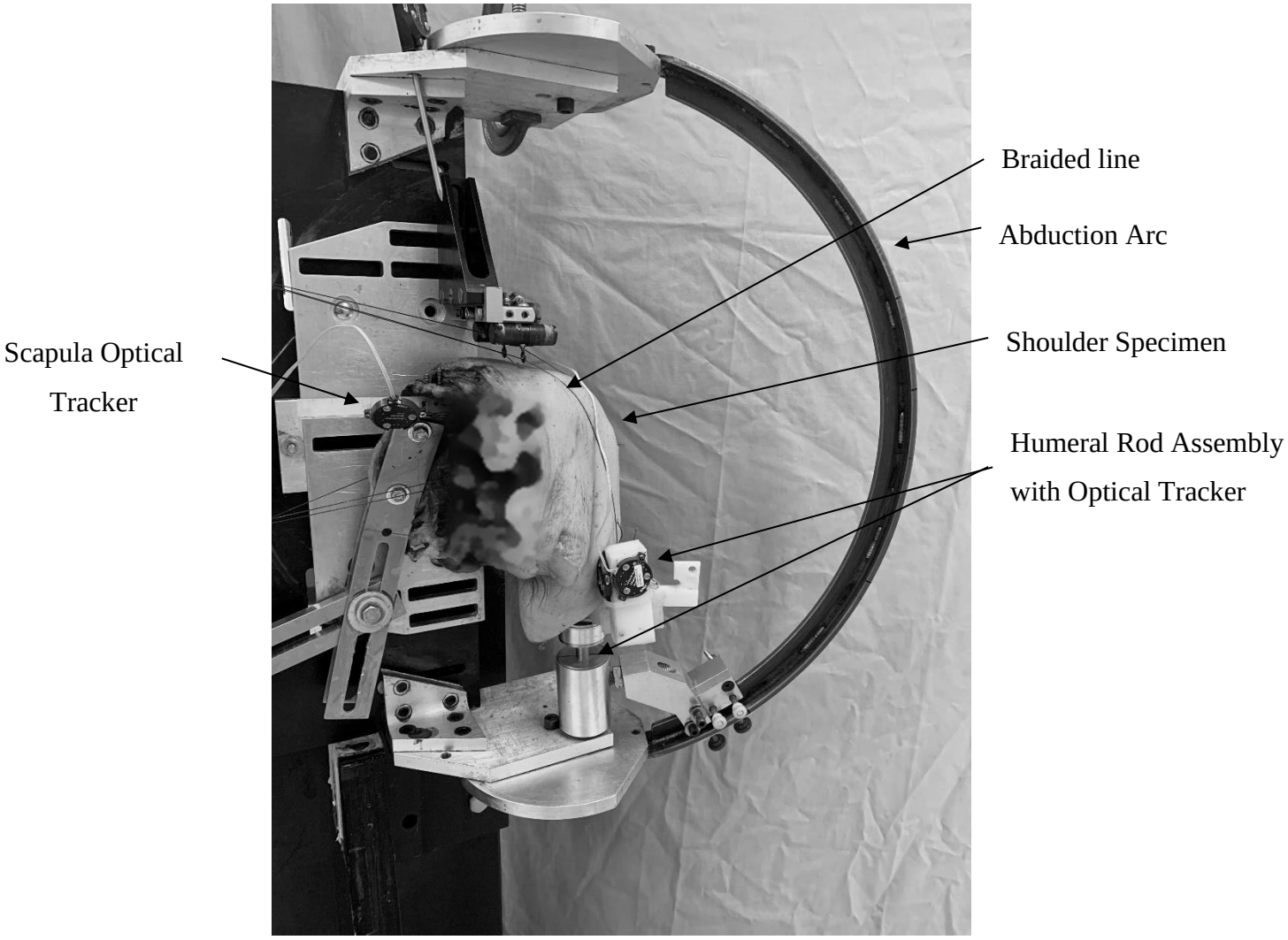

Figure 3-1: Cadaveric testing setup.

A cadaver specimen is attached to the shoulder simulator, with the scapula clamped to the base of the simulator and the humeral rod assembly placed in the abduction arc. Two optical trackers, one on both the scapula and humerus, are used to track the motion of the humerus relative to the scapula.

Static testing was conducted for all test states using an 80N force equally distributed across the deltoid (26.67N applied to each head of the deltoid) and a 10N force applied to each rotator cuff tendon. This loading protocol has previously been used in cadaveric studies to assess humeral head translation in the presence of massive, irreparable cuff tears[21,25,30]. Tests were conducted at 0, 30, and 60 degrees of glenohumeral rotation.

3.2.1 Test States

Testing was first performed on the intact shoulder joint. Next, the rotator cuff deficient or "torn" state, in which a posterosuperior massive rotator cuff tear was created and tested. This was achieved via a lateral deltoid split approach by carefully dissecting and removing the supraspinatus tendon and anterior fibers of the infraspinatus tendon. The inferior capsule of the glenohumeral joint was released to allow unrestricted proximal migration of the humeral head to simulate a chronic massive, irreparable rotator cuff tear.

A rigid subacromial implant that was 3D printed from medical grade titanium alloy was then implanted. The implant consisted of two distinct features: a fixation plate and a spacer. (Figure 3-2). The fixation plate was the long curving portion of the implant affixed to the scapula along the inferior surface of the spine using four locking screws. The subacromial spacer feature of the implant comprised the bulk end of the implant and was positioned underneath the acromion. Additionally, the implant was comprised of two different solid parts (Figure 3-3). The superior component was continuous with the fixation plate and top portion of the spacer, and contained small spikes on its superior surface that provided additional fixation between the implant and the acromion. The inferior component contained the implant's primary articular surface, which served to articulate with the native humeral head. This modular design allowed for different inferior spacer components to be tested. As a whole, the spacer feature of the implant mimicked the shape of the acromion.

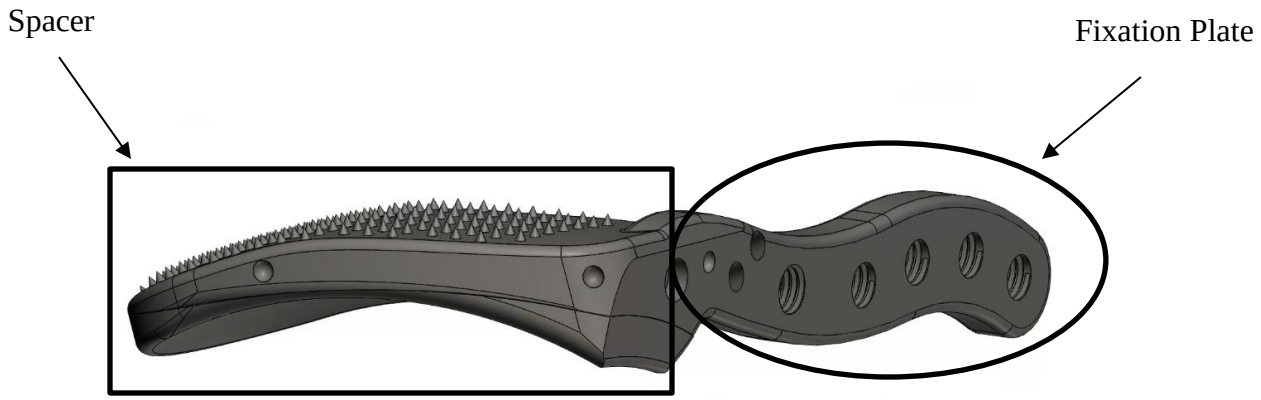

Figure 3-2: Subacromial implant design.

The overall implant shape consists of two features: the spacer (indicated by the black rectangle) and the fixation plate (indicated by the black oval).

Figure 3-3: Modular components of the subacromial implant.

The implant is split into two components, superior and inferior. The superior component comprises the top portion of the spacer feature and fixation arm. The inferior component comprises the bottom portion of the spacer feature. Inferior components were designed to capture the variations in thickness and constraint and are compatible with one common superior component.

Two implant design variables were tested by utilizing the modularity of the implant. These variables included the thickness of the implant and the constraint of the implant's articulating surface with the humerus. The thickness of the implant was measured at the junction of the middle and anterior third of the implant. Implant thickness values of 5mm and 8mm were tested. The constraint of the implant's primary articulating surface was defined according to this surface's radius Therefore, the high constraint implant had a smaller radius compared to the low constraint implant. Hence two thicknesses and two radii (Figure 3-4), resulting in four implant states, were tested.

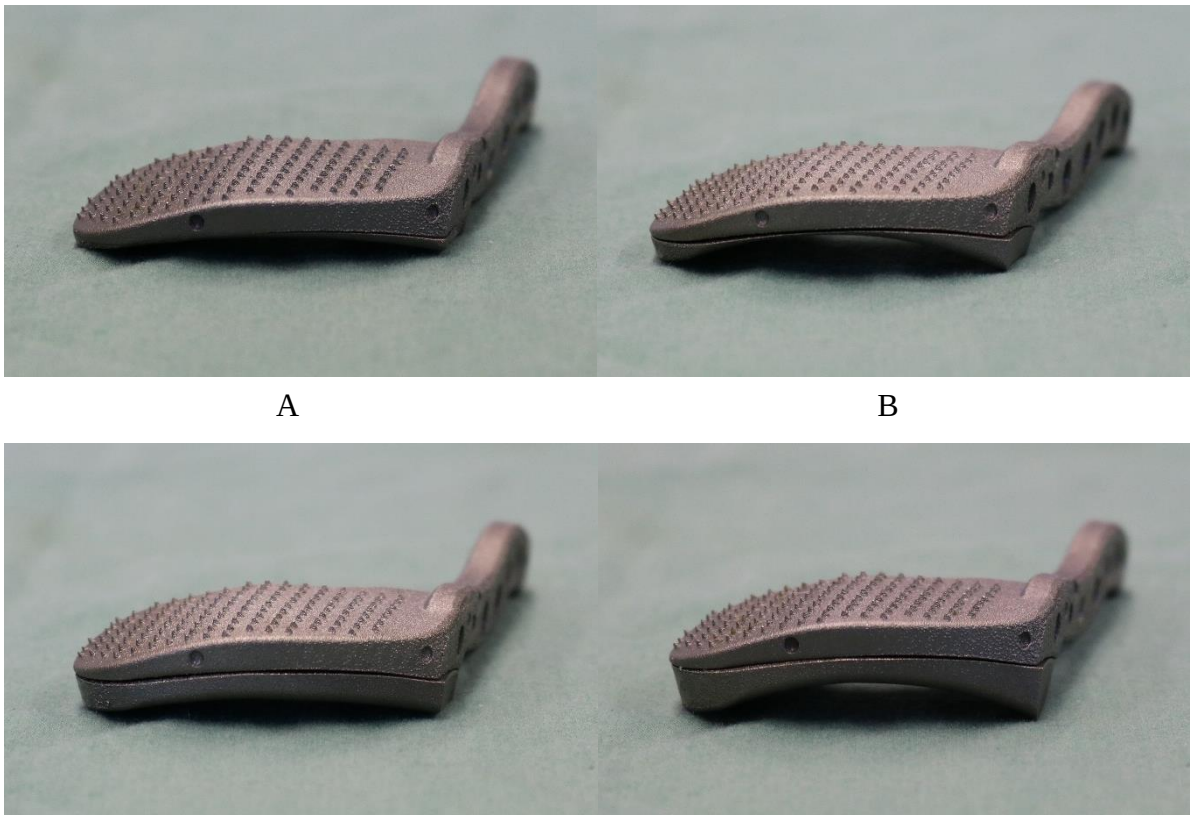

A B

C D

Figure 3-4: Final subacromial implant designs.

All implants were printed from medical grade titanium. (A) 5mm Low Constraint, (B) 5mm High Constraint, (C) 8mm Low Constraint, and (D) 8mm High Constraint.

The implant was inserted through the lateral deltoid split incision originally made to create the massive, irreparable cuff tear state. The inferior surface of the native acromion was cleared of any soft tissues before positioning the implant. Posteriorly, a transverse incision was made along the scapular spine and a small deltoid split was performed to allow access to the scapular spine. This incision was used to secure the implant's fixation plate to the scapula using four locking screws. Both incisions were closed with sutures before testing. The testing order for the different implants was randomized.

Following completion of testing, the articular surface on the humeral head was traced and point data was sphere-fitted[14] in MATLAB (MathWorks, Natick, MA, USA). A coordinate system was developed to quantify the position of the humeral head center relative to the glenoid.

3.2.2 Outcome Variables & Statistical Analysis

The outcome variables included the translation of the humeral head center in both the superior-inferior and anterior-posterior directions. All translation values were normalized with respect to the intact test state at each angle of abduction, which allowed for the position of the humeral head in the cuff deficient and implant test states to be directly compared to that of the intact state. Superior translation and anterior translation of the humeral head relative to the intact state were expressed as positive.

Statistical analysis was carried out using a two-way repeated measures analysis of variance (RM-ANOVA) in SPSS (IBM, Armonk, NY, USA). The independent variables were the abduction angle and test state, and the dependent variables were superior-inferior (SI) and anterior-posterior (AP) translation of the humeral head. A Bonferroni correction was used to correct for the multiple statistical analyses performed, with the significance value set as $p<0.05$.

3.3 Results

3.3.1 Superior-Inferior Translation

The simulation of a massive irreparable cuff tear resulted in significant superior translation of the humeral head (mean translation across all abduction angles was 2.0 ± 1.6mm,

P=0.016). All four implant designs tested were effective in decreasing the superior humeral head translation seen in the torn state. The 5mm low constraint and 5mm high constraint implants were most effective at restoring native humeral head position in the superior-inferior direction (-1.3 ± 2.0mm, P=0.223; and -1.5 ± 2.3mm, P=0.928 respectively). Both low and high constraint 8mm thick implant designs resulted in overcorrection and therefore greater inferior translation (-4.0 ± 2.2mm, P=0.060; and -3.8 ± 2.3mm, P=0.060 respectively). The 8mm low constraint implant caused 2.6 ± 1.2mm of inferiorization relative to the 5mm low constraint implant (P=0.002). This was similar to the 8mm high constraint implant, which resulted in 2.3 ± 1.4mm (P=0.007) of inferior humeral head translation relative to the 5mm high constraint implant. The difference in SI translation between high and low constraint implant models for both thicknesses was not statistically significant (P=1.000). In addition, the position of the humeral head was found to translate inferiorly with increasing abduction angles (0 degrees: -0.6 ± 2.4mm; 30 degrees: -0.9 ± 2.5mm; 60 degrees: -2.8 ± 3.0mm). Significant differences were observed between mean humeral head positions at 0 and 60 degrees of abduction (P<0.001) and 30 and 60 degrees of abduction (P<0.001). However, no significance was detected between average SI humeral head translation values at 0 and 30 degrees (P=0.898).

Figure 3-5 demonstrates the average superior-inferior humeral head translation relative to the native shoulder state at all abduction angles. Superior translation of the humeral head was greatest at 0 and 30 degrees of abduction (2.6 ± 1.9mm, P=0.090; and 2.5 ± 1.3mm, P=0.017 respectively), with superior translation decreasing at 60 degrees (0.9 ± 1.1mm, P=0.648). All implant designs were most effective in restoring native humeral head position at 0 degrees of abduction. At this abduction angle, both 5mm implant designs restored humeral head position to within 1mm of the native state. Humeral head position was found to be significantly different compared to the native state using the 8mm low constraint implant (P=0.013). Similar trends were observed at 30 degrees, with both 5mm implants again restoring humeral head position to within 1mm of the native state, although both 8mm thick implants resulted in significant inferior translation (low constraint: P=0.046, high constraint: P=0.037). At 60 degrees, all implant designs except the 5mm high constraint implant resulted in significant inferior translation of the humeral head

(5mm low constraint: P=0.009, 5mm high constraint: P=0.127, 8mm low constraint: P=0.001, 8mm high constraint: P=0.001).

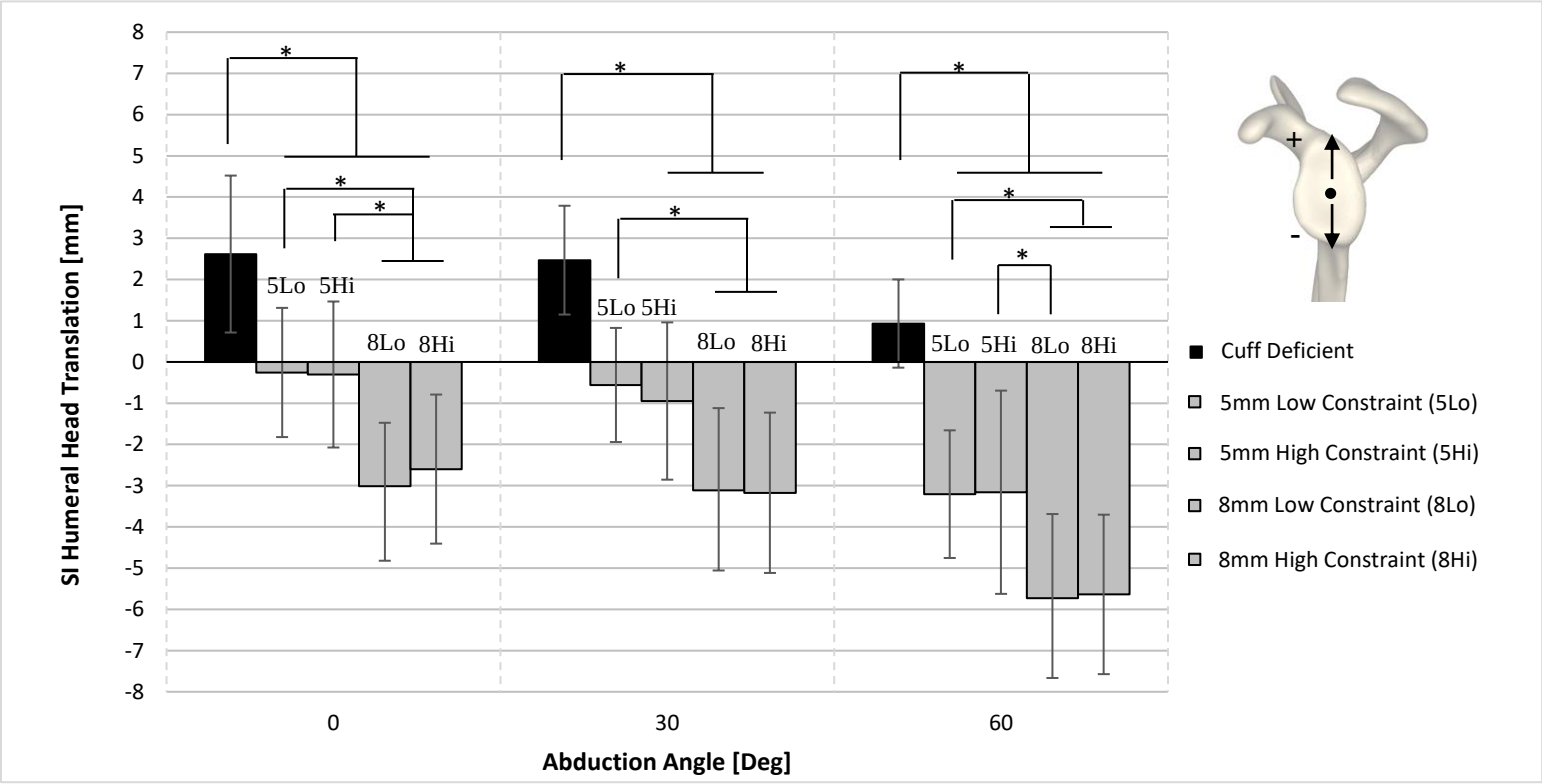

Figure 3-5: SI translation (mean ± 1 SD) of the humeral head relative to the intact test state.

Black bars correspond to the cuff deficient state and grey bars correspond to the implant test states. Significance (P<0.05) denoted by ''.*

3.3.2 Anterior-Posterior Translation

No significant differences in anterior-posterior humeral head translation were found to exist between the different test states. The cuff deficient state on average resulted in posterior translation of the humeral head (-1.4 ± 1.6mm, P=0.128). All implant designs resulted in anterior humeral head translation relative to the intact test state (5mm low constraint: 2.7 ± 3.5mm, P=0.764; 5mm high constraint: 2.0 ± 4.7mm, P=1.000; 8mm low constraint: 3.6 ± 5.4mm, P=1.000; 8mm high constraint: 1.6 ± 4.9mm, P=1.000). The 5mm low constraint implant exhibited increased anterior humeral head translation compared to the 5mm high constraint design (0.6 ± 3.4mm, P=1.000). Similarly, the 8mm low constraint implant displayed greater anterior humeral head translation relative to the 8mm high constraint implant design (1.9 ± 2.3mm, P=0.611). Minimal difference in AP translation was observed between 5mm and 8mm thick implants, for both high and low constraint models (P=1.000). Anterior translation of the humeral head was also observed with increasing abduction angle (0 degrees: 0.5 ± 3.2mm; 30 degrees: 1.0 ± 3.4mm; 60 degrees: 2.6 ± 5.3mm). However, no statistical differences were observed between the different abduction angles tested.

In the cuff deficient state, posterior translation was greatest at 0 degrees of abduction (-2.2 ± 2.2mm, P=0.411) and decreased as the angle of abduction increased (30 degrees: -1.6 ± 1.3mm, P=0.145; 60 degrees: -0.6 ± 0.6mm, P=0.368) (Figure 3-6). All implant designs were found to be most accurate at restoring normal AP humeral position at lower angles of abduction, as anterior translation increased with abduction angle for all implants. For all angles of abduction, the high constraint implants for both 5mm and 8mm thickness values were found to more accurately restore normal AP humeral head position compared to corresponding low constraint implant designs. However, the difference in AP translation between high constraint and low constraint implants, for both implant thicknesses, was not found to be statistically significant across for angles of abduction.

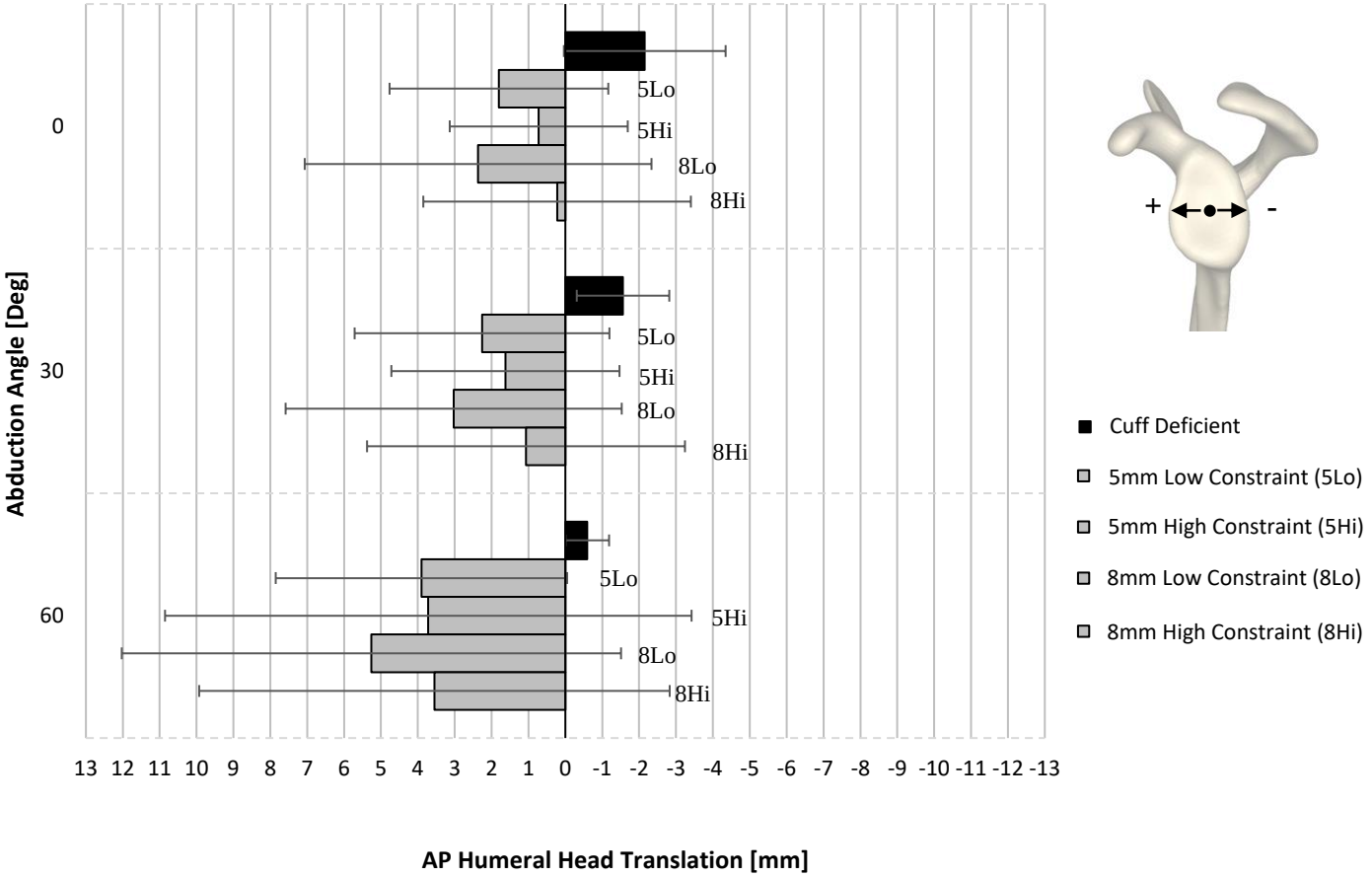

Figure 3-6: AP translation (mean ± 1 SD) of the humeral head relative to the intact test state.

Black bars correspond to the cuff deficient state and grey bars correspond to the implant test states.

3.4 Discussion

The simulated posterosuperior massive, irreparable rotator cuff tear state resulted in corresponding posterosuperior translation of the humeral head when the deltoid was activated. The greatest magnitude of humeral head migration was observed at lower abduction angles, with superior translation decreasing with increased abduction angle. The use of the subacromial implant was effective in reducing the posterosuperior translation of the humeral head observed in the torn state and helped to restore native joint position. Restoring native glenohumeral joint position in patients with massive rotator cuff tears is thought to be helpful for pain reduction and improved range of motion. Superior humeral head migration seen in the torn state also results in a reduction of the deltoid moment arm, thus increasing the deltoid force needed for abduction[6].

The different implant designs used in this study allowed for both the curvature of the implant's primary articular surface and the implant's thickness to be analyzed in their ability to restore native joint position. The implant's thickness was noted to have the greatest effect on superior-inferior humeral head translation. The opposite was observed for anterior-posterior translation, where the constraint of the implant's primary articular surface had the greater influence. Both trends were expected due to the unique constraint each variable had on the humeral head range of motion. Since the implant is positioned above the humeral head, implant thickness primarily influenced the superior-inferior position of the humeral head. Meanwhile, the constraint of the implant's primary articulating surface is determined by this surface's radius in the sagittal plane. Therefore, this variable serves to control the anterior-posterior translation of the humeral head. The results indicate an implant thickness of 5mm combined with a higher constrained primary articular surface design to be most effective at restoring native humeral head position. The 8mm implant designs were too large and overcorrected the position of the humeral head inferiorly relative to the intact test state. The results also confirmed the higher constrained implant's ability to better capture and restabilize the humerus, as greater anterior translation was observed using the lower constrained implants compared to the higher constrained implants.

The results demonstrated that superior humeral migration decreased with increasing abduction angle, implying the restoration of native humeral position to be most critical at lower angles of abduction. This trend can be explained by considering the muscle loads acting on the humerus throughout shoulder elevation. Due to the shallow nature of the glenoid articular surface, the glenohumeral joint depends on the surrounding musculature including the rotator cuff to provide dynamic stability and concavity compression[17,18,36]. However, when multiple rotator cuff muscles are absent or atrophied due to massive, irreparable tears, the concavity compressing forces become unbalanced and result in a loss of containment of the humeral head[2,13,22,32,34]. This is most problematic at lower angles of abduction as the superior pull from the deltoid muscle causes the humeral head to translate upwards. This superior migration of the humerus is less severe at higher angles of abduction as the deltoid line-of-action changes to act more medially, thus increasing concavity compression. The results showed that each implant was most effective at restoring native humeral head position at lower abduction angles. However, at 60 degrees of abduction, all implant designs, including the 5mm high constraint implant, overcorrected humeral head position with increased anterior-inferior translation. These results suggest that future implant designs should more closely consider the changing deltoid line-of-action and potentially the morphology of the entire humeral head at higher abduction angles to mitigate the overcorrection in humeral position.

To our knowledge, there are no studies examining the biomechanics of solid subacromial spacers for the management of massive irreparable rotator cuff tears. This implant is most comparable to the subacromial balloon spacer, as both treatments utilize the presence of a physical medical device in the subacromial space to function as a passive spacer to limit proximal migration of the humerus. Although these two objects have the same purpose and function, they differ significantly in their structure and operation. The balloon is positioned freely within the subacromial space during the surgical procedure while the metallic implant is rigidly fixed to the scapula, The two devices also greatly differ in structure as the implant is a rigid structure while the balloon is made from L-lactide-co-Ɛ-caprolactone, a biodegradable material designed to completely dissipate after 12 months[29]. The balloon is also available in three sizes while the modular aspect of the metallic implant allows for multiple designs to potentially be considered. The unique characteristics of each of these

designs warrant future investigation comparing their ability to restore native humeral head position.

This study has limitations. The testing apparatus applied static loads which do not accurately represent the dynamic loading of the deltoid and rotator cuff muscles *in-vivo*. In addition, the loading apparatus did not permit scapulothoracic rhythm as the scapula was rigidly fixed during testing. Although the testing procedure does not fully mimic *in-vivo* glenohumeral joint conditions, this protocol has previously been used to parametrically assess other surgical treatment options for massive, irreparable rotator cuff tears simulated in cadavers[21,25,30]. Another limitation included the use of cadaver specimens, which do not fully replicate the clinical state. It was ensured that all tissues were kept thoroughly moist throughout testing, and that test time in the laboratory was well under the critical time threshold previously demonstrated to lead to potential changes in the mechanical properties of soft tissues in-vitro[16]. Future studies are warranted to compare the implant to other treatment options for massive, irreparable cuff tears.

3.5 Conclusion

A rigid subacromial implant was biomechanically assessed for the purpose of restoring native humeral head position in patients with proximal humeral head migration due to massive, irreparable rotator cuff tears. The results indicate that the solid subacromial implant tested restored humeral head position, such that it was not significantly different than the native intact shoulder. Additionally, implant size and shape had substantial effects on the restoration of humeral head position, as the 5mm high constraint implant was most effective out of the designs tested at restoring normal humeral head position.

3.6 References

1. Altintas B, Scheidt M, Kremser V, et al. Superior Capsule Reconstruction for Irreparable Massive Rotator Cuff Tears: Does It Make Sense? A Systematic Review of Early Clinical Evidence. *Am J Sports Med*. 2020;48(13):3365-3375. doi:10.1177/0363546520904378

2. Berthold DP, Muench LN, Bell R, et al. Biomechanical consequences of isolated, massive and irreparable posterosuperior rotator cuff tears on the glenohumeral joint: A dynamic biomechanical investigation of rotator cuff tears. *Obere Extrem*. 2021;16(2):120-129. doi:10.1007/s11678-021-00622-3

3. Chalmers PN, Salazar DH, Romeo AA, Keener JD, Yamaguchi K, Chamberlain AM. Comparative Utilization of Reverse and Anatomic Total Shoulder Arthroplasty: A Comprehensive Analysis of a High-volume Center. *J Am Acad Orthop Surg*. 2018;26(24):e504-e510. doi:10.5435/JAAOS-D-17-00075

4. Chalmers PN, Salazar DH, Steger-May K, et al. Radiographic progression of arthritic changes in shoulders with degenerative rotator cuff tears. *J Shoulder Elb Surg*. 2016;25(11):1749-1755. doi:10.1016/j.jse.2016.07.022

5. Denard PJ, Brady PC, Adams CR, Tokish JM, Burkhart SS. Preliminary Results of Arthroscopic Superior Capsule Reconstruction with Dermal Allograft. *Arthrosc - J Arthrosc Relat Surg*. 2018;34(1):93-99. doi:10.1016/j.arthro.2017.08.265

6. Dyrna F, Kumar NS, Obopilwe E, et al. Relationship Between Deltoid and Rotator Cuff Muscles During Dynamic Shoulder Abduction: A Biomechanical Study of Rotator Cuff Tear Progression. *Am J Sports Med*. 2018;46(8):1919-1926. doi:10.1177/0363546518768276

7. Gerber C, Canonica S, Catanzaro S, Ernstbrunner L. Longitudinal observational study of reverse total shoulder arthroplasty for irreparable rotator cuff dysfunction: results after 15 years. *J Shoulder Elb Surg*. 2018;27(5):831-838. doi:10.1016/j.jse.2017.10.037

8. Gerber C, Fuchs B, Hodler J. The results of repair of massive tears of the rotator cuff. *J Bone Jt Surg - Ser A*. 2000;82(4):505-515. doi:10.2106/00004623-200004000-00006

9. Gerber C, Pennington S, Nyffeler R. Reverse total shoulder arthroplasty. *J Am Acad Orthop Surg*. 2009;17:284-295. doi:10.5435/00124635-200905000-00003

10. Gerber C, Wirth SH, Farshad M. Treatment options for massive rotator cuff tears. *J Shoulder Elb Surg*. 2011;20(2):S20-S29. doi:10.1016/j.jse.2010.11.028

11. Giles J, Miguel Ferreira L, Singh Athwal G, Andrew Johnson J. Development and Performance Evaluation of a Multi-PID Muscle Loading Driven in Vitro Active-Motion Shoulder Simulator and Application to Assessing Reverse Total Shoulder

Arthroplasty. *J Biomech Eng*. 2014;136(12). doi:10.1115/1.4028820

12. Hartzler RU, Steen BM, Hussey MM, et al. Reverse shoulder arthroplasty for massive rotator cuff tear: Risk factors for poor functional improvement. *J Shoulder Elb Surg*. 2015;24(11):1698-1706. doi:10.1016/j.jse.2015.04.015

13. Itami Y, Park MC, Lin CC, et al. Biomechanical analysis of progressive rotator cuff tendon tears on superior stability of the shoulder. *J Shoulder Elb Surg*. 2021;30(11):2611-2619. doi:10.1016/j.jse.2021.04.012

14. Jennings A. Sphere Fit (Least Squared). Matlab Central-File Exchange. Published 2021. Accessed October 4, 2021. https://www.mathworks.com/matlabcentral/fileexchange/34129-sphere-fit-least-squared

15. Jensen KL, Williams GR, Russell IJ, Rockwood CA. Current concepts review rotator cuff tear arthropathy. *J Bone Jt Surg - Ser A*. 1999;81(9):1312-1324. doi:10.2106/00004623-199909000-00013

16. King GJW, Pillon CL, Johnson JA. Effect of in vitro testing over extended periods on the low-load mechanical behaviour of dense connective tissues. *J Orthop Res*. 2000;18(4):678-681. doi:10.1002/jor.1100180422

17. Lee SB, Kim KJ, O'Driscoll SW, Morrey BF, An KN. Dynamic glenohumeral stability provided by the rotator cuff muscles in the mid-range and end-range of motion: A study in cadavera. *J Bone Jt Surg - Ser A*. 2000;82(6):849-857. doi:10.2106/00004623-200006000-00012

18. Lippitt SB, Vanderhooft JE, Harris SL, Sidles JA, Harryman DT, Matsen FA. Glenohumeral stability from concavity-compression: A quantitative analysis. *J Shoulder Elb Surg*. 1993;2(1):27-35. doi:10.1016/S1058-2746(09)80134-1

19. Mihata T, Lee TQ, Hasegawa A, et al. Five-Year Follow-up of Arthroscopic Superior Capsule Reconstruction for Irreparable Rotator Cuff Tears. *J Bone Jt Surg - Am Vol*. 2019;101(21):1921-1930. doi:10.2106/JBJS.19.00135

20. Mihata T, Lee TQ, Hasegawa A, et al. Arthroscopic Superior Capsule Reconstruction Can Eliminate Pseudoparalysis in Patients With Irreparable Rotator Cuff Tears. *Am J Sports Med*. 2018;46(11):2707-2716. doi:10.1177/0363546518786489

21. Mihata T, McGarry MH, Pirolo JM, Kinoshita M, Lee TQ. Superior capsule reconstruction to restore superior stability in irreparable rotator cuff tears: A biomechanical cadaveric study. *Am J Sports Med*. 2012;40(10):2248-2255. doi:10.1177/0363546512456195

22. Mura N, O'Driscoll SW, Zobitz ME, et al. The effect of infraspinatus disruption on glenohumeral torque and superior migration of the humeral head: A biomechanical

study. *J Shoulder Elb Surg*. 2003;12(2):179-184. doi:10.1067/mse.2003.9

23. Piekaar RSM, Bouman ICE, van Kampen PM, van Eijk F, Huijsmans PE. The subacromial balloon spacer for massive irreparable rotator cuff tears: approximately 3 years of prospective follow-up. *Musculoskelet Surg*. 2020;104(2):207-214. doi:10.1007/s12306-019-00614-1

24. Prat D, Tenenbaum S, Pritsch M, Oran A, Vogel G. Sub-acromial balloon spacer for irreparable rotator cuff tears: Is it an appropriate salvage procedure? *J Orthop Surg*. 2018;26(2). doi:10.1177/2309499018770887

25. Reeves JM, Singh S, Langohr GDG, Athwal GS, Johnson JA. An in-vitro biomechanical assessment of humeral head migration following irreparable rotator cuff tear and subacromial balloon reconstruction. *Shoulder Elb*. 2020;12(4):265-271. doi:10.1177/1758573219865479

26. Ruiz Ibán MA, Lorente Moreno R, Ruiz Díaz R, et al. The absorbable subacromial spacer for irreparable posterosuperior cuff tears has inconsistent results. *Knee Surgery, Sport Traumatol Arthrosc*. 2018;26(12):3848-3854. doi:10.1007/s00167-018-5083-3

27. Savarese E, Romeo R. New Solution for Massive, Irreparable Rotator Cuff Tears: The Subacromial "Biodegradable Spacer." *Arthrosc Tech*. 2012;1(1):e69-e74. doi:10.1016/j.eats.2012.02.002

28. Schoch B, Wagner E, Elhassan B. Tendon Transfers for Massive Irreparable Rotator Cuff Tear. *Oper Tech Orthop*. 2015;25(1):57-75. doi:10.1053/j.oto.2014.11.001

29. Senekovic V, Poberaj B, Kovacic L, et al. The biodegradable spacer as a novel treatment modality for massive rotator cuff tears: a prospective study with 5-year follow-up. *Arch Orthop Trauma Surg*. 2017;137(1):95-103. doi:10.1007/s00402-016-2603-9

30. Singh S, Reeves J, Langohr GDG, Johnson JA, Athwal GS. The Subacromial Balloon Spacer Versus Superior Capsular Reconstruction in the Treatment of Irreparable Rotator Cuff Tears: A Biomechanical Assessment. *Arthrosc - J Arthrosc Relat Surg*. 2019;35(2):382-389. doi:10.1016/j.arthro.2018.09.016

31. Tashjian RZ. The Natural History of Rotator Cuff Disease: Evidence in 2016. *Tech Shoulder Elb Surg*. 2016;17(4):132-138. doi:10.1097/BTE.0000000000000109

32. Tempelaere C, Pierrart J, Lefèvre-Colau MM, et al. Dynamic three-dimensional shoulder Mri during active motion for investigation of rotator cuff diseases. *PLoS One*. 2016;11(7):1-12. doi:10.1371/journal.pone.0158563

33. Tempelhof S, Rupp S, Seil R. Age-related prevalence of rotator cuff tears in asymptomatic shoulders. *J Shoulder Elb Surg*. 1999;8(4):296-299. doi:10.1016/S1058-2746(99)90148-9

34. Terrier A, Reist A, Vogel A, Farron A. Effect of supraspinatus deficiency on humerus translation and glenohumeral contact force during abduction. *Clin Biomech*. 2007;22(6):645-651. doi:10.1016/j.clinbiomech.2007.01.015

35. Woodmass JM, Wagner ER, Borque KA, Chang MJ, Welp KM, Warner JJP. Superior capsule reconstruction using dermal allograft: early outcomes and survival. *J Shoulder Elb Surg*. 2019;28(6):S100-S109. doi:10.1016/j.jse.2019.04.011

36. Wueler N, Korell M, Thren K. Dynamic glenohumeral joint stability. *J Shoulder Elb Surg*. 1998;7(1):43-52.

Chapter 4

4 The Effect of Combining a Subacromial Implant with a Tuberoplasty Procedure on Normal Joint Stability and Range of Motion

This chapter further evaluates the subacromial implant in restoring both normal joint stability and range of motion when paired with a tuberoplasty procedure. A tuberoplasty removes bone from the greater tuberosity to match the curvature with that of the articular humeral head region. It was postulated that performing a tuberoplasty with the implant in place would further improve joint stability and increase the allowable abduction range of motion. To evaluate this hypothesis, simulated muscle loading was applied to a series of cadaveric shoulders. Anterior-posterior and superior-inferior translation of the humeral head was recorded for each implant design and compared to intact rotator cuff and rotator cuff deficient models. The angle of abduction reached for different deltoid load magnitudes was also quantified.

4.1 Introduction

The previous chapter described the testing of the subacromial implant in its ability to restore normal joint position in a massive irreparable rotator cuff tear model. While all implant designs were effective in preventing superior and posterior translation of the humeral head as observed with this pathology, the 5mm constraint implant design was shown to be most effective in restoring humeral head position to that of the intact rotator cuff test state. This study however did not investigate whether impingement, particularly between the greater tuberosity of the humeral head and implant, occurred throughout abduction. Impingement between these structures could reduce the allowable range of motion of a patient and also reduce the effectiveness of the implant to minimize deltoid loads to produce abduction.

A potential solution to prevent impingement would be to combine the insertion of the subacromial implant with a tuberoplasty procedure. Tuberoplasty refers to the surgical

procedure proposed by Fenlin et al.[2] in 2002 used to smoothen the surface of the greater tuberosity to match the natural curvature of the humeral head (Figure 4-1). This procedure was originally proposed to create a smooth, congruent articulation between the humerus and acromion. Since its proposal, this treatment has also been grouped with arthroscopic debridement and biceps tendon tenotomy to form a procedure termed reversed arthroscopic subacromial decompression[9]. Studies have reported satisfactory results when using this procedure alone to treat elderly patients with massive irreparable rotator cuff tears[3,6,8,10]. Combining the tuberoplasty aspect of this procedure with the subacromial implant may be advantageous in restoring both joint stability and preventing any potential impingement with the humeral head, thereby restoring normal range of motion.

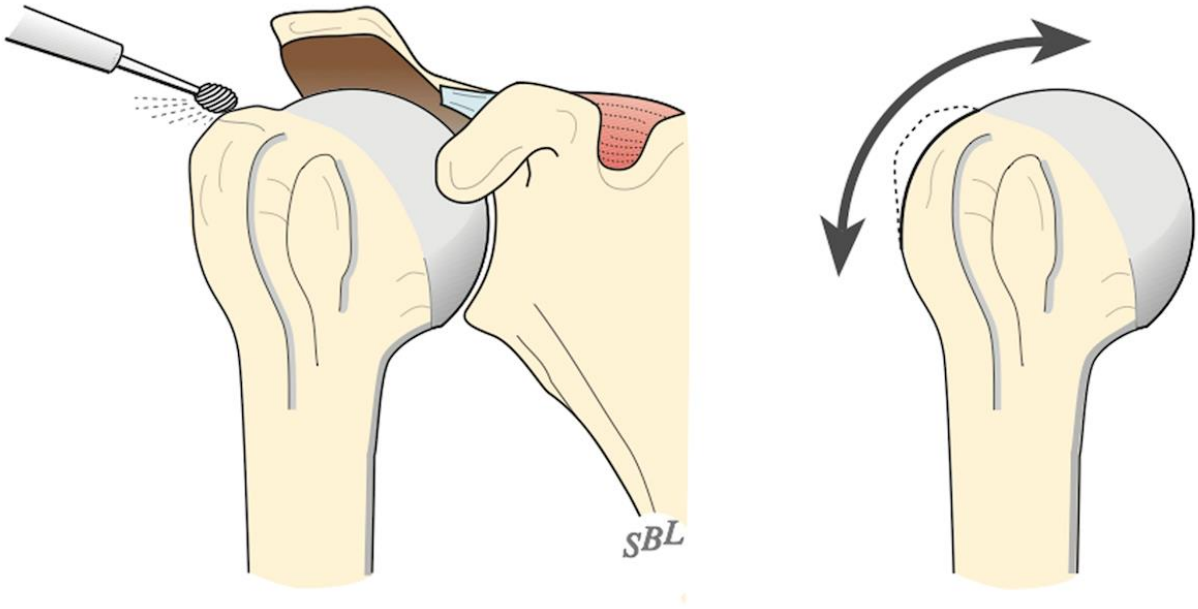

Figure 4-1: Depiction of tuberoplasty procedure

(A) Surgical representation of a tuberoplasty being performed with a burr device. (B) Greater tuberosity bone is removed so the lateral curvature of the humeral head matches that of the articular surface[4].

The first objective of this study was to assess the effect a tuberoplasty procedure, combined with the subacromial implant placement, had on the restoration of normal humeral head position. The second objective was to investigate the difference in allowable range of motion in abduction between the subacromial implant, both with and without a tuberoplasty. It was hypothesized that combining the insertion of the subacromial implant with a tuberoplasty procedure would more effectively restore normal joint position and increase glenohumeral range of motion compared to the use of the subacromial implant alone.

4.2 Methods[4]

Six male, right armed cadaveric specimens were used for the kinematic analysis (average age: 76 ± 16 years), while four male, right armed cadavers were used to conduct the range of motion analysis (average age: 70 ± 2 years). Computer tomography (CT) scans of each cadaver were reviewed prior to testing to ensure no signs of glenohumeral osteoarthritis or cuff tear arthropathy were present at the joint. All cadavers were resected mid-diaphysis, distally to the deltoid tuberosity. Each shoulder was thawed for 18 hours prior to testing. All rotator cuff tendons were tagged at their insertional footprints using #5 Ethibond sutures (Ethicon, Johnson&Johnson, New Brunswick, NJ). To gain access to the joint capsule and posterior rotator cuff insertion, a lateral incision was created with a deltoid split. High strength braided line was connected to each tagged rotator cuff insertion. A single transosseous hole was drilled into the lateral aspect of the deltoid tuberosity to serve as the insertion site for all three braided lines representing the three heads of the deltoid. A single hole was used, as opposed to three different transosseous holes, to improve the wrapping of the anterior and posterior deltoid braided lines. A humeral rod assembly was fixed into the humeral canal using acrylic dental cement which cured for a minimum of 15 minutes.

The shoulder simulator used in Chapter 3 was again used to conduct in-vitro testing with the implant, however, several changes were applied to the simulator design (Figure 4-2).

---

[4] The methods presented in this chapter are similar to those described in Chapter 3.

The abduction arc, along with its humeral fixation carriage, were replaced with a guide rail mechanism in order to reduce the constraint on the humerus during testing. The previous design required sufficient abduction force in order to overcome the friction between the abduction arc and humeral fixation carriage, and thereby did not allow for smooth abduction. This new design utilized an alignment slot which constrained motion to a single elevation plane while minimizing friction between the simulator and humeral rod. This design also allowed for the humerus and humeral rod to rotate freely internally and externally. This minimized the constraint placed on the humerus during testing, allowing the humerus to move along the path of least resistance during elevation. Fixation of the scapula relative to the base of the shoulder simulator was also changed. In the previous design, the shoulder was fixed directly to the base of the simulator. The new design introduced a system of alignment plates that allowed for the shoulder to be fixed more laterally to the base of the simulator. This was advantageous for several reasons. The new alignment plate system allowed for the position of the shoulder to be adequately adjusted in three dimensions to ensure the glenohumeral joint was aligned with the center of rotation of the abduction guide rail. This prevented impingement between the guide rail and humeral rod assembly, due to misalignment between the glenohumeral joint and simulator in the anterior and posterior direction, as was observed with the previous simulator design. Furthermore, the lateralization of the shoulder relative to the base of the simulator increased the accessibility of the cadaver specimen during testing. In the previous design, the shoulder was fixed directly to the base of the simulator, only allowing anterior and lateral surgical access to the shoulder. The new fixation location of the cadaver onto this simulator allowed for anterior, lateral, and posterior surgical access to the cadaver specimen throughout testing. Unrestricted access to the posterior shoulder was important during testing to allow for easy insertion of the subacromial implant. The shoulder was positioned on the simulator to allow for approximately 10-20 degrees of forward scapular tilt as observed in previous biomechanical studies[1,5].

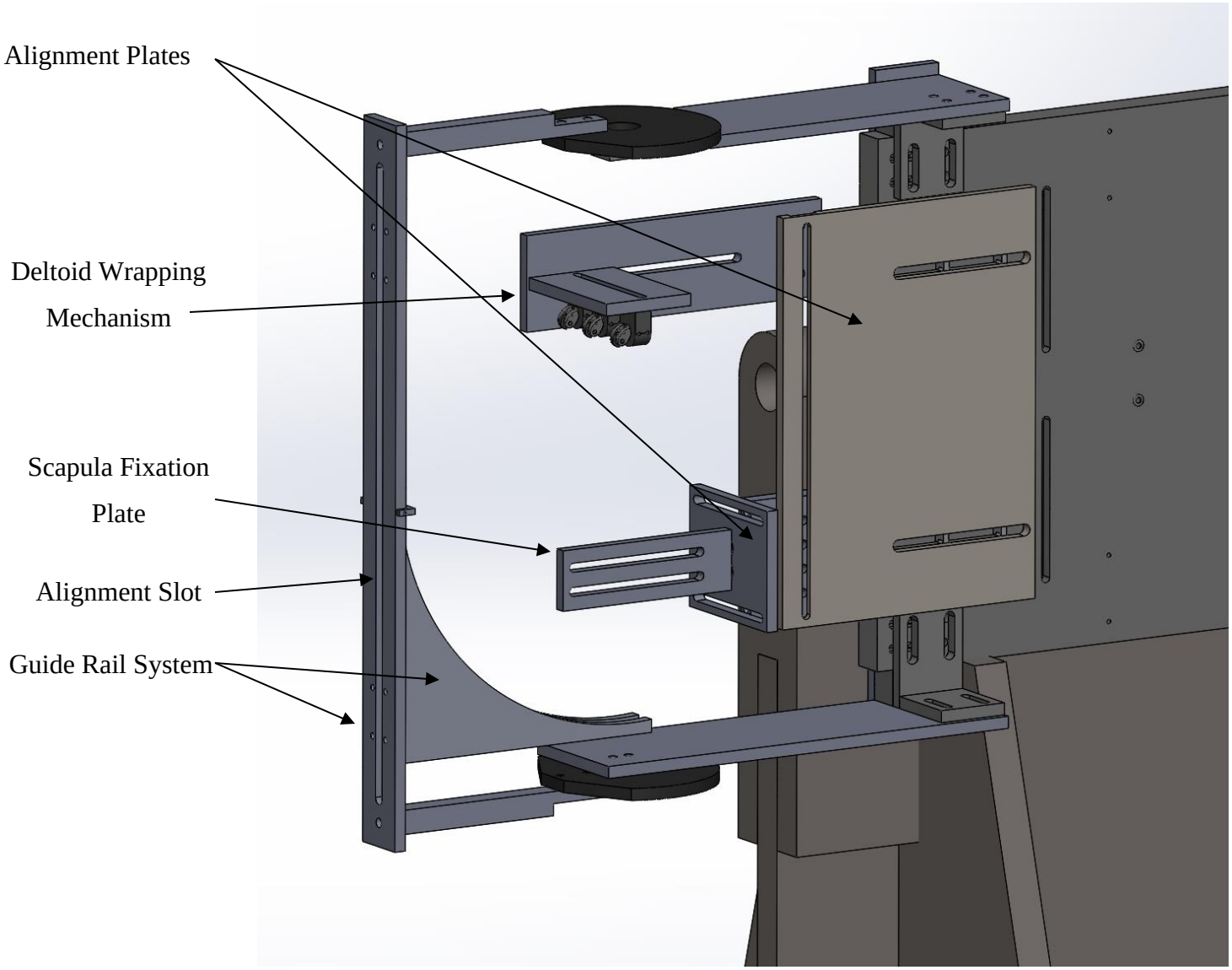

Figure 4-2: The new shoulder simulator design used for testing.

A new guide rail system utilizes a slot to constrain elevation to a single plane, while allowing for axial rotation. A system of alignment plates can be translated in three dimensions to ensure proper positioning of the scapula, which is mounted to the scapula fixation plate. Lastly, the deltoid wrapping plates can be translated to change the simulated wrapping of the deltoid muscle.

The lines, connected to all muscle insertions, were attached to individual pneumatic actuators used for muscle activation. The lines connected to the rotator cuff insertions were routed along the base of the shoulder simulator using eyebolts to best mimic each physiological muscle line of action. The three lines representing the three heads of the deltoids were each routed through 2-DOF pullies (Figure 4-3). These pullies were used for their ability to adapt to the changing muscle line of action throughout full range of abduction motion, while also minimizing the friction with the braided line. Each pulley was positioned within the sagittal plane to best represent the origin of each deltoid head. The middle deltoid pulley was aligned with the center of the acromion, the posterior deltoid pulley with the scapular spine, and the anterior deltoid pulley with the distal third of the clavicle. All three pullies were positioned directly above the scapular notch, as pilot studies demonstrated this position to most accurately replicate the deltoid muscle line of action and muscle wrapping over the acromion. To control the pneumatic actuators, and therefore muscle loading, a custom LabVIEW (National Instruments, Austin, Texas, USA) code was developed to apply static muscle loading to each individual muscle. Static muscle loading was based on previous cadaver studies investigating superior humeral head translation and different treatments for massive irreparable rotator cuff tears. An optical tracking system (Certus, Northern Digital, Waterloo, ON, Canada) was used to track the motion of both the scapula and humerus throughout testing using optical tracker markers rigidly fixed to each bone. All soft tissue was copiously hydrated using normal saline throughout testing to maintain normal muscle mechanics.

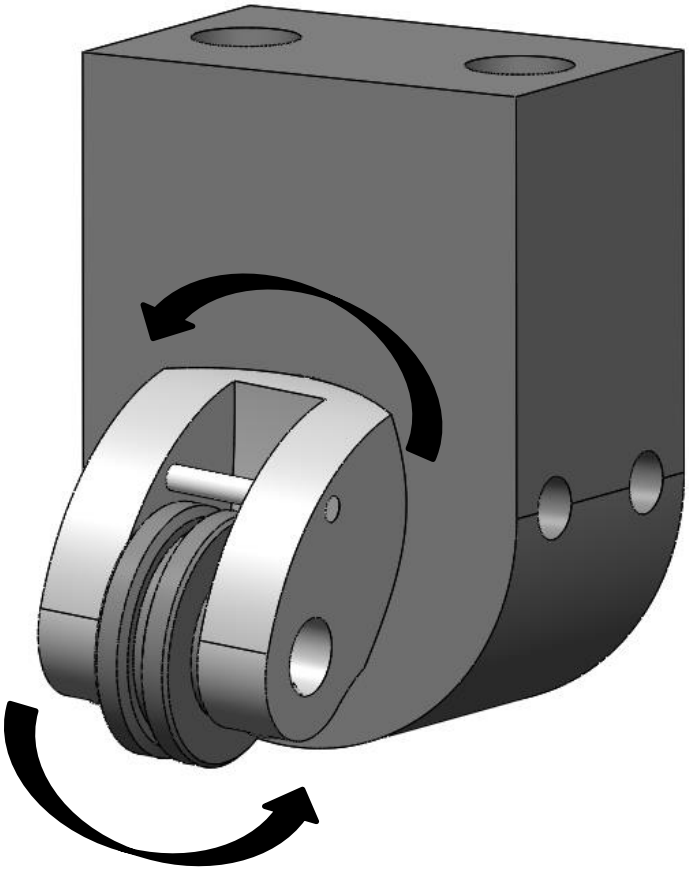

Figure 4-3: Two DOF pulley

Three of these pullies were used to control the wrapping of the deltoid lines over the acromion. The pulley rotates freely with within the encased Delrin structure.

4.2.1 Kinematic Analysis

4.2.1.1 Test States

The first state tested was the intact rotator cuff. This testing state served to represent a healthy glenohumeral joint with no rotator cuff pathology. The lateral incision used to suture the posterior rotator cuff tendons was closed using 2-0 Vicryl (Ethicon, Johnson&Johnson, New Brunswick, NJ) before testing. In this test state, the application of 80N was equally distributed across all three deltoid heads, while 10N was applied to the supraspinatus, infraspinatus, teres minor, superior subscapularis, and inferior subscapularis.

The intact test state was followed by the creation of a massive irreparable rotator cuff tear, with insertion of the subacromial implant. The massive irreparable rotator cuff tear was simulated by surgically removing the supraspinatus tendon and the anterior fibers of the infraspinatus tendon from the joint space. Results for the cuff deficient state are not presented in this chapter as this comparison was established in Chapter 3. The implant models used in this chapter were similar to those used in Chapter 3. However, the implants used in Chapter 3 were designed for left scapulae. Therefore, additional implants, capturing the same thickness and constraint variables, were required for right scapulae. These implants were created by mirroring the previous implant designs about their frontal plane using computer-aided design (CAD) software, ensuring the same geometry was obtained. Further modifications to the implant design included additional digitization features along the length of the implant's lateral edge. The setscrew hole was also shortened, allowing for a smaller length setscrew to be used during testing. The same fabrication process used in Chapter 2 was again used to create one superior implant component and four inferior components. The four inferior components captured 5mm and 8mm implant thicknesses in addition to high constraint and low constraint articular surfaces. The same surgical technique, as described in the previous chapters, was used to insert the subacromial implant into each shoulder. This was performed by a board-certified Orthopaedic surgeon (D.F.). The lateral and posterior incisions were sutured closed using 2-0 Vicryl before the start of each test. The order in which the different subacromial implant designs were tested was randomized for all specimens. During the testing for each implant, the rotator cuff muscle

loads were changed compared to those used during the intact state. While 10N was still applied to the teres minor tendon, 5N were applied to each subscapularis tendon to ensure a balanced transverse force couple.

The final test state utilized the subacromial implant with the addition of a tuberoplasty. A tuberoplasty was performed through the lateral incision by removing and smoothing exposed greater tuberosity bone on the humeral head. This included bone from the anterior aspect of the greater tuberosity (extending to the bicipital groove) up to that of the remaining intact infraspinatus rotator cuff tendon. The quantity of bone removed was assessed visually so the remaining greater tuberosity matched the curvature of the humeral head (Figure 4-4). Subacromial implant designs were then tested in reverse order compared to the previous subacromial test state discussed in the previous paragraph.

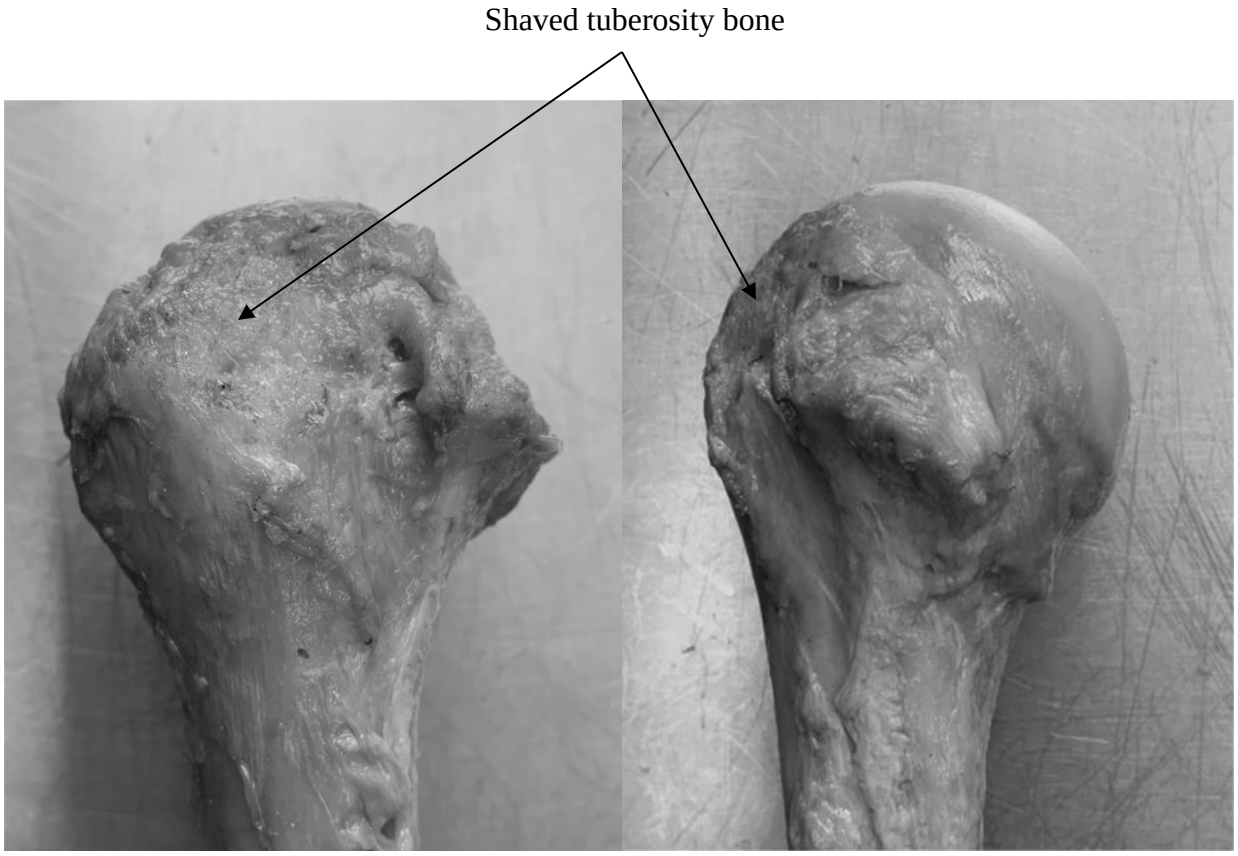

Figure 4-4: Proximal humerus with a tuberoplasty performed.

(A) Lateral view and (B) Anterior view.

4.2.1.2 Outcome Variables and Statistical Analysis

The primary outcome variables obtained from the kinematic analysis included translation of the humeral head relative to the glenoid, similar to Chapter 3. This was quantified in all test states at 0, 15, 30, 45, and 60 degrees of glenohumeral abduction, which were marked on the abduction guide rail using a digital protractor prior to testing. The abduction guide rail was set at an angle of 30 degrees relative to the frontal plane to represent elevation in the scapular plane. Translation of the humeral head center was used to quantify translation of the humerus. This point was estimated by digitizing the articular surface of the humerus and applying a sphere-fitting algorithm in MATLAB (MathWorks, Natick, MA, USA) using the digitized points. The direction of humeral head translation was quantified by creating a local coordinate system on the glenoid determined using digitized 12, 3, 6, and 9 clock points on the glenoid periphery. All translation values were normalized with respect to the intact rotator cuff testing state, with superior and anterior translation represented as positive. A two-way repeated measures analysis of variance (RM-ANOVA), for the independent variables of glenohumeral abduction angle and the testing state, was performed using SPSS software (IBM, Armonk, NY, USA) on both superior-inferior (SI) and anterior-posterior (AP) translation results. A Bonferroni correction was used to correct for the multiple statistical analyses performed, with the significance value set as $p<0.05$.

4.2.2 Range of Motion Analysis

4.2.2.1 Test States

Unlike the kinematic analysis, only the results for the implant test states are reported for the range of motion analysis. This allowed for the primary focus to be placed on the comparison of range of motion between all implant models with and without a tuberoplasty. This further allowed for the focus of this analysis to be placed on the investigation of whether impingement between the greater tuberosity and implant occurred. The same rotator cuff muscle loads as used previously in the implant test states were again used in this analysis.

At the beginning of each test state, the rotator cuff muscle loads were applied, ensuring the humeral head was within joint. Sequential deltoid loading was then performed in 10N

increments starting at 20N, and progressing to a maximum deltoid load of 80N, as this force value was shown to be sufficient for achieving maximum glenohumeral abduction in pilot studies. The total deltoid load was evenly distributed across its three heads. Glenohumeral abduction was performed in the abduction guide rail in the scapular plane to prevent out of plane motion of the humerus.

4.2.2.2 Outcome Variables and Statistical Analysis

The angle of glenohumeral abduction achieved at each deltoid load served as the primary outcome variable in this analysis, similar to that of previous biomechanical literature[7]. To quantify this angle, the optical tracking system was again used to record the position of the humerus at each sequential deltoid load value throughout testing. The angle between the long axis of the humerus in each of these positions and the long axis of the humerus when positioned in zero degrees of elevation was used to quantify the abduction angle. The long axis of the humerus was obtained by digitizing the surface of the humeral shaft and applying a cylinder-fitting algorithm to these collected points in MATLAB. The position of the humerus in zero degrees of elevation was recorded prior to the start of testing, while using a digital protractor to validate the position of the humerus. A two-way RM-ANOVA, for the independent variables of deltoid muscle load and the test state, was performed on abduction angle results using SPSS. A Bonferroni correction was used to correct for the multiple statistical analyses performed, with the significance value set as $p<0.05$.

4.3 Kinematic Analysis Results

4.3.1 Superior-Inferior Translation

Similar to the findings of Chapter 3, all implant designs prior to conducting the tuberoplasty were effective in preventing superior humeral head translation relative to the intact rotator cuff test state. The 5mm thick designs were more effective at restoring normal humeral head position relative to the 8mm thick implants. The 5mm high and low constraint implants resulted in -2.0 ± 1.2mm (P=0.134) and -2.0 ± 1.3mm (P=0.279) of SI translation respectively. The 8mm high and low constraint implant designs however caused -4.0 ± 1.5mm (P=0.031) and -4.3 ± 1.9mm (P=0.068) of SI translation relative to the intact state respectively. All implant models, when combined with the tuberoplasty procedure, were

more effective at restoring normal humeral head position compared to without the tuberoplasty. The 5mm high and low constraint implant designs were the most effective and resulted in -1.2 ± 1.0mm (P=0.800) and -1.7 ± 1.5mm (P=1.000) of SI translation relative to the intact test state respectively. The 8mm high and low constraint implant designs were also more effective compared to their non-tuberoplasty counterparts, resulting in -3.7 ± 1.2mm (P=0.003) and -4.0 ± 1.6mm (P=0.031) of SI translation relative to the intact condition respectively. However, no statistical significance was observed in average SI translation values between corresponding implant models with and without a tuberoplasty (P=1.000 for all implant models). SI translation was found to decrease as the angle of abduction increased when results were averaged across all test states. Statistical significance in SI translation however was only obtained between angles of 45 and 60 degrees (P=0.005).

SI translation relative to the intact test state was found to decrease in all implant models as the angle of abduction increased (Figure 4-5). This trend however was less severe in all implants tested with a tuberoplasty, as all implants resulted in less inferior translation compared to the intact condition at greater angles of abduction. At 60 degrees of glenohumeral abduction, the 5mm high and low implants with a tuberoplasty reduced inferior translation by 2.4 ± 1.2mm and 1.6 ± 1.2mm respectively compared to without a tuberoplasty. A similar trend was also observed in the 8mm high and low constraint implants with a tuberoplasty, which reduced inferior translation by 1.2 ± 3.2mm and 1.0 ± 2.5mm respectively compared to without a tuberoplasty. However, the SI translation differences between implant models with and without a tuberoplasty at 60 degrees were not found to be statistically significant.

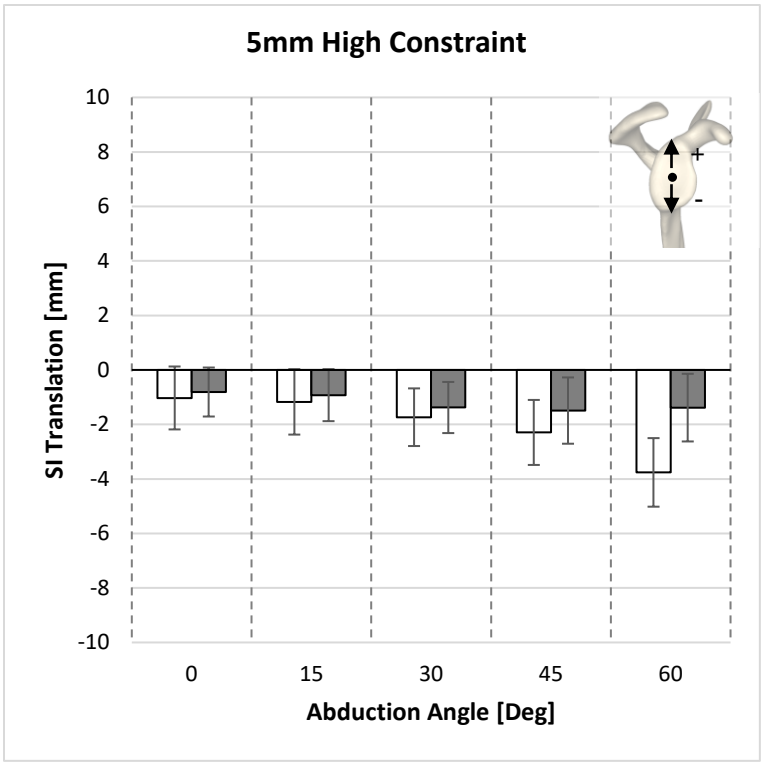

A

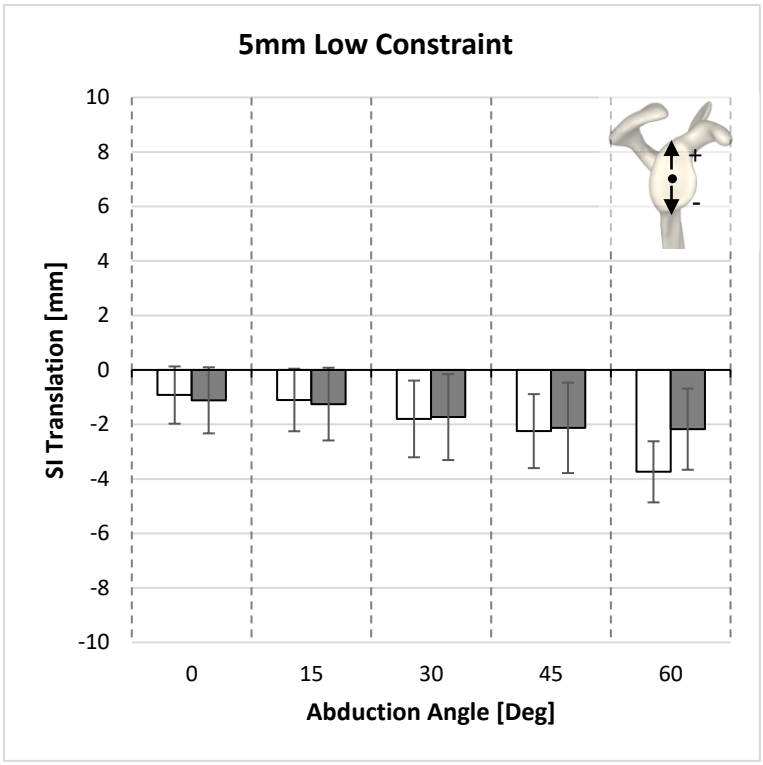

B

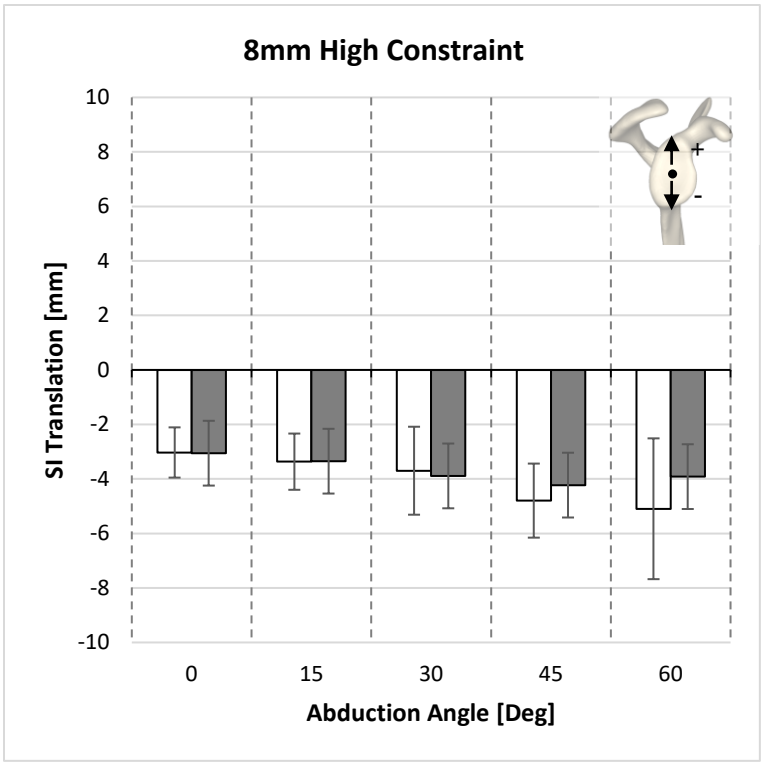

C

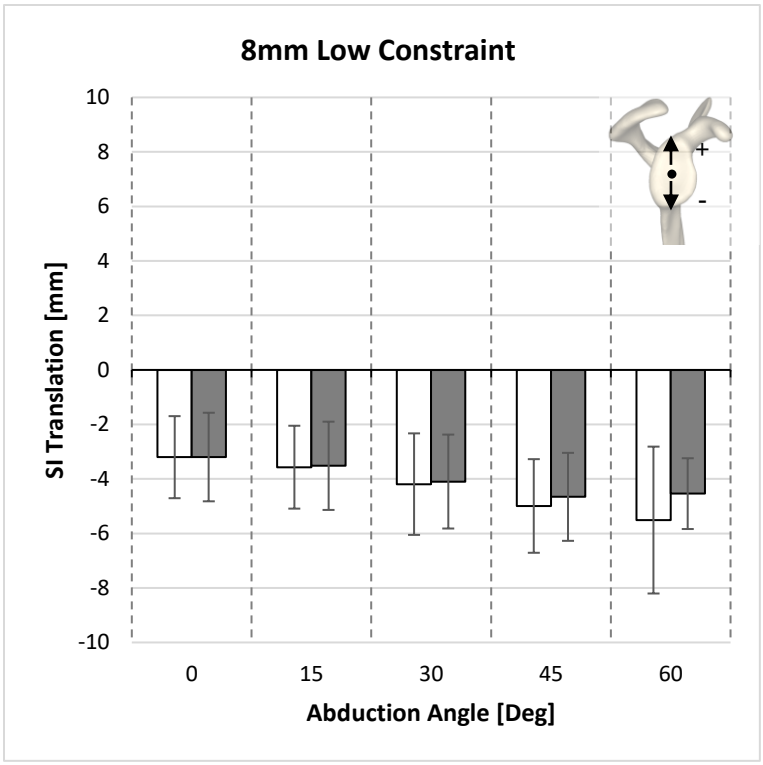

D

Figure 4-5: SI translation (mean ± 1 SD) of the humeral head relative to the intact test state.

White bars correspond to the implants tested without a tuberoplasty, while grey bars correspond to implants tested with a tuberoplasty. (A) 5mm high constraint, (B) 5mm low constraint, (C) 8mm high constraint, and (D) 8mm low constraint.

4.3.2 Anterior-Posterior Translation

All subacromial implant designs were effective in preventing excessive posterior translation of the humeral head relative to the intact state. Prior to performing the tuberoplasty, the high constraint implant designs more effectively restored normal humeral head position compared to the low constraint designs. The 5mm high constraint implant on average was the most effective implant model, which resulted in 0.3 ± 1.2mm (P=1.000) of AP translation, while the 5mm low constraint design on average resulted in 1.0 ± 1.3mm (P=1.000) of AP translation relative to the intact state. The 8mm high and low constraint models averaged 2.0 ± 2.4mm (P=1.000) and 3.0 ± 2.0mm (P=0.200) of AP translation respectively. However, all implant models on average were more effective at restoring humeral head position to that of the intact state once paired with a tuberoplasty. The 5mm high constraint implant model with a tuberoplasty was again the most effective implant design, which resulted in -0.1 ± 0.9mm (P=1.000) of translation relative to the intact rotator cuff test state. The 5mm low constraint averaged 0.7 ± 1.2mm (P=1.000). The 8mm high and low constraint implants averaged 1.2 ± 1.0mm (P=0.473) and 2.4 ± 1.6mm (P=0.321) of AP translation. No significance was observed in AP translation results between corresponding implant models with and without a tuberoplasty. Increased anterior humeral head translation was also observed with increasing angle of abduction, although no statistical significance was observed between the different abduction angles tested.

The tuberoplasty procedure, when combined with the subacromial implant, was effective in limiting anterior humeral head translation across all angles of abduction in 5mm low constraint, and 8mm high and low constraint implants (Figure 4-6). Only at 45 and 60 degrees of glenohumeral abduction was the 5mm high constraint model more effective at restoring normal humeral head position when paired with a tuberoplasty. The addition of the tuberoplasty appeared to be most effective in restoring normal AP humeral position at higher angles of abduction in the 8mm thick implants. In the 8mm high and low constraint models, the addition of the tuberoplasty more effectively restored humeral position to within 2.2 ± 5.6mm and 1.9 ± 4.7mm of the intact condition at 60 degrees of abduction respectively. However, the difference in AP translation between corresponding implant designs with and without a tuberoplasty were not significant (P=1.000).

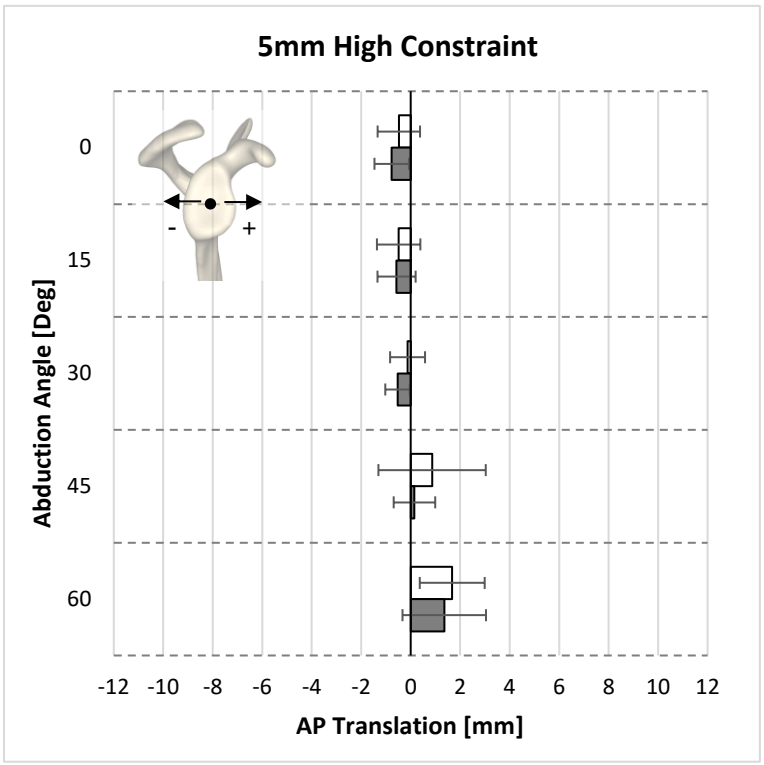

A

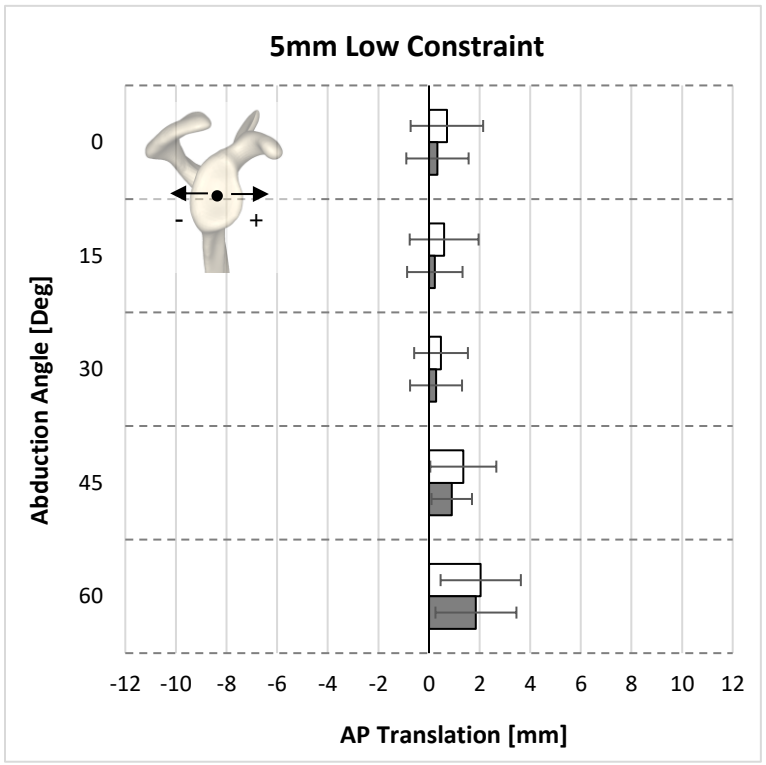

B

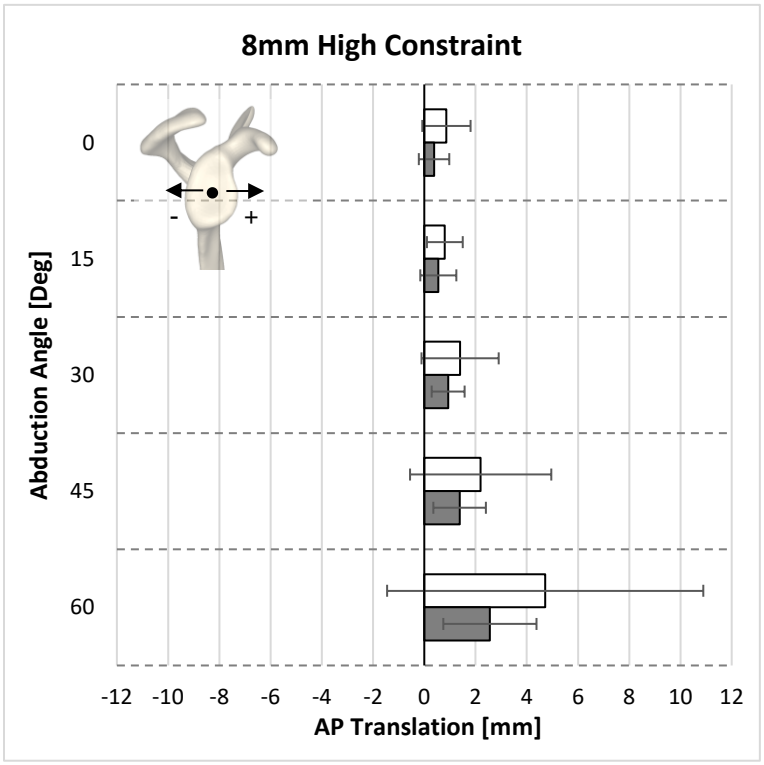

C

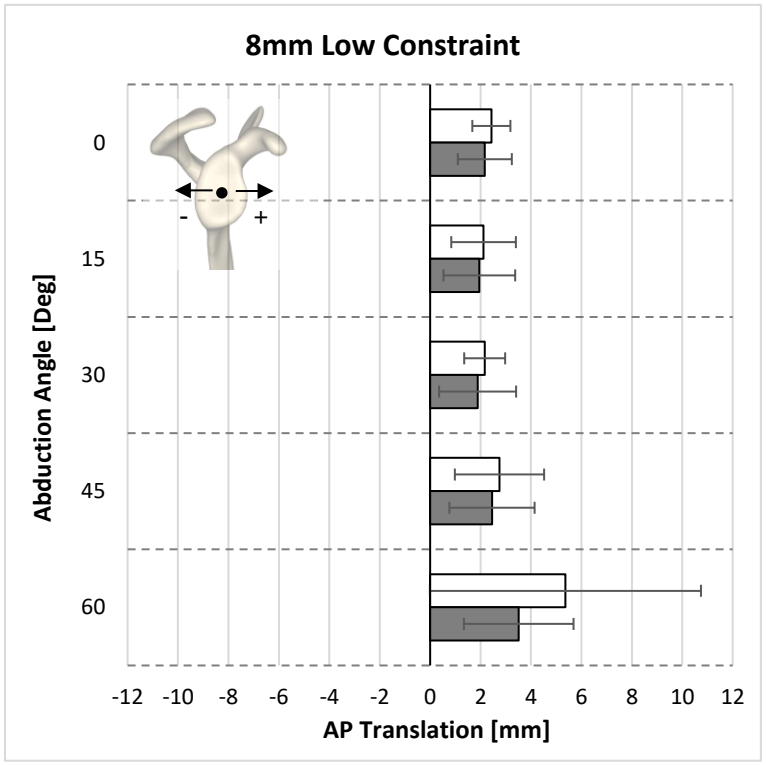

D

Figure 4-6: AP translation (mean ± 1 SD) of the humeral head relative to the intact test state.

White bars correspond to the implants tested without a tuberoplasty, while grey bars correspond to implants tested with a tuberoplasty. (A) 5mm high constraint, (B) 5mm low constraint, (C) 8mm high constraint, and (D) 8mm low constraint.

4.4 Range of Motion Analysis Results

When averaged across all deltoid loads tested, all implants displayed greater abduction angles when tested with a tuberoplasty. The 5mm high and low constraint implants achieved slightly higher abduction angles (49.6° ± 12.5° degrees and 53.9° ± 12.8° degrees respectively) compared to 8mm high and low constraint designs (49.2° ± 12.3° degrees and 49.0° ± 14.9° degrees respectively), when all tested with a tuberoplasty. The 5mm high and low constraint implants without a tuberoplasty achieved 31.2° ± 11.2° degrees and 36.3° ± 11.4° degrees of abduction, while 8mm high and low implants tested without a tuberoplasty on average achieved 32.8° ± 12.3° degrees and 34.2° ± 9.25° degrees of abduction. No statistically significant differences were present between the different testing states. It was also observed that the abduction angle increased with deltoid load when averaged across the different testing states ($P<0.001$).

At the maximum deltoid load of 80N, the 5mm high and low constraint implants, when tested with a tuberoplasty, achieved the largest abduction angles of 96.9° ± 17.8° degrees and 95.8° ± 17.6° degrees respectively (Figure 4-7). The 8mm high and low constraint tuberoplasty testing states with a tuberoplasty achieved slightly smaller angles of 86.4° ± 21.2° degrees and 84.6° ± 19.3° degrees respectively. For both thickness implants with a tuberoplasty, greater abduction was achieved with the high constraint models, however, these differences were minimal. The implant test states without the tuberoplasty achieved far smaller angles of abduction when tested at the maximum deltoid load, although no statistically significant differences between corresponding implant designs with and without a tuberoplasty were observed.

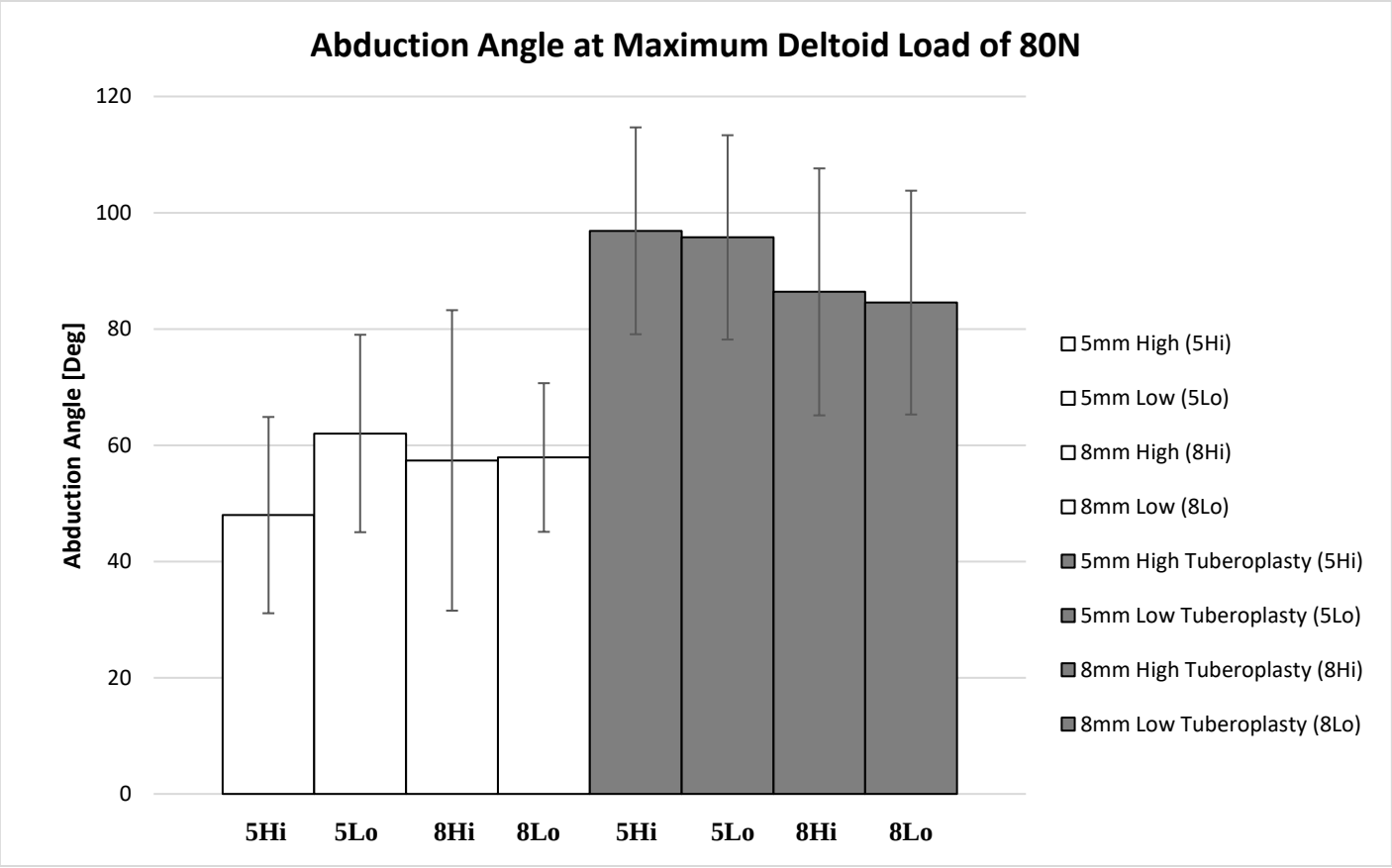

Figure 4-7: Maximum (mean ± 1 SD) angle of abduction achieved with 80N deltoid load.

White bars represent the different implant designs without a tuberoplasty, while the grey bars represent the angle of abduction achieved by the different implant designs with a tuberoplasty.

Figure 4-8 displays the progression of abduction angle with increasing deltoid load for all implants tested. Abduction angle increased with deltoid load for all implant designs, both with and without a tuberoplasty. However, it was observed that the difference in abduction angle between implants tested with and without a tuberoplasty increased around 60N, as the angle of abduction seem to converge between 40°-60° degrees for the implants tested without a tuberoplasty. No statistical significance was achieved in abduction angle between corresponding implants with and without a tuberoplasty for all deltoid loads.

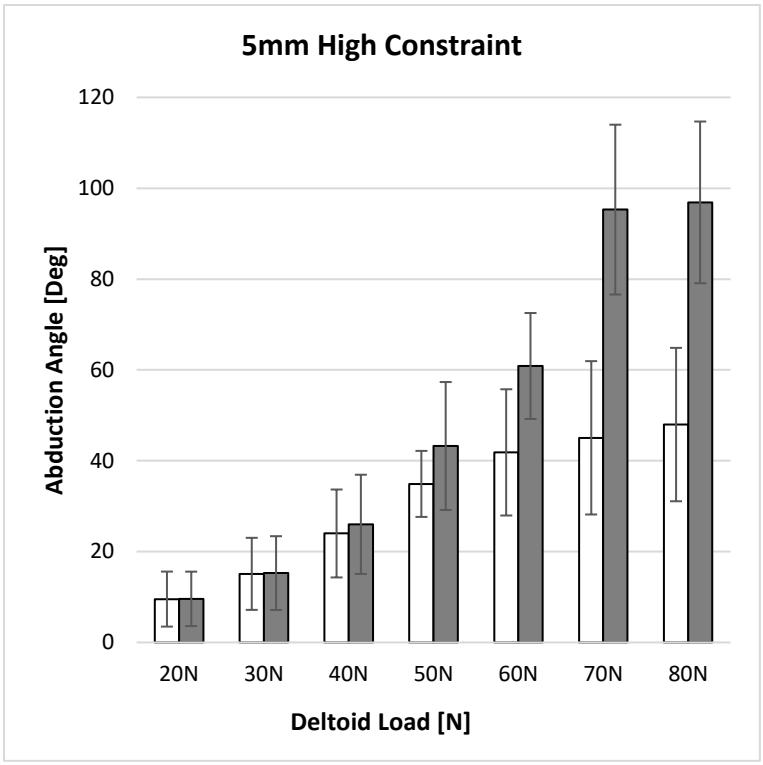

A

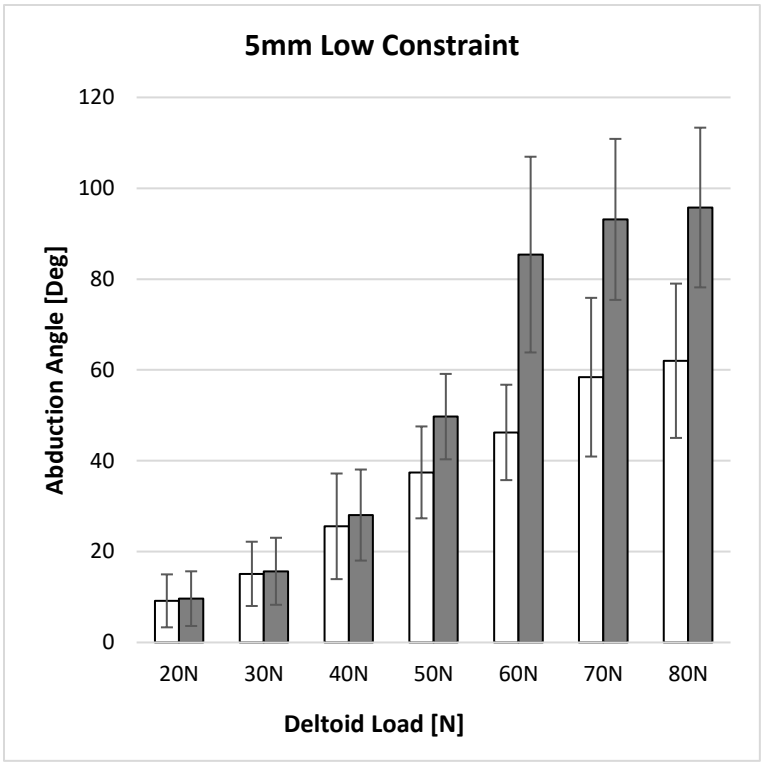

B

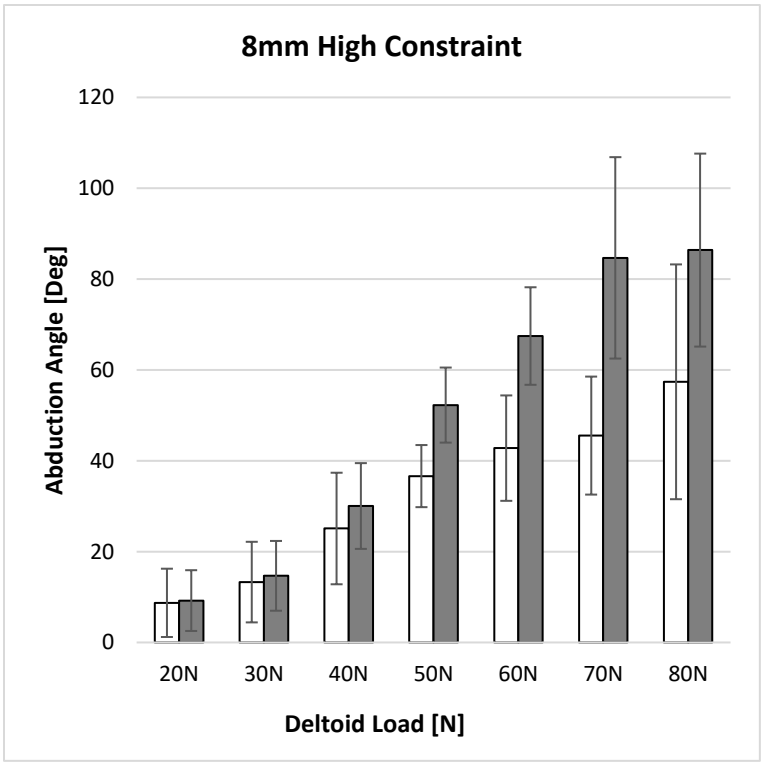

C

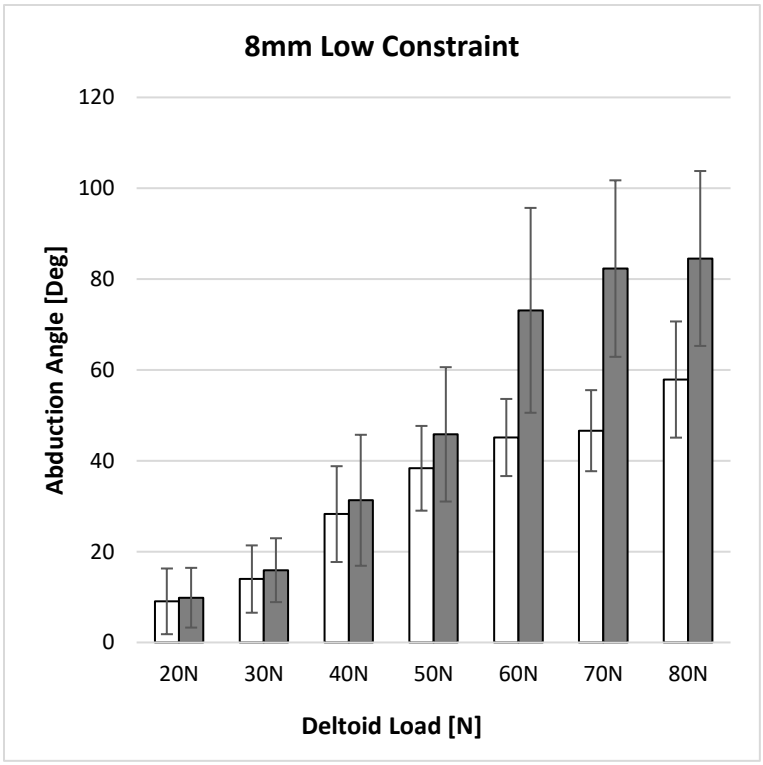

D

Figure 4-8: Abduction angle (mean ± 1 SD) versus deltoid load.

Results are presented for all implant models, both without (white) and with (grey) a tuberoplasty.

4.5 Discussion

Similar translation results to those obtained in Chapter 3 were achieved with the subacromial implant design prior to the tuberoplasty in both AP and SI directions. All implants prevented the superior and posterior translation that was observed in the cuff deficient test state. The constraint of the implant again appeared to have the greatest influence on AP position of the humerus, with the high constraint implant models more effectively restoring normal humeral head position on average. This is due to the smaller radius in the AP direction on the implant's inferior articular surface. The increased curvature of this surface provides greater constraint anteriorly and posteriorly onto the humeral head compared to the low constraint design, which more closely resembles a flatter surface and thereby provides little resistance to translation. The thickness of the implant had the greatest influence on the SI position of the humeral head. Similar to Chapter 3, the 5mm thickness was more effective at restoring normal humeral head position compared to the 8mm thick implants. The 8mm thick implants also increased the anterior translation of the humeral head, suggesting the thickness of the implant to also have an influence on AP translation of the humeral head. The translation results obtained again illustrate that the 5mm high constraint implant design, assuming no other surgical interventions, is the most effective subacromial implant design at restoring normal position of the humeral head.

It is worth noting that the results obtained for both AP and SI translation exhibited slightly different values compared to those in Chapter 3 of this thesis. These differences include lower average superior migration observed in the cuff deficient test state, greater average posterior translation in the cuff deficient state, and different average values obtained across the implant designs. The probable cause of these differences is multifactorial. It is likely that the changes applied to the shoulder simulator affected the translation of the humerus in all testing states. However, these changes were designed to reduce the constraint placed on the glenohumeral joint by the shoulder simulator, therefore more accurately modelling joint motion. Additionally, the contralateral shoulder of the cadavers used in Chapter 3 were used for testing in this chapter, which may have exhibited slight differences in both scapular and humeral morphology. Also, insertion and positioning of the implant was

completed by different board-certified surgeons in both chapters, which may have led to different subacromial implant positioning in each cadaver tested.

The addition of a tuberoplasty was found to restore normal joint position more accurately in both AP and SI directions for all implant designs. However, the difference in translation results between all implant models with and without a tuberoplasty were minimal. As previously noted, the effect of the tuberoplasty on humeral head position was most observable at greater angles of abduction. This is likely due to the anatomy of the greater tuberosity and its position relative to the implant throughout abduction. The greater tuberosity extends outwards from the surface of the humeral head, disrupting the smooth curvature of the humeral head articular surface. It is positioned both laterally and slightly posteriorly on the humeral head as it provides insertion for the supraspinatus and posterior rotator cuff muscles. At lower angles of glenohumeral abduction and neutral axial rotation, the greater tuberosity is positioned laterally relative to both the acromion and subacromial implant. As elevation increases and the humerus rotates, the greater tuberosity slides underneath both the acromion and subacromial implant. Since this feature protrudes off the surface of the humeral head, the humerus must translate in order to allow the greater tuberosity to slide underneath the implant, or impingement will result (Figure 4-9). This translation is reflected in the non-tuberoplasty translation results at 45 and 60 degrees shown in Figure 4-5 and Figure 4-6, where the humeral head exhibits increased anterior and inferior translation. It is likely that increases in both anterior and inferior translation exist due to the impingement between the subacromial implant and greater tuberosity. The lateral aspect of the greater tuberosity is likely responsible for the inferiorization of the humeral head, while the exposed posterior aspect of the greater tuberosity likely contacts the posterior implant, translating the humeral head anteriorly. With the addition of the tuberoplasty, which removes and smoothens the exposed greater tuberosity caused by the massive irreparable rotator cuff tear, each implant exhibited decreased anterior and inferior humeral head translation at these higher angles of abduction. However, only small differences in translation were observed between implants with and without a tuberoplasty likely due to the fact that only small quantities of bone were removed from the greater tuberosity.

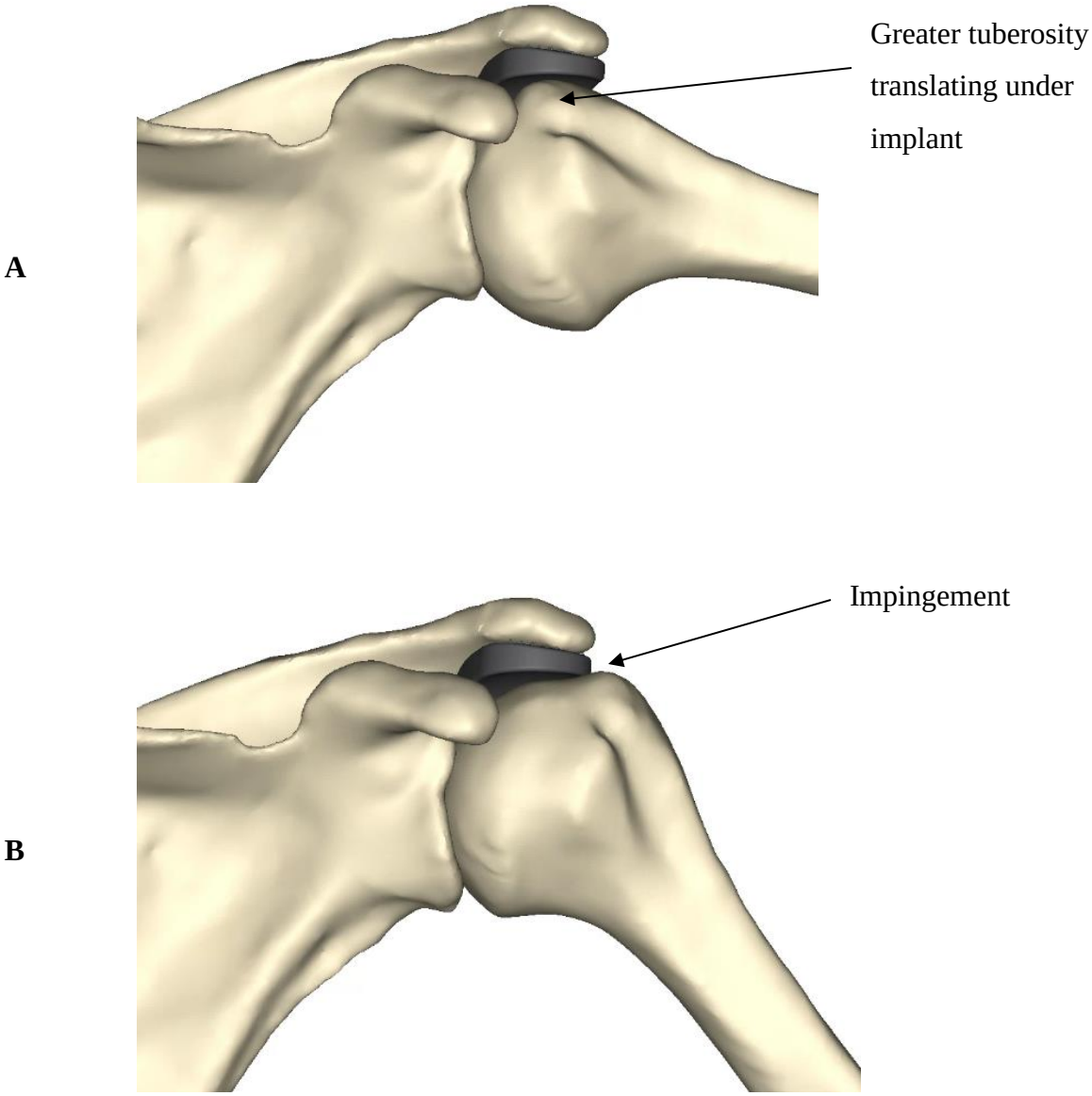

Figure 4-9: Articulation between implant and humeral head.

(A) The humeral head translates inferiorly to allow the greater tuberosity to slide under the implant. (B) Failure for the humerus to translate inferior results in impingement between the lateral edge of the implant and the greater tuberosity.

The benefits of adding the tuberoplasty procedure were perhaps most observable during the range of motion analysis. All implant designs exhibited improved range of motion when paired with a tuberoplasty. The range of motion results presented at the maximum deltoid load (Figure 4-7) are of particular interest as they represent the maximum allowable abduction angle that can be achieved under a high deltoid load. These results suggest that the insertion of the subacromial implant with a tuberoplasty does not affect the normal range of abduction motion in a patient. However, without a tuberoplasty, the subacromial implant restricts the allowable range of abduction motion to nearly half that observed in implant testing states performed with a tuberoplasty

The mechanism responsible for this motion restriction can be explained by studying the change in abduction angle versus deltoid load for all implant designs. The plots shown in Figure 4-8 illustrate that with a tuberoplasty, each implant was capable of achieving high angles of glenohumeral abduction. Without a tuberoplasty however, the angle of abduction seemed to converge between 40°-60° degrees. It is likely that impingement between the lateral edge of the implant and the greater tuberosity was the mechanism responsible for this asymptotic behavior in the implants tested without a tuberoplasty. As the humerus is elevated, the lateral most aspect of the greater tuberosity contacts the lateral edge of the implant, which protrudes off the inferior surface of the acromion. This contact likely acts as a barrier to further abduction. This impingement can be overcome by externally rotating the humerus, which rotates the greater tuberosity posteriorly relative to the glenohumeral joint. Therefore, as the arm is abducted in external rotation, the greater tuberosity does not rotate or move in a path coincident with the acromion or subacromial implant. However, externally rotating the humerus in order to achieve normal abduction is not practical when this motion can normally be performed without the need for external rotation.

While the tuberoplasty was shown to provide several different advantages when paired with the subacromial implant, alternative measures may also be advantageous to improve the function of this implant. Potentially the most suitable option as an alternative to using a tuberoplasty would be to modify the lateral morphology of the subacromial implant. More specifically, it may be warranted to consider designing the laterally aspect of the implant as a converging entity, minimizing the lateral border of the implant. This could serve to

reduce, or potentially eliminate impingement between the greater tuberosity and implant, while also allowing the implant to restore normal joint stability.

This study was not without limitations. Testing was carried out using cadaveric shoulder specimens with static loads used to control muscle activation. Although cadaveric studies have been thoroughly used previously to examine implant performance, this type of testing does not fully represent the dynamic muscle characteristics observed in-vivo. However, the use of cadavers allowed for the design of a repeated-measures study to be performed, in addition to the evaluation of multiple implant designs. This type of testing also allowed for accurate tracking of joint kinematics and for visual observations to be made regarding the interface between the subacromial implant and both scapula and humerus. Another limitation included the small sample size used to carry out this study. However, further testing using the same methods as described in this chapter will be carried out to increase both the sample size and statistical power for both kinematic and range of motion analyses. Lastly, axial rotation of the humerus was not assessed during the range of motion analysis, which may have influenced the angle of abduction achieved. However, the shoulder simulator used to conduct this testing was designed to limit the constraint placed on the glenohumeral joint, which included freeing the axial rotation degree of freedom of the humerus. Therefore, the humerus was allowed to both translate and rotate through a path of least resistance.

4.6 Conclusion

This chapter evaluated the efficacy of pairing the subacromial implant with a tuberoplasty procedure to further improve the function of the implant in restoring normal glenohumeral joint stability and range of motion. The results obtained from the kinematic analysis revealed the tuberoplasty to have minimal effect on the implants ability in restoring normal humeral head position. The 5mm high constraint implant paired with a tuberoplasty was again shown to be most effective, restoring average AP and SI humeral head position to within 1mm and 2mm of the intact rotator cuff test state respectively. Most importantly, the addition of the tuberoplasty greatly increased the allowable range of motion of all subacromial implant designs. These results suggest the pairing the insertion of the

subacromial implant with a tuberoplasty is advantageous for improving both glenohumeral stability and range of motion with this implant.

4.7 References

1. Berthold DP, Bell R, Muench LN, et al. A new approach to superior capsular reconstruction with hamstring allograft for irreparable posterosuperior rotator cuff tears: a dynamic biomechanical evaluation. *J Shoulder Elb Surg*. 2021;30(7):S38-S47. doi:10.1016/j.jse.2021.04.002

2. Fenlin JM, Chase JM, Rushton SA, Frieman BG. Tuberoplasty: Creation of an acromiohumeral articulation - A treatment option for massive, irreparable rotator cuff tears. *J Shoulder Elb Surg*. 2002;11(2):136-142. doi:10.1067/mse.2002.121764

3. Lee BG, Cho NS, Rhee YG. Results of arthroscopic decompression and tuberoplasty for irreparable massive rotator cuff tears. *Arthrosc - J Arthrosc Relat Surg*. 2011;27(10):1341-1350. doi:10.1016/j.arthro.2011.06.016

4. Matsen III F. Rotator cuff tears - what to do if they are irreparable? Shoulder Arthritis/Causes of rotator cuff tears: causes of shoulder pain. Published 2016. 1. Matsen III F. Rotator cuff tears - what to do if they are irreparable? Shoulder Arthritis/Causes of rotator cuff tears: causes of shoulder pain. Published 2016. Accessed July 26, 2022. http://shoulderarthritis.blogspot.com/2016/02/rotator-cuff-tears-what-to-do-if-they.html

5. Mihata T, McGarry MH, Kahn T, Goldberg I, Neo M, Lee TQ. Biomechanical Effects of Acromioplasty on Superior Capsule Reconstruction for Irreparable Supraspinatus Tendon Tears. *Am J Sports Med*. 2016;44(1):191-197. doi:10.1177/0363546515608652

6. Mirzaee F, Aslani MA, Zafarani Z, Aslani H. Treatment of Massive Irreparable Rotator Cuff Tear with Arthroscopic Subacromial Bursectomy, Biceps Tenotomy, and Tuberoplasty. *Arch Bone Jt Surg*. 2019;7(3):263-268.

7. Oh JH, Jun BJ, McGarry MH, Lee TQ. Does a Critical Rotator Cuff Tear Stage Exist? *J Bone Jt Surg*. 2011;93(22):2100-2109. doi:10.2106/jbjs.j.00032

8. Park JG, Cho NS, Song JH, Baek JH, Rhee YG. Long-term outcome of tuberoplasty for irreparable massive rotator cuff tears: Is tuberoplasty really applicable? *J Shoulder Elb Surg*. 2016;25(2):224-231. doi:10.1016/j.jse.2015.07.025

9. Scheibel M, Lichtenberg S, Habermeyer P. Reversed arthroscopic subacromial decompression for massive rotator cuff tears. *J Shoulder Elb Surg*. 2004;13(3):272-278. doi:10.1016/j.jse.2004.01.007

10. Verhelst L, Vandekerckhove PJ, Sergeant G, Liekens K, Van Hoonacker P, Berghs B. Reversed arthroscopic subacromial decompression for symptomatic irreparable rotator cuff tears: Mid-term follow-up results in 34 shoulders. *J Shoulder Elb Surg*. 2010;19(4):601-608. doi:10.1016/j.jse.2009.10.001

Chapter 5

5 Thesis Summary and Conclusions

This chapter revisits the objectives and hypotheses from Chapters 2, 3, and 4. The results are also revisited and are assessed relative to the original objectives and hypotheses. The strengths and weaknesses of this work are provided, followed by a discussion of future work needed to further improve and develop this implant. This chapter concludes by discussing the significance of this work from both a clinical and patient perspective.

5.1 Summary and Conclusions

Massive irreparable rotator cuff tears observed in younger, higher functioning patients continue to pose difficulty to clinicians as no clear choice of treatment for this patient demographic exists. While a variety of different treatment options are currently available, each has disadvantages that can lead to low patient satisfaction and poor surgical outcomes. A potential concept that has yet to be utilized by any current treatment options for this pathology is a rigid implant fixed within the subacromial space that functions to prevent excessive humeral head translation. Although this concept was recently proposed, no studies or scientific research has previously been conducted to determine its efficacy in treating massive irreparable rotator cuff tears. It was the overall purpose of this work to design, develop, and test a surrogate device to evaluate its ability to restore normal joint stability.

The first objective of this work (Chapter 2) was to design a subacromial implant for the purpose of restoring normal glenohumeral stability in the presence of a massive irreparable rotator cuff tear. The implant had to be designed using average scapular morphology and created as a modular device, representing different implant variables. Various methods were used to make changes to the originally proposed implant design in order to improve both the function of the implant and the fit of the implant to the scapula, while permitting in-vitro evaluations of various design options in a repeated measures fashion in each specimen tested downline. An anthropometric analysis, using a database of upper extremity

computer tomography (CT) scans, was conducted in addition to in-vitro implantation and experimentation with intermediate design prototypes. These tests served to primarily improve the shape of the implant to improve its articulation with the scapula. Implantation of this device also allowed for an insertion technique to be developed, which will be important for future clinical use. The implant was also designed as a modular device, which allowed for different implant shapes to be easily tested. The two design variables captured by the modularity of the implant were the implant thickness and constraint of its inferior articular surface. These variables were selected due to their importance in restoring normal position of the humeral head within the glenohumeral joint. This led to the creation of four unique implant designs, classified by 5mm and 8mm implant thicknesses, in addition to low and high constraint articular surfaces. All implant components were three-dimensionally (3D) printed from medical grade titanium as this material provided a rigid barrier to humeral head translation.

The second objective of this thesis (Chapter 3) was to investigate the ability of the rigid subacromial implant (designed in Chapter 2) to restore humeral head position from the superiorly migrated position. It was hypothesized that a subacromial implant would restore near normal humeral head position in a massive, irreparable rotator cuff tear state. Furthermore, it was predicted that different implants, characterized by different implant design variables, would be more effective in improving the implant's ability in restoring axial glenohumeral stability. This objective was accomplished using an in-house shoulder testing apparatus to apply physiologic and static muscle loading at varying angles of glenohumeral abduction. All four implant designs were compared to the intact rotator cuff and cuff deficient testing states, where the cuff deficient testing state simulated a massive irreparable rotator cuff tear. The results from this study found the 5mm high constraint implant model to be most effective at restoring humeral head position to that of the intact cuff state in both anterior-posterior (AP) and superior-inferior (SI) directions. This result confirmed both hypotheses made prior to this study as this implant design prevented the humerus from translating both superiorly and posteriorly, as commonly observed with the rotator cuff tear state. Furthermore, the 5mm high constraint implant design was more effective at restoring both AP and SI humeral head position compared to the other implant variables tested. This confirmed that the implant could be optimized to improve its overall

function. The results showed the 5mm thick implant designs to restore SI humeral head position more accurately compared to the 8mm thick designs, which caused greater inferiorization relative to the intact test state. A similar trend was observed between the high and low constraint implant designs, as the low constraint implant designs allowed for greater anterior translation of the humeral head compared to the high constraint implants. However, it was observed that all implant models were most effective at restoring normal joint position at lower and medium angles of glenohumeral abduction compared to higher angles of abduction. At 60 degrees, all implant models exhibited greater anterior and inferior humeral head translation, suggesting that contact between the humerus and implant may be responsible for such overcorrection in humeral position at higher abduction angles.

The third objective of this thesis (Chapter 4) was to assess the effect a tuberoplasty procedure, combined with the subacromial implant placement, had on the restoration of normal humeral head position. Additionally, the objective was to investigate the difference in allowable range of motion in abduction between the subacromial implant, both with and without a tuberoplasty. It was hypothesized that combining the insertion of the subacromial implant with a tuberoplasty procedure would more effectively restore normal joint position and increase glenohumeral range of motion compared to the use of the subacromial implant alone. The same shoulder simulator as used in Chapter 3 was used to carryout in-vitro testing with the subacromial implant. However, several design changes to the shoulder simulator were made prior to testing to reduce the constraint placed on the motion of the glenohumeral joint, and importantly to permit unrestrained arm abduction upon varied deltoid loading. The same four implant designs as used in Chapter 3 were tested, first without a tuberoplasty, and then repeated in reverse testing order with a tuberoplasty. Two different analyses were performed during this study. The first analysis examined the kinematics of the humeral head within the glenohumeral joint at varying angles of abduction with static muscle loading. The second analysis examined the angle of abduction achieved in each implant test state throughout sequential deltoid loading, to a maximum total deltoid load of 80N. The results from the first analysis in this study found all implant designs, on average, to more effectively restore normal humeral head position when paired with a tuberoplasty. However, the benefits provided by the tuberoplasty procedure were minimal, with no statistical differences observed between corresponding implant designs

with and without a tuberoplasty. The effect of the tuberoplasty was most observable in the second analysis performed, which illustrated increased allowable abduction range of motion when the implant was paired with a tuberoplasty procedure. The subacromial implant when used without a tuberoplasty greatly limited the allowable range of motion, suggesting that impingement between the lateral edge of the implant and greater tuberosity on the humerus occurs during abduction.

5.2 Strengths and Limitations

The most significant strength of this study was the testing of a novel implant device that utilizes a rigid spacer to function as a passive barrier to humeral head translation. Furthermore, this device does not require the replacement of joint surfaces to properly function. These unique attributes suggest this device may be more advantageous to younger, more active patients. The implant was also created as modular, which allowed for several different implant designs to be tested. This study also performed experimentation using repeated measures methodology, using the same cadaver specimens to test all implant designs. This permitted all implant models, including those paired with and without a tuberoplasty, to be evenly compared within the same physiological environment.

Some limitations were present within this work. The utilization of cadavers for testing the subacromial implant was a limitation as cadaveric testing does not replicate active muscle loading or the complex, dynamic joint environment as in-vivo. However, the use of cadaver specimens not only allowed for several implant designs to be tested within the same joint environment, but also permitted the implant to be compared directly to healthy and pathologic soft tissue conditions. Another limitation present in this work included that motion during in-vitro testing was limited to the scapular plane. Abduction in the scapular plane is performed in studies examining superior humeral migration as the activation of all deltoid heads maximizes the superior force acting on the humerus to exhibit the greatest superior humeral head translation. While the primary focus of this study was to analyze the implant in its ability to prevent superior humeral migration, other motions should also be studied to investigate whether any other instances of impingement occur between the humerus and implant.

This study was also limited by the modular design of the subacromial implant. Although two important implant design variables were tested, the quantity of both design variables and the different values of these design variables were limited by several factors. An increase in the number of implant designs tested would have significantly extended the in-vitro testing time. The modular aspect of the implant, combined with how the different implant components were connected, limited the allowable implant thickness to be tested. Although the setscrew fixation design used to secure implant components allowed for the quick and efficient interchanging of design components throughout testing, this design limited the minimum thickness of the spacer to approximately 5mm. Implant thickness of less than 5mm could not be evaluated as sufficient implant volume was needed for insertion of the setscrew through the implant itself. Further investigation of thinner implant designs must be conducted as the results obtained from this work suggest an implant design with a thickness smaller then 5mm may be optimal in restoring normal joint position.

5.3 Future Work

This work was the first to evaluate the efficacy of using a subacromial implant to restore normal joint stability in the presence of a massive irreparable rotator cuff tear. Therefore, these were the earliest stages of design and development for this device. Extensive research, including further optimizing and implant testing, is needed to improve the effectiveness of this device while also ensuring patient safety and satisfaction.

Continuing optimization of the morphology of this implant will further improve the implant's capability in restoring normal humeral head position in the presence of a massive irreparable rotator cuff tear. The results obtained in both Chapters 3 and 4 suggest an implant thickness of 5mm was too large, as both 5mm implant designs inferiorly translated the humeral head relative to the intact rotator cuff testing state. Future evaluation of smaller implant thickness values is necessary to determine the optimal implant size. Additional constraint values should also be further investigated to optimize the restoration of anterior-posterior humeral head position. Implant design modifications also need to be considered to improve the function of this device at higher angles of abduction. Although it was shown that pairing this device with a tuberoplasty improved humeral head position at higher angles of abduction, it may be possible to modify the lateral aspect of the implant to prevent

humeral impingement. Such modifications could include designing the implant with a thinner lateral edge or decreasing the length of the implant in the medial-lateral direction. Computational modelling would provide the most cost efficient, and time efficient method for conducting the analyses discussed above as this would permit a large quantity of different implant designs to be tested without fabrication.

Several other attributes of the subacromial implant that were not focused on within this thesis must also be further studied to ensure proper functioning of this device. Perhaps the most important of these attributes includes the effect that insertion of this device will have on the stress within the scapular spine. It is critical to ensure that fixation of this implant to the scapular spine does not compromise the structural integrity of this bony structure, thereby increasing the risk of a scapular spine fracture. Both in-vitro testing and computational analysis using Finite Element Analysis (FEA) should be conducted going forward to investigate the impact that fixation with this device has on scapular spine and acromial stresses. Further optimization should also be performed to improve the conformity of the implant to both acromion and scapular spine surfaces. Proper fixation of the implant to both of these surfaces will also be critical in minimizing implant loosening, ensuring the longevity of this device. Such optimization would include further modifying the superior aspect of the implant to improve its conformity with different acromion shapes and curvatures. This could also include modifying the shape of the fixation plate so the device is fixed to the thickest and highest density cortical bone in the scapular spine. The concept of utilizing this implant as a patient specific device should also be considered moving forward, where the design of individual implant models could be created using patient Computer Tomography (CT) scans, similar to recent advances in mandibular and cranial reconstruction research. This could potentially lead to a significant improvement in the fixation and conformity of the implant to both the acromion and scapular spine. Optimization of other implant design variables must also be considered going forward. These variables include, but are not limited to, the constraint of the implant's articulating surface in the medial-lateral direction and the angulation of this inferior surface relative to the center of the glenohumeral joint. Lastly, the material used for future fabrication of the implant should be assessed to improve contact mechanics at its articulation with the humeral head. Some early thoughts include the use of pyrolytic carbon which has a

demonstrated advantage with regard to minimizing friction against cartilage and bone. It will be imperative to investigate potential materials with low stiffness values to improve contact mechanics between both the implant and cartilage, and implant and bone.

5.4 Significance

The importance of treating massive irreparable rotator cuff tears is obvious with an aging population that continues to be more active, demanding a safe and quick return to either employment and/or recreational activities. Current treatments contain different attributes that have contributed to poor clinical outcomes and low patient satisfaction when treating this demographic. This thesis presented a novel device that utilizes a rigid subacromial implant to function as a passive barrier to prevent against posterosuperior translation of the humeral head as observed in a rotator cuff tear model. The unique attributes of this medical implant may be advantageous for treating this patient demographic, improving their quality of life and allowing for safe return to daily activities.

Curriculum Vitae

Cole T. Fleet

Education

2020-2022

Master of Engineering Science – Mechanical and Materials Engineering

The University of Western Ontario, London, Canada
- Collaborative Specialization in Musculoskeletal Health Research (CMHR) at Western University

2016-2020

Bachelor of Engineering Science – Mechanical and Materials Engineering

The University of Western Ontario, London, Canada
- Graduated with distinction

Relevant Work Experience

2020-Present

Teaching Assistant

The University of Western Ontario
- MME2259 – Product Design and Development
- MME2285 – Engineering Experimentation
- MME3380 – Mechanical Components Design
- MME4469 – Biomechanics of the Musculoskeletal System

Honours and Awards

2022-2023:

Ontario Graduate Scholarship - $15,000 (Declined)

2022-2025:

Canada Graduate Scholarship-Doctoral (NSERC CGS D) - $105,000

2021-2022:

Ontario Graduate Scholarship - $15,000 (Declined)

2021-2022:

Canadian Graduate Scholarship – Master's (NSERC CGS-M) - $17,500

2019:

Undergraduate Student Research Award (NSERC USRA) - $7,000

2018:

Undergraduate Student Research Award (NSERC USRA) -$6,500

2017-2020:

Dean's Honor List (Four years)

2016-2019:

Western's Continuing Admissions Scholarship (Four years) - $10,000

Publications

Submitted:

1. **Fleet, C.T.**, McNeil, D.M, Trenholm, J.A.I., Johnson, J.A., Athwal, G.S., Development and Evaluation of a Rigid Subacromial Implant to Treat Massive Irreparable Rotator Cuff Tears. *Submitted to the Journal of Shoulder and Elbow Surgery.*

Published:

1. **Fleet, C.T.** and Straatman, A.G. (2021). A model for the conduction shape factor in spherical void phase porous materials. *International Journal of Heat and Mass Transfer,* 164, 120583.

Peer Reviewed Abstracts and Conferences

Presentations:

1. **Fleet, C.T.**, Boux de Casson, F., Urvoy, M., Chaoui, J., Johnson, J.A., Athwal, G.S. (2022) Peripheral Glenoid Bone Remodeling in Patients with Type A2 Glenohumeral Arthritis. *Canadian Orthopaedic Research Society (CORS)*, Quebec City, Quebec, Canada.
2. **Fleet, C.T.**, McNeil, D.M., Trenholm, J.A.I., Johnson, J.A., Athwal, G.S. (2022) The Efficacy of a Subacromial Implant to Restore Normal Glenohumeral

Kinematics in a Massive Rotator Cuff Tear Model. *Canadian Orthopaedic Research Society (CORS)*, Quebec City, Quebec, Canada.

3. **Fleet, C.T.**, Boux de Casson, F., Urvoy, M., Chaoui, J., Johnson, J., Athwal., G. (2021) Validation of a Patient Specific Statistical Shape Model for Predicting Premorbid Glenoid Morphology. *Canadian Orthopaedic Research Society (CORS)*, June 15-19, Vancouver (Virtual), Canada, CORS Top Canadian Research Paper Session Founder's Award Candidate.

Posters:

1. **Fleet, C.T.**, Vannitamby, K.D., Mistry, M., Johnson, J.A., King, G.J.W. (2022) A Biomechanical Study Investigating Overcorrection of Ulnar Angulation on Radial Head Stability in Anterior Monteggia Fractures. *London Health Research Day (LHRD),* London, Ontario, Canada
2. **Fleet, C.T.**, Klarer, J., Abdic, S., Johnson, J.A., Athwal, G.S. (2022) Analysis of Bone Loss Depth in Favard Type E3 Gleniod Erosions. *Canadian Bone and Joint Conference (CBJC),* London, Ontario, Canada
3. Benitah, J., **Fleet, C.T.**, Cunningham, D.E., Johnson, J.A., King, G.J.W. (2022) Viscoelastic Properties of Articular Cartilage Affect the Contact Mechanics of Both the Native and Hemiarthroplasty Articulations. *Canadian Orthopaedic Research Society (CORS)*, Quebec City, Quebec, Canada.
4. Cunningham, D.E., **Fleet, C.T.**, Athwal, G.S., Johnson, J.A. (2022) Evaluating Micromotion Measurements in Orthopaedic Implants Relative to Bone. *Canadian Orthopaedic Research Society (CORS)*, Quebec City, Quebec, Canada.
5. Vannitamby, K.D., **Fleet, C.T.**, Mistry, M., Johnson, J.A., King, G.J.W. (2022) Analysis of Four Different Annular Ligament Reconstructions to Restore Radial Head Stability in Anterior Monteggia Fractures. *Canadian Orthopaedic Association (COA)*, Quebec City, Quebec, Canada.
6. Vannitamby, K.D., **Fleet, C.T.**, Mistry, M., Johnson, J.A., King, G.J.W. (2022) Overcorrection of Ulnar Angulation Improves Radial Head Stability in Anterior Monteggia Fractures: An In-Vitro Biomechanical Study. *Canadian Orthopaedic Association (COA),* Quebec City, Quebec, Canada.
7. **Fleet, C.T.**, Copp, G., Athwal, G.S., Johnson, J.A. (2021) The Effect of High Velocity Shoulder Motion on Joint Loading: An Analysis in OpenSim. *Canadian Orthopaedic Research Society (CORS)*, June 15-19, Vancouver (Virtual), Canada.

Non-Peer Reviewed Work:

1. McNeil, D.M., **Fleet, C.T.**, Johnson, J.A., Athwal, G.S., Johnston, D.A., Trenholm, J.A.I. (2021) A Biomechanical Study of a New Implant for Treatment of Massive Rotator Cuff Tears. *2nd Annual Fellows Research Day*, London, Ontario, Canada.
2. Vannitamby, K.D., **Fleet, C.T.**, Van Osch, N., Mistry, M., Johnson, J.A., King., G.J.W. (2021) The Effect of Overcorrection of Ulnar Angulation on Radial Head Stability in Anterior Monteggia Fractures. *Orthopaedic Surgery Residents' Research Day*, London, Ontario, Canada.